Phytochemicals for prostate cancer prevention: Integrating redox signaling, epigenetics and genetics *in vitro* and *in vivo*

by

Ying Huang

A dissertation submitted to the

Graduate School-New Brunswick

Rutgers, The State University of New Jersey

In partial fulfillment of the requirements

For the degree of

Doctor of Philosophy

Graduate Program in Pharmaceutical Science

Written under the direction of

Professor Ah-Ng Tony Kong, Ph.D.

And approved by

_____

_____

_____

_____

New Brunswick, New Jersey

January, 2015

ABSTRACT OF THE DISSERTATION

Phytochemicals for prostate cancer prevention: Integrating redox signaling, epigenetics and genetics *in vitro* and *in vivo*

by Ying Huang

Dissertation Director: Dr. Ah-Ng Tony Kong

Prostate cancer is the most prevalent type of non-skin cancer among men in the United States. The development of prostate cancer generally consists of three stages—initiation, promotion and progression. Many phytochemical display preventive effects against prostate cancer by blocking the tumor initiation and/or suppressing the promotion and progression. Nrf2 is a master regulator of the antioxidant response and xenobiotic metabolism through the regulation of a wide range of antioxidant and phase II detoxification genes. Nrf2 protects cells from stressors, including endogenous substances, reactive oxygen species, radiation, environmental toxins, and xenobiotics from food. The protective role of Nrf2 points its potential importance in prostate carcinogenesis. Coincidentally, our group has reported that as prostate progresses in the transgenic adenocarcinoma of mouse prostate (TRAMP) model, there is a progressive loss of expression of Nrf2 and its downstream target genes, which is associated CpG hypermethylation in the promoter region. Curcumin (CUR), tocopherols (T) and tocotrienols (T3) were found to be powerful cancer chemopreventive agents using animal models of different cancers including prostate cancer. Using TRAMP C1 cells, we demonstrated that CUR is a potent demethylation agent and it restores the epigenetically silenced Nrf2 gene through DNA demethylation. In addition, we showed

that a γ-tocopherol-rich mixture of tocopherols (γTmT) treatment reduced the incidence of palpable tumor incidence in TRAMP mice. γTmT also inhibited the CpG hypermethylation in the Nrf2 promoter during prostate cancer progression and maintained Nrf2 and its downstream target NQO1 in the prostate. A global gene expression analysis comparing the TRAMP and non-transgenic mice revealed dramatic difference in the prostate, including genes encoding phase II detoxification enzymes and cell cycle controlling proteins. Short-term treatment of γTmT could partly prevent the alteration of genes identified in the prostate of TRAMP mice. Furthermore, we found that a mixture of tocotrienols, a less-recognized subclass of vitamin E, suppressed xenografted VCaP prostate tumor in nude mice in part by modulating cell cycle progression.

ACKNOWLEDGEMENTS

I would like to gratefully and sincerely thank my advisor Dr. Ah-Ng Tony Kong for his incessant support and guidance throughout the course of my graduate study at Rutgers. He encouraged me to not only grow as an experimentalist but also as an independent thinker. For everything you've done for me, Dr. Kong, thank you! I would also thank the other members of my committee Drs. Audrey Minden, Li Cai and Leonid Kagan for their valuable comments and input on the projects.

I would also like to thank Drs. Tin Oo Khor and Constance Saw for their help and guidance in getting my graduate study started, and Drs. Zheng-Yuan Su and Limin Shu, with whom I worked closely. I would also thank Dr. Xi Zheng and Dr. Chuang S. Yang's group for their collaboration. Additionally, I am very grateful for the friendship of all the members of Dr.Kong's group. My special thanks to Ms. Hui Pung for her administrative support in the past six years. I would also thank Ernest Mario School of Pharmacy for providing me teaching assistantships.

Finally, I would like to thank my family, especially my mother, for their endless love, support and encouragement.

Table of Content

List of Tables

List of Figures

1 Chapter 1. Background and Significance

Prostate cancer (PCa) is a frequently diagnosed cancer in men worldwide. The incidence of PCa shows strong variation across different regions, with the highest rate in North American, Australia, Western and Northern Europe, and the lowest rate in Asian countries [1]. In the US, PCa is the most common non-skin cancer in men. In 2014, it was estimated that approximately 233,000 new cases would be diagnosed and 29,480 Americans would die from PCa [2].

1.1 Phytochemicals in prostate cancer prevention

A growing body of evidence suggests that PCa results from the accumulation of genetic and epigenetic alterations [3, 4]. PCa most likely origins from prostatic intraepithelial neoplasia (PIN), which is an androgen-dependent proliferation of neoplastic cells. PIN further progresses to latent low-grade carcinoma and subsequently high-grade metastatic tumor [3]. The development of PCa generally consists of three stages—initiation, promotion and progression. Initiation involves irreversible genetic and epigenetic changes caused by genotoxic species such reactive oxygen species and carcinogens. Promotion and progression of PCa are controlled by various signal transduction cascades triggered by hormones, growth factors, and chronic inflammation.

Cancer chemoprevention is defined as the use of relatively non-toxic chemicals to reverse, suppress or prevent cancer development [5]. Many epidemiological and preclinical animal studies have highlighted the potential of micronutrients and non-nutritive phytochemicals as chemopreventive agents against PCa [6]. These include curcumin (from Curcuma longa), epigallocatechin gallate (EGCG from green tea), soy isoflavones, sulforaphane (from cruciferous vegetables), resveratrol (from grape), tocopherols and tocotrienols (from vegetable oil and palm oil). They are currently under various phases of clinical trial (www.clinicaltrials.gov). Our laboratory and others have

demonstrated that their preventive effects again prostate cancer in animal models. Chemopreventive agents can be categorized as blocking agents, which impede the initiation stage, and suppressing agents, which delay or reverse the promotion and progression of tumor [7]. The chemopreventive effects of these agents might be attributed to a combination of effects on modulating phase I metabolizing enzymes (activation of carcinogens), phase II metabolizing enzymes (detoxification of carcinogens), proliferation, apoptosis, hormone activity, nuclear receptors, and epigenetic events [8].

1.2 Nuclear factor E2-related factor 2 (Nrf2)

Nrf2 is a master regulator of the antioxidant response and xenobiotic metabolism through the regulation of a wide range of antioxidant and phase II detoxification genes [9, 10]. Nrf2 protects cells from stressors, including endogenous substances, reactive oxygen species, radiation, environmental toxins, and xenobiotics from food. Therefore, activation of the Nrf2 pathway might be a promising strategy for chemoprevention. This view is supported by a number of studies demonstrating that Nrf2 is essential for chemopreventive agents, such as sulforaphane and oltipraz, to block carcinogenesis and that Nrf2-deficient mice are more prone to chemical-induced cancer development [11-13]. Regulation of the Nrf2 pathway

1.2.1 Molecular mechanisms of Nrf2 regulation

The Nrf2-Keap1 axis: As depicted in Figure 1-1, Keap1 is a key Nrf2 repressor and plays a pivotal role in regulating the Nrf2 signaling pathway [14-17]. Nrf2 has two binding motifs in the Neh2 domain, the ETGE and DLG motifs, and recruits two molecules of Keap1 in the absence of stimuli [18, 19]. Keap1 serves as a bridge between Nrf2 and ubiquitination ligase Cullin-3 (Cul-3), which is required for the ubiquitination of lysines in the Neh2 domain and subsequent proteasomal degradation [15, 17, 20, 21].

The negative regulation of Nrf2 by Keap1 has been confirmed in mouse models. Keap1-knockout mice express constitutively high levels of Nrf2, and select heterozygous Keap1 mutations abrogate the repressive effects of wild-type Keap1 on Nrf2 [22, 23].

Oxidative stressors or electrophiles inhibit the ubiquitination-dependent degradation and increase nuclear accumulation of Nrf2. As a cysteine-rich protein, Keap1 is an excellent sensor for chemical inducers [24]. Accumulating evidence lead to the "cysteine code" hypothesis, which proposes that different classes of Nrf2 activators have unique preferences in modifying specific cysteines (reviewed in [25]). Sulforaphane and tBHQ activate Nrf2 in a Cys151-dependent manner, whereas endogenous alkenal metabolites prefer Cys273/288 [26-28]. Cysteine modifications alter the proper conformation of the Keap1-Nrf2-Cul3 complex but do not dissociate Keap1 from the Neh2 domain of Nrf2 [29]. In the "hinge & latch" model, Nrf2 activators disrupt the relatively weak interaction between Keap1 and the DLG motif, but not the one between Keap1 and the ETGE motif [18, 19]. The switch from two-site to one-site binding inhibits Nrf2 ubiquitination, thereby rescuing Nrf2 from degradation. Nrf2 accumulates in the nucleus, where it dimerizes with small Maf proteins and binds to the ARE cis-regulatory sequences to trigger transcriptional expression [9, 30]. A large number of genes have been identified as downstream targets of Nrf2, including NAD(P)H:Quinone Oxidoreductase 1 (NQO1) and certain glutathione S-transferases (GSTs) (reviewed in [31]).

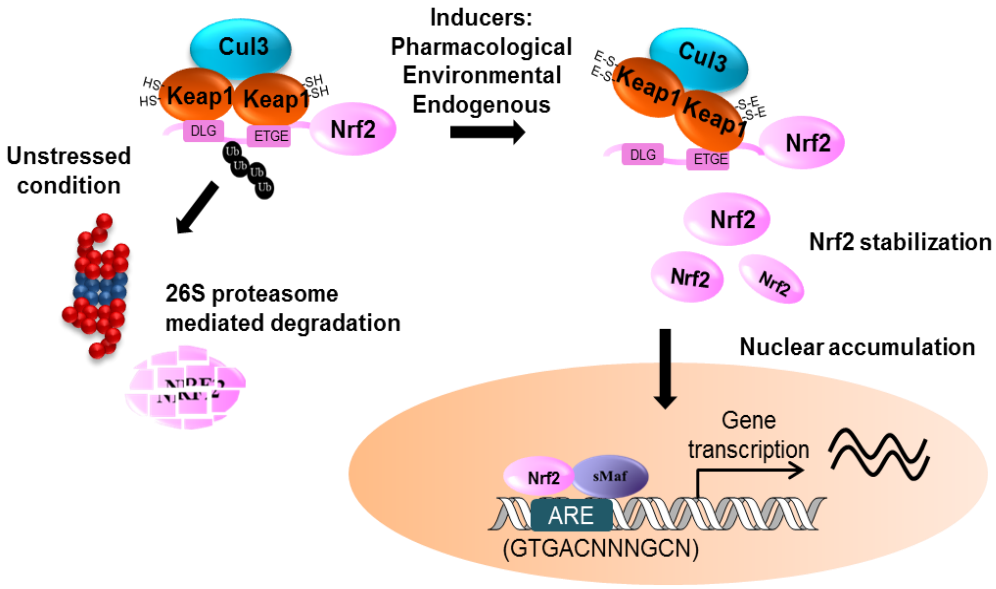

Figure 1-1. The classical Nrf2-Keap1 signaling pathway

Posttranslational regulation of Nrf2: Phosphorylation of Nrf2 can be detected by radioactive 32P labeling, phosphorylation-specific antibodies and mass spectrometry [32, 33]. A number of studies have examined the upstream regulators of Nrf2 phosphorylation, including protein kinase C (PKC), mitogen-activated protein kinases (MAPKs), PKR-like endoplasmic reticulum kinase (PERK), phosphatidylinositol 3-kinase (PI3K), and glycogen synthase kinase-3 (GSK-3). PKC phosphorylates Nrf2 at Ser40, a residue located in the Neh2 domain that binds Keap1. PKC activates the Nrf2 pathway, likely through disturbing the Nrf2-Keap1 interaction [33-35]. The effects of MAPKs on Nrf2 signaling appear to depend on the specific MAPK. In general, activation of JNK1 and ERK2 promotes the Nrf2 pathway, whereas activation of p38 is inhibitory [36]. Multiple sites in Nrf2 are phosphorylated by various forms of MAPKs (JNK1/2, ERK2, p38, and MEKK3/4) in HEK293T cells, but the Nrf2-mediated ARE response is unaffected by mutation of these sites [33]. This finding raises the question whether MAPK-mediated activation of Nrf2 occurs through direct phosphorylation. PERK enhances the nuclear accumulation of Nrf2 under endoplasmic reticulum stress [37]. PI3K also promotes the nuclear translocation of Nrf2 and induces

the expression of ARE-containing genes [38]. By contrast, GSK-3, negatively regulated by PI3K, inhibits Nrf2 by promoting its degradation [39-42]. GSK-3 catalyzes the phosphorylation of Nrf2 at the Neh6 domain and decreases its stability independent of Keap1-mediated degradation [41]. Taken together, protein kinases play a crucial role in Nrf2 signaling. However, it remains unclear whether the phosphorylation of critical Nrf2 residues directly affects Nrf2 signaling. Protein kinases might regulate the Nrf2 pathway through direct phosphorylation or indirect signaling cascades, which need to be dissected in the future.

Transcriptional regulation: Regulation of Nrf2 at the transcriptional level is far less studied compared to its regulation at the protein level. DeNicola et al. demonstrated that oncogenic alleles of Kras, Braf and Myc induce mRNA expression of Nrf2 and its target genes [43]. The transcriptional upregulation may involve the binding of Myc and Jun to the Nrf2 promoter, although detailed molecular mechanisms are not clear. Enhanced Nrf2 expression leads to the reduction of intracellular ROS and may provide a more favorable environment for cancer cell proliferation.

Translational regulation: We have reported the translational machinery that controls protein synthesis of Nrf2 [44]. Human Nrf2 mRNA contains an internal ribosomal entry site (IRES) at the 5' untranslated region that is required to initiate the internalization of Nrf2 mRNA into ribosomes for protein synthesis. In addition, an inhibitory element (IE) exists upstream of the IRES, blocking ribosomal internalization of mRNA. Hydrogen peroxide and sulforaphane treatment induces the entry of Nrf2 mRNA into polysomal fractions and augments its translation in an IRES-dependent manner. These findings suggest that the Nrf2 translation efficiency is

low in normal conditions and markedly increases under stress such that cells can consume energy efficiently for protein synthesis and degradation.

Epigenetic regulation: Accumulating research demonstrates that the transcriptional expression of some specific genes is controlled by epigenetic modification involving chromatin structural alterations. Epigenetic modulations can be caused by DNA methylation, histone modifications, and microRNAs [45]. DNA methylation is catalyzed by DNA methyltransferases (DNMTs) that transfer a methyl group to the 5′ position of the cytosine residue within CpG dinucleotides [46, 47]. Inappropriate DNA methylation of CpG islands in tumor suppressor genes and oncogenes has been observed in many cancer cells and is one of the potential carcinogenic mechanisms during the development of human cancers [45, 48-51].

Our group has reported that the transcription of Nrf2 is suppressed in prostate tumors of TRAMP mice and tumorigenic TRAMP-C1 cells due to the hypermethylation of select CpGs in the promoter of Nrf2 [52]. Repressive proteins, such as methyl-CpG-binding protein 2 (MBD2) and trimethyl-histone H3 (Lys9), are enriched in this region. Because DNA methylation is reversible, combined treatment with 5-aza-29-deoxycytidine (a DNMT inhibitor) and trichostatin A (a histone deacetylase inhibitor) restores Nrf2 expression in TRAMP-C1 cells [52]. Recently, a variety of natural compounds were found to modulate DNA methylation and/or histone modification, effectively restoring Nrf2 expression [53-56].

Recently, several microRNAs have been found to regulate the Nrf2-Keap1 pathway. MicroRNAs, transcribed from genetic loci, are small (20-22 nucleotides) non-protein-coding RNAs [57]. MicroRNAs regulate gene expression by inhibiting translation or inducing degradation of their target mRNAs [57]. Overexpression of four microRNAs, including miR-144, miR-153, miR-27a, and miR-142-5, either individually or as a

group, can reduce Nrf2 mRNA and protein levels, leading to reduced glutathione production in neuronal SH-SY5Y cells [58]. MiR-144 and miR-28 mediate the degradation of Nrf2 mRNA by targeting the 3'-untranslated region (3'-UTR) [59, 60]. Moreover, miR-34a is elevated in the livers of aged rats, which is associated with suppressed expression of Nrf2 [61]. The negative regulation of miR-34a on Nrf2 was further confirmed by the transfection of miR-34a in HEK293 cells. In addition, miR-200a mediates the degradation of Keap1 mRNA in breast cancer cells, and the reduction of Keap1 activates the Nrf2 pathway [62].

1.2.2 Nrf2 activators: diverse structures and distinct mechanisms

Nrf2 activators comprise a range of structurally diverse chemicals, classified as isothiocyanates, Michael reaction acceptors, dithiolethiones, oxidizable diphenols/phenylenediamines/quinones, thiocarbamates, polyenes, hydroperoxides, trivalent arsenicals, heavy metals and dimercaptans (Table 1) [63, 64]. Keap1 is the primary target of Nrf2 activators, most of which are electrophilic or reactive to thiol groups. Select Keap1 cysteine residues undergo covalent modifications depending on the nature of the Nrf2 inducers [24, 29, 65-67]. It is intriguing whether the position of the modified cysteine affects the subsequent biological effects. In addition to Keap1, some Nrf2 activators also modulate other machinery in Nrf2 signaling, as discussed in the preceding section.

Sulforaphane, an isothiocyanate, can be digested from cooked cruciferous vegetables and a variety of oral supplements containing purified sulforaphane or broccoli sprout extract [82-86]. Sulforaphane activates the Nrf2-Keap1 pathway through direct modifications of critical Keap1 cysteines, especially Cys151, as evidenced in mass spectrometry analysis, site-directed mutagenesis and in vivo experiments [27, 28, 65, 68, 69]. Sulforaphane treatment also promotes the ribosomal

internalization of Nrf2 mRNA for protein synthesis [44]. Recently, we demonstrated that sulforaphane restores Nrf2 mRNA expression epigenetically through the demethylation of promoter CpGs in TRAMP-C1 and JB6 cells [54, 56]. Following acute or long-term administration of sulforaphane, antioxidant and phase II drug metabolizing enzymes are induced in the liver, intestines, skin, prostate, and blood lymphocytes [70-76]. Sulforaphane has been shown to be protective against carcinogenesis in various types of carcinogen-induced and transgenic cancer models (reviewed [31, 77]). Clinical studies have demonstrated that the consumption of broccoli sprout extract changes the disposition of aflatoxin-DNA adducts and is well-tolerated in humans [78-80].

Synthetic oleanane triterpenoids such as 2-cyano-3,12-dioxooleana-1,9(11)-dien-28-oic acid (CDDO) and its derivatives are the most potent Nrf2 inducers ever discovered, activating Nrf2 signaling at nanomolar concentrations [81, 82]. These compounds belong to the Michael reaction acceptors and are reactive to nucleophiles containing –SH groups when incubated with dithiothreitol (DTT), cysteine, or reduced glutathione [83]. Given the chemical properties of these compounds, they very likely modify one or more Keap1 cysteine residues, although the exact 'cysteine code' remains to be elucidated [28, 84]. Oral administration of CDDO-Im, an imidazole derivative of CDDO, elevates the expression of HO-1 and NQO1 in the liver and other organs in mice in an Nrf2-dependent manner [81, 85]. A variety of CDDO derivatives are effective for preventing or treating cancer in preclinical models (reviewed in [86]). In addition, CDDO-Im also provides protection against kidney injury, emphysema and cardiac dysfunctions through the Nrf2 pathway [87, 88].

Oltipraz is a synthetic dithiolethione, which is a class of organosulfur compounds. Dithiolethiones are reactive to thiols and potentially modify Keap1 cysteine residues

[89, 90]. 3H-1,2-dithiole-3-thione, a dithiolethione structurally similar to oltipraz, induces intermolecular disulfide bonds between two Keap1 molecules at Cys273 and Cys288 [66]. Other studies suggest that dithiolethiones activate the Nrf2 pathway through the generation of H2O2 or other superoxides, which are another class of Nrf2 inducers [90-92]. Oltipraz stimulates a battery of antioxidant and phase II detoxification enzymes, such as NQO1, GSTs and UGTs, and elevates GSH in vitro and in vivo [11, 12, 93, 94]. Oltipraz, an ancient compound used in early chemoprevention studies in the 1980s [95-98], suppresses tumorigenesis induced by a broad range of carcinogens (reviewed in [89, 99]). Its chemopreventive efficacy in carcinogen-induced models appears to depend on Nrf2, as its efficacy is lost in Nrf2 knockout (KO) mice [11, 12, 93]. A clinical study reported that oltipraz increased aflatoxin-mercapturic acid conjugates in urine in subjects with high exposure to aflatoxin B1, indicating faster excretion of aflatoxin B1 [100].

tBHQ and tBQ are oxidized products from butylated hydroxyanisole (BHA), which is an oxidizable diphenol and commonly used as an antioxidant food preservative. Cys151 of Keap1 is a specific sensor for tBHQ. Nrf2 induction by tBHQ is diminished in cell culture and zebrafish by the ectopic expression of Keap1-C151S mutants, as well as in mouse embryonic fibroblasts (MEFs) and primary peritoneal macrophages derived from transgenic mice expressing the Keap1-C151S mutant [27, 28, 69, 101]. Although tBHQ-Cys151 adduct has not been detected by mass spectrometry, the oxidized quinone metabolite of tBQ forms a covalent adduct with Keap1 at Cys151 in a cell-free system [67]. Furthermore, tBHQ enhances the ubiquitination of Keap1, possibly from the switch of Cul3-mediated ubiquitination from Nrf2 to Keap1, leading to the stabilization of Nrf2 protein [102]. Nrf2 induction by BHA and tBHQ is associated with the activation of JNK1 and ERK2, respectively [103]. BHA regulates a wide array of

genes involved in phase II detoxification, ubiquitination, transporters and protein kinases in the small intestine and liver in mice through an Nrf2-dependent pathway [104]. Notably, the in vivo effects of BHA might be due to the combined action of BHA itself and its oxidized metabolites such as tBHQ and tBQ, which are more potent Nrf2 activators [105, 106]. The health concerns of the use of BHA as a food additive have been debated since the 1960s. One early study reported that BHA feeding (0.5% w/w) for 60 weeks inhibited ciprofibrate-induced hepatic tumorigenesis in rats [107]. By contrast, other studies found that BHA increased the toxicity of other chemicals or radiation, but BHA feeding (0.4%) alone for 104 weeks did not lead to carcinogenesis in rats [108, 109].

Arsenic is a ubiquitous environmental toxin, found in ground water, soil, and air. Arsenic exposure leads to prolonged Nrf2 activation through unique mechanisms that are not observed in sulforaphane or tBHQ treatment [110, 111]. Nrf2 induction by arsenic is associated with elevated p62 and the accumulation of autophagosomes, and knockdown of p62 diminishes the induction [111]. The proper interaction of Nrf2 and Keap1 is likely to be disordered due to the Keap1-p62 interaction and the sequestration of Keap1 in autophagosomes during arsenic-induced autophagy deficiency [111, 112]. The half-life of Nrf2 is markedly extended by approximately 10-fold when Nrf2 ubiquitination is inhibited by arsenic [110]. Although Nrf2 deletion rescues liver dysfunction in autophagy-deficient mice, it is not clear whether prolonged Nrf2 activation contributes to arsenic toxicity. By contrast, Nrf2 deficiency exacerbates arsenic toxicity in liver and bladder [113].

1.3 Nrf2 and cellular functions

1.3.1 Redox balance and xenobiotic metabolism

Reactive oxygen species (ROS), such as superoxides, hydrogen peroxide, and hydroxyl free radicals, are constantly produced in aerobic organisms. Aerobic respiration, during which some electrons leak from the electron transport chain and activate oxygen molecules, is the major source of ROS. Exposure to radiation, ultraviolet light, tobacco smoke, or metal can also trigger ROS production. Nitric oxide (NO), a reactive nitrogen species (RNS) generated by a group of NO synthases, has important physiological functions in regulating muscle contraction, inflammatory response, vasodilation, and platelet aggregation. Balanced cellular ROS/RNS is essential to maintain normal physiological processes, whereas excess amounts of ROS/RNS are harmful to intracellular macromolecules and are associated with chronic diseases, including Alzheimer's disease (AD), Parkinson's disease (PD), amyotrophic lateral sclerosis (ALS), diabetes, cardiovascular disease, inflammatory diseases, and cancer [114]. Mammalian cells have evolved with complicated antioxidant systems for survival, consisting of non-enzymatic antioxidants such as vitamin C and E and inducible antioxidant enzymes. Nrf2 coordinates the expression of ARE-containing genes, including superoxide dismutases (SODs), glutathione peroxidase (GPx), NQO1, heme oxygenase-1 (HO-1), and many enzymes involved in glutathione production, which can respond quickly to oxidative stress and maintain a balanced redox state in cells [115].

Humans also face carcinogenic and mutagenic stresses caused by xenobiotics from environmental pollutants. In general, xenobiotics undergo metabolism through two distinct phases: phase I metabolism that includes oxidation, reduction and hydrolyses, and phase II metabolism that comprises conjugation reactions such as

glucuronidation, glutathione conjugation and sulfation [116]. Phase I metabolism of xenobiotics often produces carcinogenic intermediates, as exemplified by benzo[*a*]pyrene and aflatoxin [117, 118]. Phase II metabolism often yields more water-soluble and fewer toxic metabolites. Nrf2 controls many phase II metabolizing enzymes, such as the GST family, the sulfotransferase 3A family, and the UDP-glucuronosyl transferase (UGT) family [31, 115]. Indeed, Nrf2 deficiency predisposes the toxicity of various carcinogens such as benzo[*a*]pyrene and aflatoxin [13, 93].

1.3.2 Inflammation

Excessive and chronic inflammation contributes to many acute and chronic diseases, including autoimmune, neurological and cardiovascular diseases and cancer [119, 120]. Increasing evidence suggests that Nrf2 may also protect against inflammation as well as oxidative stress [121-127]. Nrf2 mitigates chemical-induced pulmonary injury and inflammation [128, 129]. Severe tobacco smoke-induced emphysema, airway inflammation and asthma in mice with genetic ablation of Nrf2 may be caused by the reduction of antioxidant gene expression and the induction of interleukin (IL)-4 and IL-13 in bronchoalveolar lavage fluid and in splenocytes [130, 131]. Nrf2 is also involved in the modulation of the innate immune response, as demonstrated in Nrf2-deficient MEFs [132]. Nrf2 may block lipopolysaccharide (LPS)-induced ROS generation of tumor necrosis factor alpha (TNF-α), IL-6 and chemokines (Mip2 and Mcp-1) in mice peritoneal neutrophils [133]. Compared with wild-type mice, LPS stimulates a high level of inflammatory-related signals, such as TNF-α, IL-1, cyclooxygenase 2 (COX-2), and iNOS, in primary peritoneal macrophages in Nrf2-KO mice [134, 135]. More severe DSS-induced colitis was observed in the colon tissues of Nrf2-KO mice than in wild-type mice, and a lower induction of phase II antioxidant and detoxification enzymes and a higher induction of

pro-inflammatory biomarkers were observed in Nrf2-KO mice [124]. This finding suggests that Nrf2 may indirectly protect cells from inflammatory damage through antioxidant activation [133, 136].

NF-κB is a key regulator in the innate immune/inflammatory pathway, and the activation of NF-κB has been demonstrated in many cancer types [137, 138]. When cells are exposed to various stimuli, such as TNF-α, IL-1, H_2O_2, LPS, or microbial infection, the induced proteasome-mediated degradation of IκB proteins leads to the translocation of NF-κB from the cytoplasm to the nucleus [139, 140]. Activated NF-κB may further trigger the expression of downstream target genes, including various inflammatory cytokines and chemokines, adhesion molecules, COX-2, and NO synthase as well as other stress response genes [140-143]. This suggests that there is cross-talk among Nrf2, NF-κB and inflammation [144]. The Nrf2-ARE signaling pathway may be downregulated by pro-inflammatory signaling, as NF-κB could block the binding between CREB-binding protein (CBP) and Nrf2 or promote the interaction of HDAC3 with either CBP or MafK [145]. Additionally, higher activation of NF-κB in response to LPS and TNF-α has been observed in Nrf2-deficient MEFs compared with wild type MEFs [132]. NF-κB activation can also be affected by Nrf2 target genes such as HO-1, NQO1 and thioredoxin (TRX) [146-149].

1.3.3 Transporters and drug resistance

Transporters mediate the deposition of endogenous substances and xenobiotics, including drugs. For example, efflux transporters in the intestine and brain limit the permeability across the gastrointestinal tract and blood-brain barrier [150]. Overexpression of efflux transporters is a common mechanism of drug resistance, causing failure of cancer chemotherapy (reviewed in [151-153]). One superfamily of

efflux transporters is the ATP-binding cassette (ABC) family, which uses the energy of ATP hydrolysis to pump xenobiotics out of cells against a concentration gradient.

A growing body of evidence suggests that Nrf2 is involved in regulating the expression of efflux transporters, especially those belonging to the ABC family. ARE-like sequences are identified in the promoters of genes encoding multidrug resistance-associated proteins (MRP), including Mrp1, Mrp2, Mrp3, Mrp4, and Abcg2 [154-157]. The binding of Nrf2 to AREs has been confirmed in chromatin immunoprecipitation (ChIP) or ChIP-seq experiments [154-158]. In addition, the Nrf2 activators tBHQ, butylated hydroxyanisole (BHA), oltipraz, and ethoxyquin induce the expression of MRPS in cultured cells as well as in mouse and rat livers [154, 157, 159-161]. Nrf2-knockout mice exhibit lower basal expression of Mrp3 and Mrp4 and are less sensitive to BHA and oltipraz-induced expression of Mrp2, Mrp3 and Mrp4 compared with Nrf2 wild-type mice [157, 162]. Constitutive overexpression of Nrf2 confers chemoresistance in some advanced cancer cells, including human lung adenocarcinoma A549 cells and pancreatic carcinoma Panc1 and Colo357 cells. The knockdown of Nrf2 using siRNA or Nrf2 inhibitors sensitizes cellular responses to common chemotherapeutic drugs or natural compounds [163-166]. Collectively, Nrf2 is a potential target to circumvent chemoresistance.

1.4 Nrf2 and carcinogenesis

1.4.1 The protective role of Nrf2 in carcinogenesis

The protective role of Nrf2 in carcinogenesis has been demonstrated in animal models of different types of cancer. In early chemoprevention studies, it was observed that chemopreventive agents modulate the disposition of carcinogens and inhibit carcinogenesis through induction of phase II metabolizing enzymes [96, 167, 168]. Nrf2 is required for sulforaphane and oltipraz to exert chemopreventive effects, as

shown by comparing their efficacy in Nrf2 WT and KO mice [11, 12, 169]. Furthermore, Nrf2 deletion markedly increases susceptibility to carcinogen-induced tumor development in various organs, including colon, skin, breast, bladder and liver [13]. Nrf2-KO mice exhibit more pronounced inflammation in a dextran sulfate sodium-induced colitis model [124, 170, 171]. These results strongly suggest that Nrf2 protects against tumorigenesis by modulating the disposition of carcinogens and inflammatory response.

1.4.2 The dark side of Nrf2 in carcinogenesis

Given the protective role of Nrf2 in counteracting different stressors and toxins, it is logical to speculate that it also provides protection for cancer cells. Indeed, an increasing body of evidence demonstrates that Nrf2 is constitutively elevated in many types of cancer cells or tumor samples from cancer patients [125, 172-178]. Overexpression of Nrf2 is associated with poor prognosis in cancer patients [179-181]. A recent study reported that urethane-induced lung tumors from Nrf2-KO mice failed to engraft in nude mice, whereas those from Nrf2 WT mice grew progressively [182]. Knockdown of Nrf2 led to cell cycle arrest at the G1 phase in A549 and NCI-H292 lung cancer cells [165]. Nrf2 might be required to sustain proliferative signaling and reprogram energy metabolism, which are hallmarks of cancer [165, 183, 184].

1.4.3 The complexity of the Nrf2 pathway: Strength and duration of activation, disease stages, and multiple targets of Nrf2 activators

Transcription factor activity is commonly a double-edged sword. The strength of its action is a crucial factor in determining which side is predominant. Kensler *et al*. proposed a U-shaped relationship of Nrf2 expression and cancer risk [185]. According this paradigm, extreme low or high Nrf2 levels increase disease risk. The U-shaped relationship effectively describes the observations that Nrf2 deletion increases

susceptibility to carcinogens, neuronal toxins and bacterial and viral infection, whereas Nrf2 overexpression promotes drug resistance and cancer cell proliferation. Therefore, effective prevention occurs within a range between the biologically effective dose (BED) and the maximal-tolerated dose (MTD).

The duration of Nrf2 activation, which is determined by the underlying mechanism for activation, has profound biological consequences. For instance, chemical inducers and genetic modifications exhibit different response-time profiles for Nrf2 induction. Chemical inducers often exhibit a transient effect on Nrf2 pathway activation. We performed a pharmacokinetic-pharmacodynamic study of sulforaphane in rats and found that the expression of Nrf2-target genes peaks at 1-2 hours in blood lymphocytes after intravenous injection and returns to basal level after 24 hours [76]. By contrast, some chemical inducers have a prolonged effect on Nrf2 induction, likely through mechanisms other than the classical Nrf2-Keap1 interaction. One such example is arsenic, which recruits p62 and traps Keap1 in autophagosomes [111]. Furthermore, genetic factors such as Keap1 deletion, Keap1 mutation, Nrf2 mutation, and oncogenes generally lead to persistent activation of Nrf2, which is linked to the "dark side" of Nrf2 [186]. Transient Nrf2 activation through an intact Nrf2-Keap1 axis appears beneficial, whereas persistent Nrf2 activation might be harmful.

The dual role of Nrf2 is exemplified in different stages of tumorigenesis. Nrf2 blocks or delays tumorigenesis in normal and premalignant cells by relieving oxidative, mutagenic and inflammatory damage and by modulating carcinogen disposition. However, Nrf2 becomes undesirable when the defensive effects are hijacked by the malignant cells. The dual role is demonstrated in a recent study comparing WT and Nrf2-KO mice with urethane exposure [182]. Nrf2 prevents lung cancer initiation but enhances its progression in the late stage.

Many Nrf2 activators concomitantly exert multiple effects, such as inhibition of the NF-κB pathway and modulation of epigenetics, which appear to contribute to protective effects in addition to Nrf2 activation. For example, sulforaphane, 3H-1,2-dithiole-3-thione, and synthetic triterpenoid CDDO-Me repress the NF-κB mediated pro-inflammatory response by inhibiting the binding of NF-κB to DNA and the degradation of the NF-κB inhibitory protein IKK [135, 187-189]. In addition, several Nrf2 activators regulate epigenetic changes by affecting the enzymatic activity of HDACs and DNMTs. Class I, II and IV HDACs are zinc metalloproteins whose activity is dependent on Zn^{2+} [190]. Some Nrf2 activators interfere with HDAC activity, possibly through chemical characteristics (i.e., isothiocyanates, organosulfides and phenols) that may chelate Zn^{2+} [191]. Various Nrf2 activators inhibit the expression or the activity of DNMTs (i.e., sulforaphane and curcumin) or deplete the cellular pool of methyl donors (i.e., catechol polyphenols), resulting in altered DNA methylation [56, 192, 193]. The beneficial effects of Nrf2 activators may be due to a combination of Nrf2 activation, NF-κB inhibition and epigenetic regulation.

1.5 Summary

As a master regulator in the antioxidant response and xenobiotic disposition, Nrf2 plays a profound role in physiological and pathological processes. Loss of antioxidant and detoxifying systems may lead to increased susceptibility to prostate cancer. Phytochemical can enhance antioxidant and detoxification enzymes through Nrf2/ARE signaling pathway. Phytochemicals can also prevent loss of Nrf2 through epigenetic mechanisms. This dissertation compiles the results of the various investigations using both *in vitro* cell culture and *in vivo* animal models: 1) Nrf2 mediates the adaptive response to oxidative stress, exemplified by an endogenous oxidative molecule 4-hydroxynoneol; 2) Curcumin, as a DNA hypomethylation agent, restores the expression

of Nrf2 via promoter CpG demethyaltion in TRAMP-C1 cells; 3) TRAMP is a transgenic prostate cancer mouse model that closely mimics key events in human prostate cancer progression. We have shown that dietary feeding of γ-tocopherol-rich mixture of tocopherols (γ-TmT) inhibits prostate tumorigenesis in TRAMP model. γ-TmT also maintains Nrf2 expression in prostate tumors of TRAMP mice via inhibition of CpG methylation; (4) Mechanisms of prostate carinogenesis in TRAMP mice by identifying the differentially expressed genes/pathways compared to age-matched control mice, and prevention of the alteration of these pathways by γ-TmT; (5) Many chemopreventive agents act as suppressing agents. Herein, we show that mixed tocotrienols can effectively inhibit human prostate tumor growth in nude mice. Tocotrienols, especially δ-tocotrienol, can block cell cycle progression by suppressing the cyclins and induction of cyclin dependent kinase inhibitor p21 and p27.

2 Chapter 2. Anti-oxidative stress regulator NF-E2-related factor 2 mediates the adaptive induction of antioxidant and detoxifying enzymes in response to 4-hydroxynonenal

2.1 Introduction

Polyunsaturated fatty acids (PUFA), essential components of cell membrane, are susceptible to oxidation initiated by free radicals [194]. 4-hydroxylnonenal (4-HNE) is an end product from lipid peroxidation of omega-6 (*n*-6) PUFA [195]. The physiological concentration of 4-HNE is generally at the low micromolar level, but is remarkably increased under continuous oxidative stress [196]. As an α,β-unsaturated aldehyde, 4-HNE is highly reactive to a variety of nucleophilic sites in DNA and proteins [197]. Exposure to excessive 4-HNE can cause cytotoxicity, inactivation of enzymes, redox imbalance and multiple signaling transductions, and 4-HNE is implied in the detrimental pathogenesis of a number of degenerative diseases including cancer [198, 199]. Several metabolic pathways are involved in the detoxification of 4-HNE, including conjugation with glutathione (GSH) catalyzed by glutathione S-transferases (GST) and reduction of the aldehyde group to corresponding alcohol by aldoketone reductases (AKR)[198].

---

[1] Part of this chapter has been published as a research paper: **Huang, Y**, Wenge Li, Kong, A.-N. T. *Cell & Bioscience.* 2012, 2:40

[2] **Key Words**: NRF2, 4-hydroxynonenal (4-HNE), antioxidant response element (ARE), oxidative stress

[3] **Abbreviations:** ARE, antioxidant response elements; AKR1C1, aldoketone reductase 1C1; EGFP, the enhanced green fluorescent protein; GSH, glutathione; GSTA4, glutathione S-transferase A4; HO-1, heme oxygenase-1; 4-HNE, 4-hydroxynonenal; KEAP1, Kelch-like ECH-associated protein 1; NRF2, NF-E2-related

Eukaryotic cells have developed highly efficient machineries to counteract oxidative stress from environmental insults and aerobic metabolisms [200]. Antioxidant response elements (*ARE*) are identified in the regulatory region of many cytoprotective genes that encode phase II drug metabolizing/detoxifying enzymes, antioxidant enzymes and phase III efflux transporters [201, 202]. When oxidative stress is elevated, NF-E2-related factor 2 (NRF2) will be activated to trigger gene expression through binding to *ARE* [9]. Subsequently, it leads to enhanced cellular capability to remove excess electrophiles and restore redox homeostasis [13] .

NRF2 activity is regulated in part by a repressor protein, Kelch-like ECH-associated protein 1 (KEAP1), which retains NRF2 in the cytoplasm and mediates its degradation under homeostatic conditions [203]. Stimuli such as dietary antioxidants, heavy metals and reactive oxygen species (ROS) can disrupt the NRF2-KEAP1 binding and induce nuclear translocation of NRF2 where it dimerizes with small Maf proteins and binds to *ARE* [203]. In addition, some studies have shown that the subcellular distribution of NRF2 can also be controlled by the net driving force of nuclear location signals (NLS) and nuclear export signals (NES) [204] and phosphorylation of NRF2 [200] .

In this study, we investigated the role of NRF2 in regulating the gene expression of antioxidant and detoxifying enzymes upon the exposure to 4-HNE. Our results show that NRF2 rapidly translocates into nucleus after exposure to 4-HNE and induces transcriptional activity of *ARE* and mRNA expressions of *AKR1C1*, *GSTA4* and heme oxygenase-1 (*HO-1*). The induction of these detoxifying enzymes is diminished when *NRF2* is knocked down using small interfering RNA.

2.2 Materials and Methods

2.2.1 Cell culture and chemicals

Human cervical squamous cancerous HeLa cells and human hepatoma HepG2 cells were obtained from ATCC (Manassas, VA). The establishment of stably expressed HepG2 cells with the ARE luciferase reporter was described previously [205]. Cells were cultured in Dolbecco's modified eagle medium supplemented with 10% FBS. 4-HNE was purchased from Cayman Chemical (Ann Arbor, Michigan).

2.2.2 Cell fractionation and Western blotting

HeLa cells were treated with 10 μM of 4-HNE for 0, 0.5, 1 and 4 h, and then rinsed with ice-cold PBS and harvested. Nuclear protein was extracted using NE-PER nuclear and cytoplasmic protein extraction kits (Thermo scientific) according to the manufacturer's instruction. The protein concentration of each sample was measured, and 10 μg of nuclear proteins were used for Western blotting analyses. The details of Western blotting procedures were described previously [206]. Antibodies against NRF2 and Lamin A were from Epitomics and Santa Cruz, respectively. The densitometry of the bands were analyzed by ImageJ program.

2.2.3 Epifluorescent Microscopy

HeLa cells were cultured on ethanol-sterilized glass coverslips and transfected with 1 μg of EGFP-NRF2 or its EGFP-NRF2ΔN using the Lipofectamine method (Invitrogen) and further cultured in DMEM for 24 h. The generation of plasmids was described in our previous study [206]. After transfection, cells were treated with 10 μM of 4-HNE for 30 min. The expression and subcellular distribution of EGFP-tagged NRF2 and NRF2ΔN were examined using a Nikon Eclipse E600 epifluorescent microscope and a Nikon C-SHG1 UV light source purchased from Micron-Optics (Cedar Knolls, NJ). The EGFP signals were examined using FITC

filters. The epifluorescent images were digitalized using the Nikon DXM1200 camera and Nikon ACT-1 software.

2.2.4 Luciferase Activity Assay

The HepG2-C8 cell line with a stably expressed p*ARE*-TI-luciferase construct was previously established [205] and used to test the ARE transcriptional activity in this study. Cells were seeded in 6-well plates overnight, and then treated with 10 μM of 4-HNE for 18 h with or without pretreatment of 5 mM glutathione (GSH) for 2 h. Cells were then washed twice with ice-cold PBS and lysed with 1× reporter lysis buffer (Promega). A 10 μl lysate was mixed with the luciferase substrate (Promega) and the luciferase activity was measured using a Sirius luminometer (Berthold Detection System) and normalized by protein concentration.

2.2.5 Reverse Transcription-PCR

RNA was extracted using RNeasy mini kit (Qiagen, Valencia, CA) according to manufacturer's instructions and reverse transcribed (RT) using TaqMan® reverse transcription reagents (Applied Biosystems). The RT products were further analyzed by PCR reactions. The RT-PCR products were resolved in 1.5% agarose gel with ethidium bromide and visualized in UV light.

2.2.6 Transfection with siRNA

The sense and antisense sequences of siRNA against *NRF2* and nonspecific sequences were described previously [125]. The siRNA oligomers were synthesized by Integrated DNA technologies. HeLa cells were transfected using Lipofectamin RNAiMAX reagent (Invitrogen) following the manufacturer's instructions. Cells were transfected for 48 h with 50 nM siRNA in Opi-MEM medium without antibiotics and serum. Then, the cells were treated with 10 μM 4-HNE for 6 h.

2.2.7 Statistical analyses

Fold induction of *ARE*-luciferase and relative densitometry of nuclear NRF2 protein were analyzed using one-way ANOVA, where 4-HNE concentration or the exposure time of 4-HNE was treated as the main effect, followed by Tukey's studentized range test.

2.3 Results

2.3.1 NRF2 translocates into the nucleus after 4-HNE treatment

When expressed in HeLa cells, NRF2 tagged with the enhanced green fluorescent protein (EGFP) exhibited a heterologous distribution pattern (Figure 2-1). Cell percentage assay showed that 64% of cells exhibited a whole cell distribution pattern. About 15% of cells showed a nuclear distribution (Figure 2-1B, arrow) and 21% of cells showed a cytosolic distribution (Figure 2-1B, arrowhead). After treatment with 10 μM 4-HNE for 30 min, nearly 90% of cells exhibited a nuclear distribution (Figure 2-1B), indicating robust nuclear translocation of NRF2.

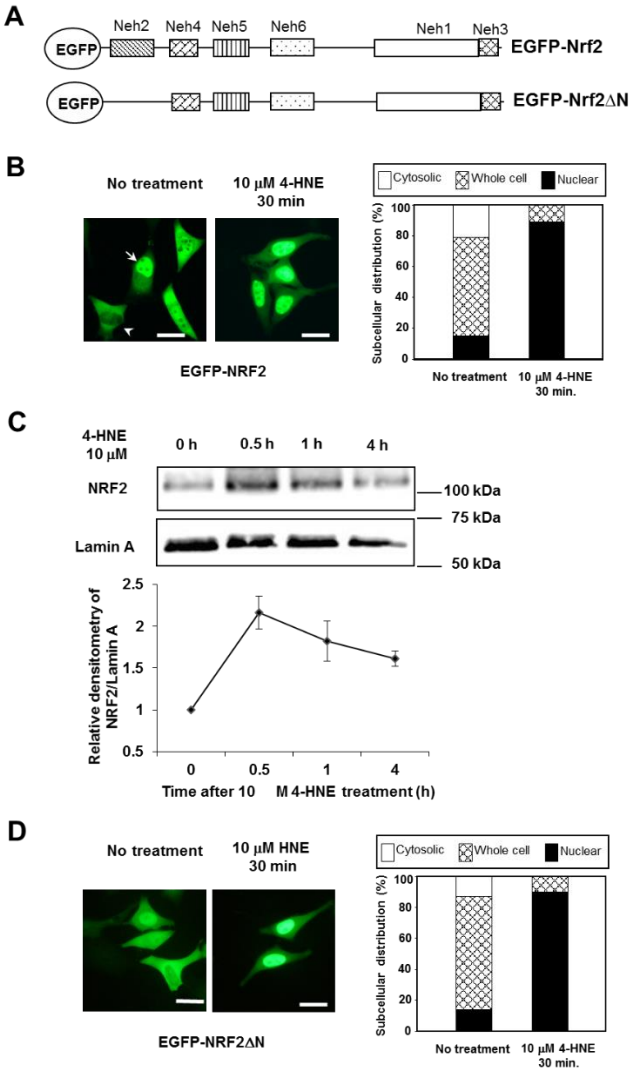

Figure 2-1. 4-HNE induces NRF2 nuclear translocation.

(A) The schematic diagram showing the structures of NRF2 constructs used in the study. (B) Under the untreated condition, EGFP-NRF2 exhibited a mixed pattern of nuclear (arrow), whole cell and cytosolic (arrowhead) distribution. After treatment of 10 μM 4-HNE for 30 min, a predominantly nuclear distribution was observed. Scale bar: 10 μm. (C) Time course of nuclear NRF2 accumulation after 10 μM 4-HNE treatment. ∗: $P < 0.05$. (D) Deletion of the KEAP1-binding domain (NRF2ΔN) did not affect 4-HNE induced nuclear translocation of NRF2.

To further confirm the nuclear translocation effect elicited by 4-HNE, we examined the nuclear NRF2 protein level by Western blotting analyses. HeLa cells

were treated with 10 μM 4-HNE for 0, 0.5,1 and 4 h. 4-HNE markedly elevated the nuclear NRF2 protein level, with the highest accumulation at 0.5 h after treatment (Figure 2-1C). Similar effects have been observed in PC12 cells and vascular endothelial cells [207, 208]. Next, the N-terminal truncation mutant of NRF2 (EGFP-NRF2ΔN, Figure 2-1D) lacking the KEAP1 domain, was expressed in HeLa cells. Under the unstressed condition, EGFP-NRF2ΔN demonstrated a heterologous distribution pattern (Figure 2-1D). Treatment with 10 μM 4-HNE (30 min) converted the distribution of EGFP-NRF2ΔN to a predominant nuclear pattern (Figure 2-1D). Previous study showed that no NRF2ΔN/KEAP1 binding was detected when NRF2ΔN was co-expressed with KEAP1 [209]. Since NRF2ΔN is free from KEAP1 sequestration in the cytosol, the NRF2ΔN distribution can be deemed as free floating in the cell. These results show that 4-HNE can directly affect the subcellular distribution of NRF2 into the nucleus.

2.3.2 *ARE*-luciferase activity increases after 4-HNE treatment

To determine whether the nuclear accumulation of NRF2 could increase the transcriptional activity of *ARE*, we co-expressed 0.5 μg pcDNA3.1-*NRF2* with 0.25 μg *ARE*-luciferase reporter in HeLa cells. Twenty-four hours after transfection, cells were treated with 0, 0.01, 0.1, 1, 10 μM 4-HNE for 30 min and then cultured in fresh medium for 6 h. HNE treatments elicited significant *ARE*-luciferase inductions in a dose-dependent manner (Figure 2-2A).

HepG2-C8 cells with stably expressed p*ARE*-TI-luciferase constructs [205] were treated with 0 and 10 μM 4-HNE for 18 h. *ARE*-luciferase activity was significantly induced with 10 μM 4-HNE treatment compared with the untreated cells (Fig. 2-2 B). Since the conjugation to GSH is the major metabolism pathway for 4-HNE, it will

result in a net loss of intracellular GSH and redox imbalance. We found that when cells were pretreated with 5 mM GSH, the induction of *ARE*-luciferase activity was completely blocked (Fig. 2-2 B).

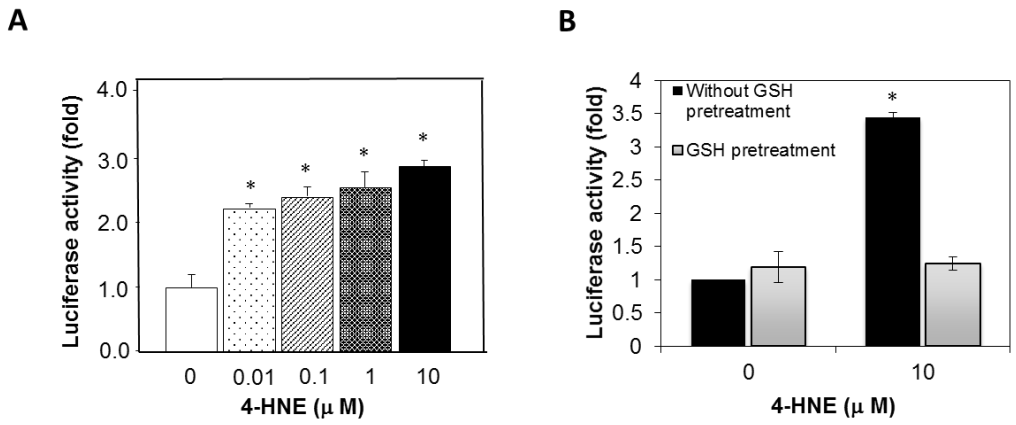

Figure 2-2. 4-HNE significantly increases ARE-luciferase activity.

(A) HeLa cells were transiently transfected with *ARE*-luciferase construct for 24 h and treated with 0.01-10 μM 4-HNE. Cells were harvested and lysed after 6 h, and luciferase activity was measured. (B) HepG2 cells stably expressed with *ARE*-luciferase reporter gene were treated with 10 μM 4-HNE with or without 2 h pretreatment of 5 mM GSH. Cells were harvested and lysed after 18 h, and luciferase activity was measured. Relative fold of induction was obtained as compared to the untreated cells. ∗: $P < 0.05$.

2.3.3 NRF2 is critical in regulating the expression of detoxifying genes

When HeLa cells were treated with 4-HNE, in agreement with the enhanced *ARE*-luciferase activity, RT-PCR results showed that 4-HNE induced the transcription of *AKR1C1*, *GSTA4* and *HO-1* in a dose-dependent manner (Figure 2-3A). To examine whether the induction of these detoxifying and antioxidant genes was dependent on NRF2, HeLa cells were transfected with *NRF2* specific siRNA or nonspecific siRNA as a control. *NRF2* expression was down-regulated by the siRNA transfection (Figure 2-3B). In the cells transfected with control siRNA, the expression of *AKR1C1*, *GSTA4* and *HO-1* was markedly induced by 10 μM 4-HNE, while in the cells transfected with *NRF2* siRNA, the induction of these genes was attenuated (Figure 2-3B).

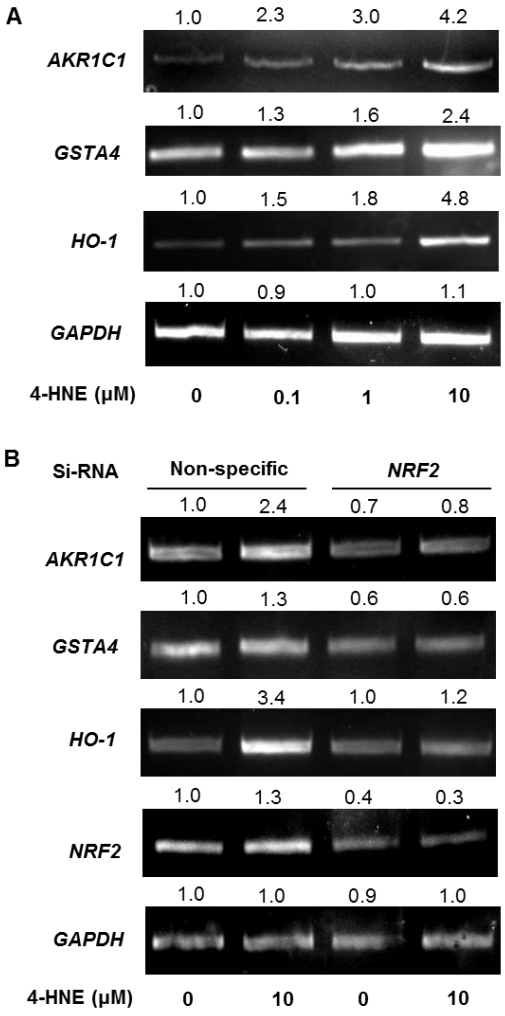

Figure 2-3. Effects of NRF2 on the mRNA expression of phase 2 metabolizing and antioxidant enzymes.

(A) HeLa cells were treated with 0, 0.1, 1 and 10 μM of 4-HNE for 6 h. mRNA expression of *AKR1C1*, *GSTA4* and *HO-1* was induced by 4-HNE in a dose-dependent manner. (B) HeLa cells were transfected with *NRF2* specific or non-specific siRNA for 24 h, followed by 4-HNE treatment for 6 h. Knocking-down of NRF2 attenuated the induction of *AKR1C1*, *GSTA4* and *HO*-1by 4-HNE. Densitometry analyses of the PCR products were performed by Image J program, and the numbers at the top of each band are relative density compared to the control.

2.4 Discussion

It is well recognized that our body has a comprehensive antioxidant system to counter oxidative stress. 4-HNE, an oxidative stressor, causes adaptive induction of detoxifying enzymes such as AKR1C1 and GSTA4 in different cell lines [210, 211], although the molecular pathway is not fully understood. The common feature of these detoxifying genes is that they have *ARE*-like sequences in their 5'-flanking regions [212, 213]. In this study, we demonstrate that NRF2 mediates 4-HNE induced gene expression of key antioxidant and detoxifying enzymes, resulting in enhanced 4-HNE metabolism.

4-HNE is a highly reactive electrophile, and several studies have reported that it is a potent NRF2 inducer [207, 208]. Our current results further confirmed that the nuclear translocation of NRF2 is significantly increased by 10 μM 4-HNE treatment in HeLa cells (*Figure 2-1*). There are several mechanisms proposed for the 4-HNE-induced NRF2 activation. 4-HNE can react with cysteine sites in the KEAP1 protein and that may disrupt the KEAP1-dependent degradation of NRF2 [214]. In addition, 4-HNE may activate NRF2 through activation of upstream kinases such as protein kinase C, extracellular signal-regulated protein kinase and phosphoinositide 3-kinase [34, 207, 215]. In this study, we showed that 4-HNE could induce nuclear translocation of the NRF2 mutant lacking the KEAP1 binding domain, indicating that 4-HNE may have a direct effect on NRF2 itself. We found that 4-HNE could modify NRF2 protein in an *in vitro* testing system (Figure 2-4), and future studies will be needed to identify the specific amino acid sites modified by 4-HNE and their impacts in NRF2 signaling. In addition, several studies have reported that 4-HNE treatment leads to dramatic decrease of intracellular GSH[216, 217], and depletion of GSH can activate NRF2 signaling [218]. In the present study, we showed that pretreatment of

GSH could block the induction of ARE transcriptional activity by 4-HNE, suggesting that 4-HNE may activate NRF2 via depletion of GSH.

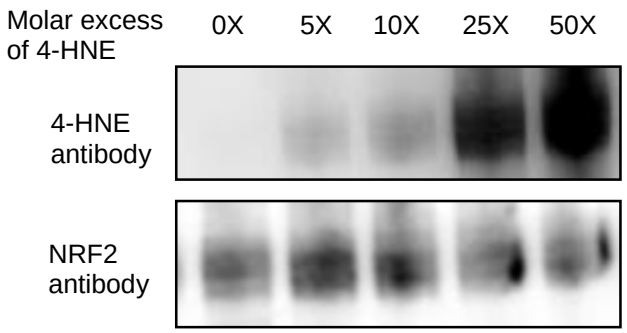

Figure 2-4. Nrf2 protein is modified by 4-HNE.

NRF2 protein is modified by 4-HNE. Purified 6×His-NRF2 protein (10 μg, 0.146 nmol) was incubated with different molar excess of 4-HNE in 30 μL phosphate buffer (50mM, pH=7.4) for 30 min. Reaction was terminated by adding 10 μL of Laemmli's SDS buffer and samples were boiled at 95^{o}C. 20 μL of each sample was subject to Western blotting analyses. Primary anti-4-HNE antibody (Alpha Diagnostic) was used to detect 4-HNE modifications. Then, the primary antibody was stripped off and anti-NRF2 antibody was used to detect NRF2 protein as a loading control.

GSTA4 and AKR1C1 are two important enzymes for detoxification of 4-HNE. In the large GST family, GSTA4 is the most active isoform in catalyzing conjugation of GSH to 4-HNE [197]. The higher expression level of GSTA4 in DU145 prostate cancer cells is associated with faster 4-HNE metabolism rate, compared to PC3 or LNCaP prostate cancer cells [219]. It is also reported that overexpression of GSTA4 protects HepG2 cells from 4-HNE mediated oxidative injuries [220]. AKR1C1 has high catalytic activity in reducing 4-HNE to less toxic 1,4-dihydroxynonenol [211]. The role of HO-1 in the detoxification of 4-HNE is not clear. The induction of HO-1 may enhance the overall cellular antioxidant capacity and prevent oxidative stress induced cytotoxicity [208]. Therefore, the induction of gene expression of these cellular protective enzymes by 4-HNE appears to be an adaptive response to enhance elimination of 4-HNE and reduce its toxicity. The transcriptional induction of these detoxifying and antioxidant genes is attenuated when *NRF2* is knocked down (*Figure 2-3*), indicating that the induction is mediated by NRF2.

2.5 Conclusions

In this study, we demonstrate that NRF2 regulates the enhanced gene expression of antioxidant and detoxifying enzymes by 4-HNE. Our study highlights the importance of the NRF2-*ARE* signaling mechanism in the detoxification of reactive lipid metabolites such as 4-HNE.

3 Chapter 3. Curcumin as DNA hypomethylation agent in restoring the expression of Nrf2 via promoter CpGs demethylation

3.1 Introduction

Unlike genetic alterations, changes in gene expression due to epigenetic regulation can be potentially reversed by chemicals. Gene silencing by promoter hypermethylation has been implicated in the development of many human malignancies including prostate cancer (PCa)[221]. There is increasing evidence that in human PCa, epigenetic alterations occur earlier than genetic defects [222]. Therefore, drugs that target enzymes responsible for DNA methylation and/or histone modification leading to reactivation of epigenetically silenced genes can be useful in cancer prevention and treatment. The histone deacetylases (HDACs) and DNA methyltransferases (DNMTs) inhibitors have been approved for use in hematological malignancies and are currently in different phases of clinical trials (reviewed in [223, 224]). However, adverse side effects have hindered the development of these compounds as a cancer chemopreventive/therapeutic agent.

---

[1] Part of this chapter has been published as a research paper: Khor T., **Huang Y.,** Wu T., Shu L., Lee J., Kong T. *Biochemical Pharmacology.* 2011; 82(9):1073-8.

[2] As the second author, Ying Huang was involved in conducting experiments, data analysis, and preparation of part of the manuscript.

[3] **Key Words**: Curcumin, DNA hypomethylation, Nrf2, Prostate cancer, TRAMP C1, Epigenetics

[4] **Abbreviations:** PCa, prostate cancer; Nrf2, nuclear factor erythroid-2 (NF-E2) related factor-2; CUR, curcumin; BGS, bisulfite genomic sequencing; MeDIP, Methylation DNA immunoprecipitation; anti-mecyt, anti-methycytosine; HDAC, histone deacetylases; DNMTs, DNA methyltransferases; GST, glutathione-S-transferases; NQO1, NAD(P)H:quinone oxidoreductase-1; HO-1, heme oxygenase-1.

Despite its poor bioavailability, curcumin (CUR) was found to be a very powerful cancer chemopreventive agent using animal models of different cancers (reviewed in [225]). In our laboratory, we have demonstrated that CUR is effective against the growth and progression of prostate tumor in immunodeficient and TRAMP mice [73, 226]. In humans, CUR has shown promising results in a phase II trial involving patients with advanced pancreatic cancer [227]. It has been suggested that the pharmacological effect of CUR is achieved through the accumulation of hydrophobic CUR and its metabolites in tissue as a result of long term oral exposure. Accumulating evidence indicates that CUR may exert its chemopreventive/therapeutic effect through epigenetic modification, which is achievable at lower concentrations [228]. Although the underlying mechanisms remain unclear, CUR has been shown to possess inhibitory effects on HDACs, HATs and more recently DNMT activity through different approaches and systems [229-234] .

Epidemiological and experimental evidence have linked oxidative stress and chronic inflammation with neoplastic transformation and carcinogenesis ([235-237]). Previous studies from our as well as other laboratories have demonstrated that nuclear factor erythroid-2 (NF-E2) related factor-2 (Nrf2 or NFE2L2) plays critical roles in defense against oxidative stress [8, 238-245]. Through the antioxidant or the electrophile response element (ARE/EpRE; GTGACNNNGC), Nrf2 regulates the induction of anti-oxidative stress proteins such as phase II detoxification enzymes glutathione-S-transferases (GST), NAD(P)H:quinone oxidoreductase-1 (NQO1), and antioxidant proteins heme oxygenase-1 (HO-1), and glutathione peroxidases (Gpx) [246-248]. Nrf2 deficiency has been shown to be closely correlated with increased susceptibility to carcinogen induced tumorigenesis in mice [73, 249] [12, 250]. We have reported that Nrf2 and its target gene HO-1 were attenuated in the skin tumors of mice induced by

DMBA-TPA [73]. We also found that the development of prostate tumors in TRAMP mice was associated with gradual down-regulation of Nrf2 as well as its downstream target genes such as NQO-1, UGT1A1 and GSTM1 [75]. Likewise, Frolich et al. found that the expression of Nrf2 and GST mu genes was significantly decreased in TRAMP prostate tumor [251]. Most recently we reported that as PCa progresses in TRAMP mice, there was a progressive loss of expression of Nrf2 and its downstream target genes such as NQO-1, UGT, GST and HO-1 2 [75, 226]. Treatments with γ-rich tocopherols [75] inhibited TRAMP mice prostate carcinogenesis with concomitant restoration of Nrf2 and its target genes such as UGT, GST, Gpx and HO-1. The aim of our current study is to investigate the potential of CUR to restore the expression of Nrf2 through DNA demethylation.

3.2 Materials and Methods

3.2.1 Reagents and Cell Culture

The CUR used in this study (cat# C1386) contains approximately 70% of CUR as determined using HPLC method by Sigma-Aldrich (St. Louis, MO, USA) (the remaining 30% comprises demethoxycurcumin and bidemethoxycurcumin). TRAMP C1 cells (generously provided by Dr. Barbara Foster, Department of Pharmacology and Therapeutics, Roswell Park Cancer Institute, Buffalo, NY) were maintained in DMEM supplemented with 10% heat-inactivated fetal bovine serum at 37℃ in a humidified 5% CO_2 atmosphere as described previously [52]. Cells were seeded in 10 cm plates for 24 hours (hr), and then treated with either 0.1% DMSO (control), azadeoxycytidine (5-Aza) (Sigma-Aldrich, St. Louis, MO, USA) and Trichostatin A (TSA) (Sigma-Aldrich, St. Louis, MO, USA) or different concentrations of CUR in 1% FBS containing medium. The medium was changed every two days. For the 5-aza and TSA combination treatment, 500 nM TSA was added to the 5-Aza containing medium on

day 4 and then incubated for another 20 hr. Cells were harvested for protein, DNA or total RNA analyses on day 5.

3.2.2 Bisulfite Genomic Sequencing (BGS)

Genomic DNA was isolated from CUR treated or control TRAMP-C1 cells using the DNeasy tissue kit (Qiagen, Valencia, CA). The bisulfite conversion was carried out with 750 ng of genomic DNA using EZ DNA Methylation Gold Kits following the manufacturer's instructions (Zymo Research Corp., Orange, CA). The converted DNA was amplified by PCR using Platinum PCR SuperMix (Invitrogen, Grand Island, NY) with the primers that amplify the first 5 CpGs located between -1086 to -1226 of the murine Nrf2 gene, with the translation initiation site (TIS) defined as position 1 [52]. The PCR products were purified by gel extraction using the Qiaquick™ gel extraction kit (Qiagen, Valencia, CA), then cloned into pCR4 TOPO vector using a TOPO™ TA Cloning kit (Invitrogen, Grand Island, NY). Plasmids DNA from at least 10 colonies per treatment groups from 3 independent experiments were prepared using QIAprep Spin Miniprep Kit (Qiagen, Valencia, CA) and sequenced (DNA Core Facility, Rutgers/UMDNJ, Piscataway, NJ), as we have previously reported [52].

3.2.3 Methylation DNA Immunoprecipitation (MeDIP) Analysis

The MeDIP analysis was performed as previously described with some modifications [252, 253]. Briefly, 8 μg DNA extracted from control and CUR treated cells was adjusted to 150 μl using TE buffer, followed by sonication on ice using a Bioruptor sonicator (Diagenode Inc., Sparta, NJ) to shear the DNA to an average size of 300 -500 base pairs (bp). One-tenth of the fragmented DNAs was kept as inputs and the remaining DNA was denaturated at 95^{o}C for 10 min, and followed by immunoprecipitation (IP) in 1x IP buffer (10 mM sodium phosphate pH 7.0, 140 mM NaCl, 0.25% Triton X-100) using anti-methylcytosine antibody (anti-mecyt; Anaspec,

Fremont, CA) or negative control antibody (anti-cMyc, Santa Cruz, Santa Cruz, CA) for 2 hr at 4°C, respectively. After the incubation, 30 µl magnetic beads (Cell signaling, Boston, MA) were added, and rotated at 4 ℃ for another 2 hr, the pulled-down DNA beads complex were washed four times using ice cold IP buffer and digested with proteinase K at 50 ºC overnight, and followed by DNA purification using miniprep kit from Qiagen (Valencia, CA). One µl of each of the purified enriched or input DNA was used as template for 30 cycles of PCR amplification using primer set covering the DNA sequence from position −1190 to −1092 of the murine Nrf2 gene in which the first 5 CpGs are located as previously described [52]. The PCR products were then analyzed by agarose gel electrophoresis and visualized using ethidium bromide (EB) staining.

3.2.4 RNA Isolation and Reverse Transcription-PCR

Total RNA was extracted from the treated cells using the Trizol (Invitrogen, Carlsbad, CA). mRNA expression levels of Nrf2 and NQO1 were determined by quantitative real time-polymerase chain reaction (PCR) (ABI7900HT) using delta delta Ct method. First-strand cDNA was synthesized from 1 µg of total RNA using SuperScript III First-Strand Synthesis System for the subsequent Reverse transcription (RT)-PCR (Invitrogen, Grand Island, NY) according to the manufacturer's instructions. The cDNA was used as the template for PCR reactions performed using Power SYBR Green PCR Master Mix (Applied Biosystem, Carlsbads, CA). The PCR primers to specific genes to be amplified have been reported in our previous publication [52].

3.2.5 Preparation of protein lyses and Western Blotting

The treated cells were harvested using radioimmunoprecipitation assay (RIPA) buffer supplemented with protein inhibitor cocktail (Sigma, St Louis, MO). The protein concentrations of the cleared lysates were determined using the bicinchoninic acid (BCA) method (Pierce, Rockford, IL), and 20 µg of the total protein were resolved by

4%–15% SDS-polyacrylamide gel electrophoresis (Bio-rad, Hercules, CA). After electrophoresis, the proteins were electro-transferred to polyvinylidene difluoride (PVDF) membrane (Millipore, Bedford, MA). The PVDF membrane was blocked with 5% BSA in phosphate-buffered saline-0.1% Tween 20 (PBST), and then sequentially incubated with specific primary antibodies and HRP-conjugated secondary antibodies. The blots were visualized by SuperSignal enhanced chemiluminiscence (ECL) detection system and documented using a Gel Documentation 2000 system (Bio-Rad, Hercules, CA). The antibodies, anti-Nrf2, actin and NQO-1 were purchased from Santa Cruz biotechnology (Santa Cruz, CA).

3.2.6 In vitro methylation assay

The in vitro methylation assay was performed as previously described with slight modifications [254]. The substrate DNA for the *in vitro* methylation assay was a 850-bp fragment; −444/+401 relative to the initiation codon from the promoter region of the human $p16^{Ink4a}$ gene. The methylation reaction contained 350 to 400 ng of the substrate DNA and 4 units of *M.SssI* methylase (0.5 μmol/L, New England Biolabs, Frankfurt, Germany) in a final volume of 50 μL. Inhibitors were added to final concentrations of 5, 50, and 100 μM. Reactions were performed at 37°C for 1 hr followed by 1 hr digestion at 60 ℃ with 30 units of *Bst*UI (New England Biolabs) and analyzed on 2% agarose gels.

3.3 Results

3.3.1 Hypermethylation of specific CpG sites in the CpG island of Nrf2 gene in TRAMP C1 cells was reversed by CUR treatment

We have previously reported that the first 5 CpGs in the CpG island of Nrf2 gene are hypermethylated in TRAMP prostate tumors and in the tumorigenic TRAMP C1 cells but not in normal prostate tissues and non-tumorigenic TRAMP C3 cells [52]. We

also found that the promoter activity of Nrf2 was significantly suppressed when these 5 CpGs were hypermethylated [52]. To test if CUR treatment can reverse the methylation status of these 5 CpGs on Nrf2 promoter, bisulfite sequencing was performed. In agreement with our previous report, these 5 CpGs was hypermethylated in TRAMP C1 cells (Figure 3-1, untreated control, 92% methylation). However, when the cells were treated with either 5 or 10 μM of CUR or a combination of 2.5 μM 5-Aza and 500 nM of TSA for 5 days, methylation of these 5 CpGs was significantly reduced (Figure 3-1, 27, 57.6 and 30% methylation, respectively).

MeDIP analysis has been previously shown to be able to enrich methylated DNA in an unbiased manner [252]. Enrichment of methylated DNA fragments can be achieved via immunoprecipitation of DNA obtained from treated and untreated cells with the anti-mecyt antibody that binds specifically to methylated cytosine. The enriched DNA was then purified and used as template to amplify the Nrf2 promoter region that contains the first 5 CpGs. In agreement with the bisulfite sequencing results, MeDIP analysis revealed that CUR significantly reduced the anti-mecyt antibody binding to the first 5 CpGs of Nrf2 promoter (Figure 3-2).

3.3.2 Expression of Nrf2 and its downstream target gene, NQO-1 was induced by CUR

To examine if demethylation of Nrf2 promoter is associated with transcriptional activation of the gene, the mRNA and protein expression levels of Nrf2 were determined. TRAMP C1 cells were treated with 2.5 μM of CUR for 5 days. Using Western Blotting and real-time PCR, we found that the expression of Nrf2 was increased in TRAMP C1 cells upon CUR treatment (Figure 3-3). 2.5 μM instead of 5 μM of CUR was selected for this experiment since the results from the bisulfite

sequencing showed that 2.5 μM of CUR have a better demethylation effect than 5 μM of CUR.

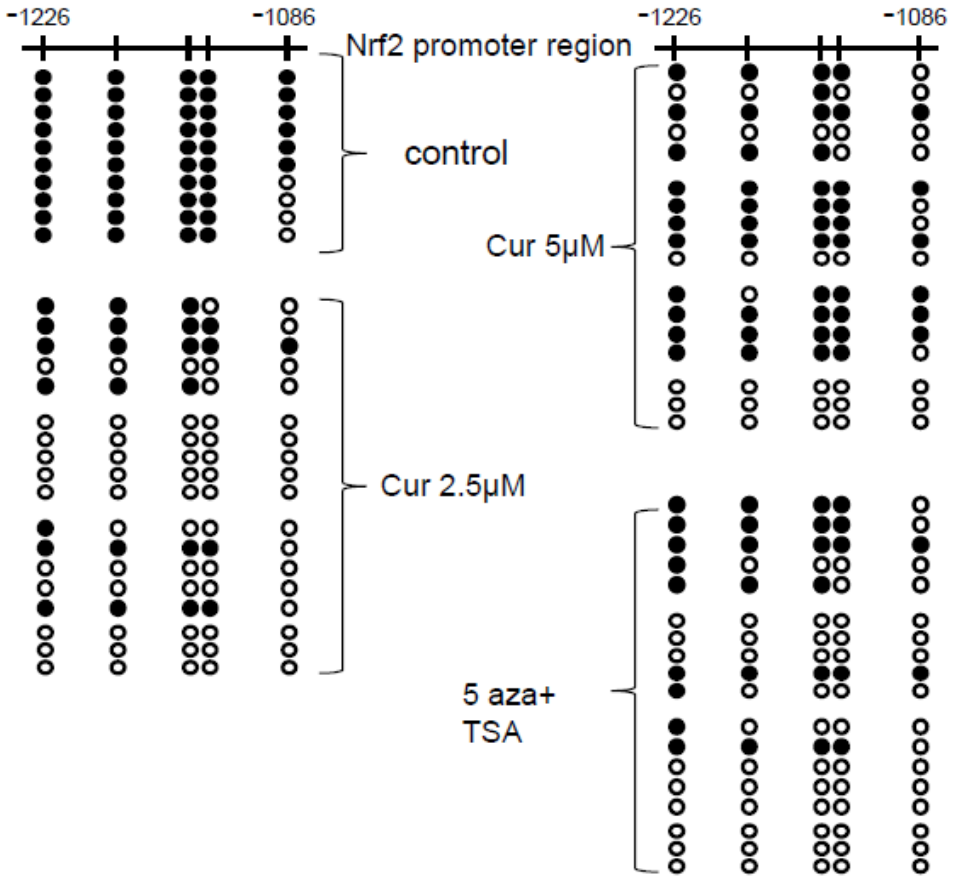

Figure 3-1. The methylation patterns and extents of the first 5 CpGs in the promoter of Nrf2 gene.

Black dots indicate methylated CpGs and open circles indicate non-methylated CpGs. The methylation status was determined using bisulfite genomic sequencing (BGS) as described in Material & Methods. 92% of the control TRAMP C1 cells were found to be methylated. Treatment with 2.5 μM, 5 μM or combination of 5-aza/TSA (2.5 and 0.5 μM, respectively) significantly reduces the methylation level to 27, 57.6 and 30%, respectively (Fisher exact test $P< 0.0001$). At least three clones from three independent experiments were selected for BGS.

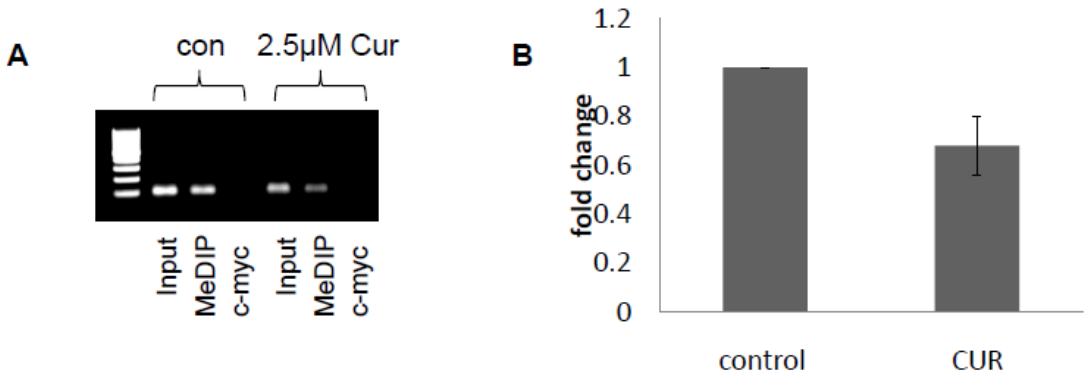

Figure 3-2. Methylation DNA immunoprecipitation analysis.

8 μg genomic DNA extracted from control or CUR treated TRAMP C1 cells were sonicated, denatured and subjected to DNA immuniprecipitation (IP) with anti methyl cytosine antibody. A: Semi-quantative PCR was performed to compare the immunoprecipitated DNA with their inputs and negative control (c-myc as non specific binding control). Primers covering the first 5 CpGs in Nrf2 promoter region were used; B: The bands (MeDIP) were visualized using a Gel Documentation 2000 system (Bio-Rad, Hercules, CA) and quantified using Quantity One software. Bars represent mean fold change +/- SDEV from 3 independent experiments (normalized with inputs and compared to control value).

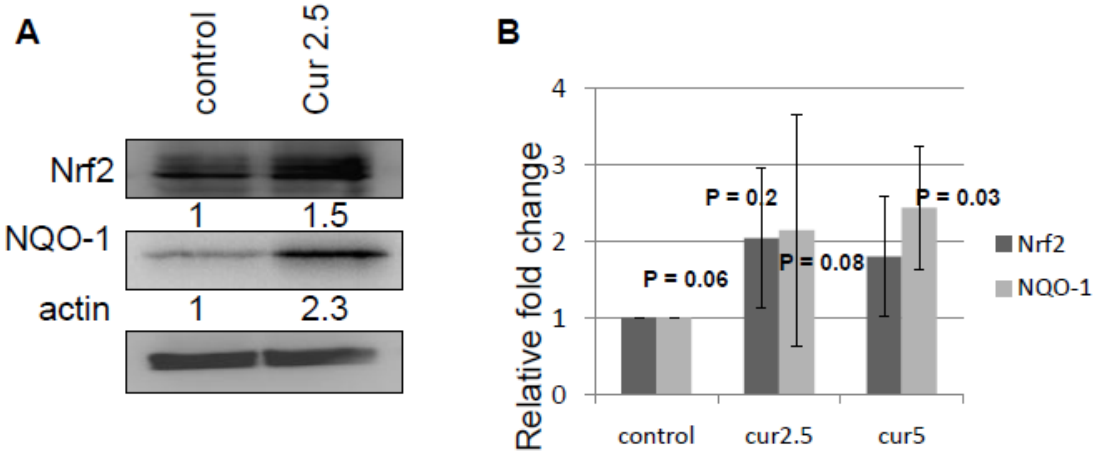

Figure 3-3. The mRNA and protein expression level of Nrf2 and NQO1.

A) mRNA and B) protein expression level of Nrf2 and its target gene NQO-1. The bands were visualized using a Gel Documentation 2000 system (Bio-Rad, Hercules, CA) and quantified using Quantity One software.

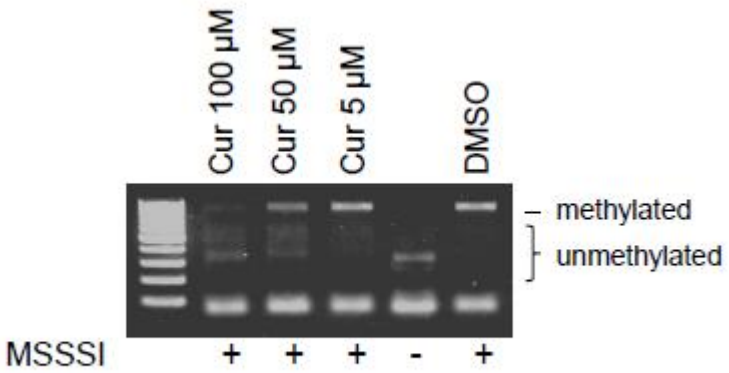

Figure 3-4. In vitro methylation assay.

CUR inhibits *M.SssI* DNA methyltransferase activity in a dose dependent manner as demonstrated by the increase of unmethylated fragment (unprotected, smaller fragments) and decrease of methylated (protected larger).

3.3.3 CUR inhibits the activity of recombinant CpG methylase *M.SssI*

DNA methylation, which involves the addition of a methyl group at the carbon-5 position of cytosine residues in the DNA, is mediated by a family of enzymes known as DNA methyltransferases (DNMTs) [255]. There are three major DNMTs identified in human including the two *de novo* methyltransferases (DNMT3a and DNMT3b) and the maintenance methyltransferase (DNMT1). To examine if the demethylation effect of CUR could be mediated through transcriptional activation of DNMTs, real-time PCR as well as Western Blotting were performed using total RNA and protein extracted from CUR treated and control TRAMP C1 cells. We found that CUR treatment has no effect on either the mRNA or protein expression level of DNMT1, 3A and 3B (data not shown). To examine if CUR can inhibit the activity of DNA methyltransferase, a cell-free *in vitro* DNA methylation assay was performed. The purified recombinant CpG methylase *M.SssI*, an enzyme shown to possess strong activity and significant structural similarities with the DNMT1 catalytic domain, was used in this assay. As described in Materials and Methods, a 850-bp PCR fragment from the promoter region of the human p16Ink4a gene was used as a substrate for the DNA methyltransferase which was subsequently digested by the methylation-sensitive restriction enzyme BstUI. Our result shows that CUR inhibited DNA methyltransferase activity in a dose-dependent manner as demonstrated by the increase of unmethylated fragment (unprotected, smaller fragments) and decrease of methylated (protected larger) (Figure 3-4).

3.4 Discussion

Accumulating evidence suggests that some dietary chemopreventive phytochemicals may prevent cancer by modifying epigenetic processes in the cells [192, 256, 257]. Selenium, a potent cancer chemopreventive agent has been reported to be able to induce global DNA hypomethylation and re-activate epigenetically silenced

tumor suppressor genes through inhibition of DNMT activity [258]. Isothiocyanates (ITCs), such as sulforaphane and PEITC from cruciferase vegetables and allyl compounds from garlic, have all been reported as potent HDAC and/or DNMT inhibitors [259-261]. In addition, polyphenols such as (–)-epigallocatechin 3-gallate (EGCG) from green tea and genistein from soybean have also been shown to inhibit DNMTs *in vitro* [192]. Recently, the potential of CUR as an epigenetic modifier has been delineated based on its inhibitory effect on HDACs, HATs and DNMTs [262]. Molecular docking studies showed that the human HDAC8 inhibitory effect of CUR is comparable to Trichostatin A and vorinostat but stronger than valproic acid and sodium butyrate [229]. Likewise, Liu et al. reported that CUR suppressed the expression of HDAC1, 3, and 8 protein levels in a dose-dependent manner associated with increased acetylated histone H4 level [263]. CUR has also been identified as a specific inhibitor of p300/CBP HAT activity [233, 264, 265]. Using a molecular docking approach, CUR has been shown to exert its DNA methyltransferase I inhibitory effect through covalent binding to the catalytic thiolate of C1226 of DNA methyltransferase I [266]. Subsequent validation experiments demonstrated that CUR has an IC50 of 30 nM in inhibiting *M.Sss1*activity. A recent report from Jha et al. showed that CUR can reverse the hypermethylation leading to activation of the RARβ2 gene in cervical cancer cell lines [267]. However, Liu et al. found that demethoxycurcumin and bisdemethoxycurcumin but not CUR demethylate the WIF-1 promoter region in A549 cells [268]. Given all the promising data indicating the possible epigenetic effects of CUR, hence we proceeded to test the hypothesis whether CUR treatment could reactivate the expression of Nrf2 gene in TRAMP C1 cells through promoter DNA demethylation. Nrf2 was selected as a target because: 1) we as well as others have previously shown that Nrf2 was epigenetically silenced during the development of

prostate cancer in TRAMP mice [52]; 2) the first 5 CpGs of Nrf2 promoter region were found to be hypermethylated in prostate tumors from TRAMP mice and TRAMP C1 cells; and 3) the cancer chemopreventive effect of some of the dietary compounds was associated with concomitant restoration of Nrf2 and its target genes such as UGT, GST, Gpx and HO-1 [75].

As one of the most precise methods to identify promoter methylation, bisulfite sequencing was used to dissect the effect of CUR on the methylation status of 5 CpGs of the Nrf2 promoter region. This observation is further supported by the MeDIP analysis that CUR significantly reduces the anti-mecyt antibody binding to the first 5 CpGs of the Nrf2 promoter. Our results show that CUR, at its sub-toxic doses (2.5 and 5 μM) was as effective as 5-AZA/TSA combination in demethylating the first 5 CpGs of the Nrf2 promoter region. Furthermore, the demethylation of these CpGs was associated with increased expression of Nrf2 and its downstream target gene, NQO-1. To investigate the underlying mechanisms by which CUR exerts its DNA demethylation effect, we examined the effect of CUR on the expression of DNMT1, DNMT3a and 3b. However, CUR was found to be possess minimal, if any, effect on the expression of DNMTs both at mRNA and protein levels (data not shown). On the other hand, in agreement with previous finding [266], CUR significantly inhibited the enzymatic activity of CpG methylase *M.SssI* in a dose dependent manner (Figure 3-4).

CUR is a multi-targeting agent as evidenced by its ability to interact with at least 33 different proteins covering different signaling pathways [269, 270]. CUR is known as a strong activator of Nrf2-mediated transcription of the ARE-luciferase reporter gene as well as an inducer of endogenous Nrf2 protein. For the first time, we showed that CUR can modulate the expression of Nrf2 through epigenetic pathways. Our findings also shed some light on the possible mechanisms by which CUR exert its cancer

chemopreventive effect in TRAMP mice [226]. We have previously reported that Nrf2 and its downstream target genes are gradually down-regulated during the prostate tumorigenesis in TRAMP mice [75] . Therefore, the ability of CUR to epigenetically restore the expression of these genes could play an important role in preventing the progression and development of prostate cancer in TRAMP mice.

3.5 Conclusions

Based on these data, we draw a possible conclusion that CUR is a potent hypomethylation agent that restores the epigenetically silenced Nrf2 gene, as well as potentially other genes, in TRAMP C1 cells through DNA demethylation. Our findings would provide important information for the future clinical development of CUR as well as other cancer chemopreventive phytochemicals as a cancer epigenetic modifying chemopreventive and therapeutic agents.

4 Chapter 4. A γ-tocopherol-rich mixture of tocopherols maintains *Nrf2* expression in prostate tumors of TRAMP mice via epigenetic inhibition of CpG methylation[1, 2]

4.1 Introduction

Nrf2 is a transcription factor that plays pivotal role in maintaining cellular redox homeostasis and elimination of carcinogens and reactive intermediates [204, 271]. Accumulating evidences have demonstrated that *Nrf2*-decient mice are more susceptible to carcinogenic, inflammatory and oxidative insults [185, 272]. Furthermore, it has been found that Nrf2 and its downstream target GST are suppressed in human and TRAMP prostate cancer, associated with excessive ROS [251]. Higher ROS level could cause genetic and epigenetic instability and transduce a variety of signals for tumor cell survival, proliferation and invasion [251, 273]. Although the direct relationship between the loss of *Nrf2* and prostate carcinogenesis is yet to be established, maintaining *Nrf2* expression appears to be critical in retaining cellular adaptability to environmental and endogenous stresses and to delay or prevent the development of prostate cancer.

---

[1] Part of this chapter has been published as a research paper: **Huang Y.**, Khor T., Shu L., Saw C., Wu T., Suh N., Yang C., Kong T. *The Journal of Nutrition.* 2012; 142(5):818-823.

[2] **Key Words**: tocopherol, TRAMP, *Nrf2*, DNA methylation, DNA methyltransferases

[3] **Abbreviations:** 5-aza, 5-aza-2'-deoxycytidine; DNMT, DNA methyltransferase; GST, glutathione-S-transferase; γ-TmT, **γ**-tocopherol-rich mixture of tocopherols; HDAC, histone deacetylase; GAPDH, glyceraldehyde 3-phosphate dehydrogenase; Nrf2, nuclear factor-erythroid 2-related factor 2; NQO1, NAD(P)H:quinone oxidoreductase 1; ROS, reactive oxygen species; TRAMP, the transgenic adenocarcinoma of the mouse prostate; TSA, trichostatin A.

The suppression of *Nrf2* in prostate tumors of TRAMP mice and TRAMP-C1 cells is found to be caused by CpG hypermethylation in the promoter, especially at the first 5 CpG [52]. These CpG are hypermethylated in tumorigenic TRAMP-C1 cells, but not in non-tumorigenic TRAMP-C3 cells [274]. Treatment with DNMT inhibitor 5-aza and HDAC inhibitor TSA could restore *Nrf2* expression in TRAMP-C1 cells [52]. However, it may not be feasible to use 5-aza as a cancer chemopreventive agent chronically due to its toxicity, and therefore great effort has been made in looking for effective epigenetic interventions through the use of relatively non-toxic natural compounds [275].

Vitamin E refers to a group of lipid-soluble compounds consisting of eight structurally related tocopherols (α-, β-, γ-, δ-) and tocotrienols (α-, β-, γ-, δ-). They are well-known natural antioxidants and are abundant in a variety of food including vegetable oils, nuts and whole grains [276]. Epidemiological studies revealed that higher serum γ-tocopherol level is associated with a reduced risk of prostate cancer [277], but large-scale clinical trials with α-tocopherol supplementation demonstrated inconsistent efficacy against prostate cancer [278, 279]. γ-TmT is a by-product during the refining of soybean oil and typically contains 57% γ-tocopherol, 24% δ-tocopherol, 13% α-tocopherol, and 1.5% β-tocopherol. γ-TmT has been shown to inhibit carcinogenesis in different types of cancer including prostate, colon, lung, and mammary [280-283].

We have reported that dietary feeding of 0.1% γ-TmT could inhibit prostate tumorigenesis in TRAMP mice along with higher *Nrf2* expression, but potential mechanisms remain unknown [283]. Hence, the present study was undertaken to investigate whether γ-TmT would maintain *Nrf2* expression by inhibiting CpG methylation in TRAMP mice and in TRAMP-C1 cells.

4.2 Methods and materials

4.2.1 Animals

Female heterozygous C57BL/TGN TRAMP mice, line PB Tag 8247NG, and male C57BL/6 mice were purchased from Jackson Laboratory (Bar Harbor, ME). TRAMP females were crossed with C57BL/6 males, and the first or second generations of transgenic males were chosen for the study. The genotype of the offspring was determined by a PCR-based method [284]. Mice were housed in cages with wood chip bedding in a temperature-controlled room (20 ^{o}C-22 ^{o}C) with a 12-h light-dark cycle, with a relative humidity of 45–55% in Rutgers Animal Care Facility. The study was carried out under IACUC-approved protocol at Rutgers University.

4.2.2 Animal study design

To test whether higher *Nrf2* expression in TRAMP prostates after γ-TmT treatment was associated with decreased promoter methylation, we repeated treatment of 0.1% γ-TmT diet in 8-wk-old TRAMP mice for 16 wk, as we have performed previously [283]. Eight-week old male TRAMP mice were randomized into treatment group (n = 7) and control group (n = 6). Mice in the treatment group were fed 0.1% mixed tocopherols in an AIN-93M diet [285]. γ-TmT was purchased from Cognis Corporation (Cincinnati, OH) and it contains 130.0 mg of α-tocopherol, 15.0 mg of β-tocopherol, 243.0 mg of δ-tocopherol, and 568.0 mg of γ-tocopherol per gram. At wk 24, mice were killed by CO_2 asphyxiation, and the genitourinary apparatus including the prostate, the seminal vesicles, and the bladder were collected, snap-frozen in liquid nitrogen, and stored in -80^{o}C for further analysis.

Archived prostate tissues of TRAMP mice at age of 12 wk (n = 4), 18 wk (n = 3) and 24 wk (n = 5) and non-transgenic C57BL/6 mice at age of 12 wk (n = 2) and 24 wk (n = 2) were used for DNA extraction to determine the methylation status of the *Nrf2*

promoter at different ages. These tissues were from our unpublished study, and they were kept in -80^{o}C for less than one year before DNA collection. Mice were fed Purina Mouse Chow 5015.

4.2.3 Cell culture and treatment

TRAMP-C1 cells were cultured in DMEM containing 10% FBS and antibiotics. Cells were grown at 37^{o}C in a humidified 5% CO_2 atmosphere. γ-TmT was dissolved in DMSO to make a stock solution containing 100 mmol/L total tocopherols, consisting of 13.0 mmol/L of α-tocopherol, 1.5 mmol/L of β-tocopherol, 25.0 mmol/L of δ-tocopherol, and 60.5 mmol/L of γ-tocopherol. TRAMP-C1 cells were treated with 30 μmol/L of γ-TmT in DMEM containing 1% FBS for 5 d and harvested.

4.2.4 Bisulfite sequencing

Genomic DNA was isolated from TRAMP prostate tissues and TRAMP-C1 cells, using QIAamp mini kit (Qiagen, Valencia, CA). DNA (800 ng) was bisulfite converted using EZ DNA Methylation-Gold kit (Zymo Research, Orange, CA). TA cloning was performed as described previously [52]. For each sample, 5 to 10 clones were chosen for sequencing. Plasmid DNA was sequenced using T7 primer (Genewiz, South Plainfield, NJ) at the Rutgers Sequencing Core facility. The methylation percentage was calculated as the number of methylated CpG over the total number of CpG examined.

4.2.5 Western blot analyses

DNMT are key enzymes catalyzing the addition of the methyl group to cytosine and play critical role in establishing DNA methylation patterns [286]. To investigate whether inhibition of methylation in the *Nrf2* promoter was related with down-regulation of any of DNMT, we determined the protein expression of DNMT in the prostate tissues of TRAMP mice and in TRAMP-C1 cell. Two prostate specimens in

the same group were combined for protein extraction. The detailed procedure of Western blotting was described previously [52]. Protein bands were visualized by Supersignal West Femto (Pirece, Rockford, IL) and documented by Gel Documentation 2000 system (Bio-rad, Hercules, CA). Protein expressions were semi-quantitated by densitometry using ImageJ program. Antibodies against DNMT1, DNMT3A and DNMT3B were purchased from Imgenex (San Diego, CA). Antibodies against Nrf2 (sc-722), NQO1(sc-16464), and β-actin (sc-1616) were purchased from Santa Cruz Biotechnology.

4.2.6 RNA extraction and reverse transcription PCR

RNA was extracted using Qiagen RNeasy mini kit and converted to cDNA (TaqMan®). Conditions for qPCR were described [284]. Relative expression was analyzed by a ΔΔ Ct method using RQ Manager 1.2 and GAPDH expression was used as internal control. The forward and reverse primers for *Nrf2* amplification were 5'-TCACACGAGATGAGCTTAGGGCAA-3' and 5'-TACAGTTCTGGGCGGCGACTTTAT-3'. Primers for *Nqo1* were 5'-AAGAGCTTTAGGGTCGTCTTGGCA-3' and 5'-AGCCTCCTTCATGGCGTAGTTGAA-3'. Primers for GAPDH were 5'-TCAACAGCAACTCCCACTCTTCCA-3' and 5'-ACCCTGTTGCTGTAGCCGTATTCA-3'.

4.2.7 Statistical analyses

Data are expressed as mean ± SEM. Palpable tumor incidence was evaluated using the Fisher exact test. The methylation percentage of the *Nrf2* promoter in the archived prostate samples over age of TRAMP mice were analyzed using one-way ANOVA, where age was treated as the main effect, followed by Tukey's studentized range test. For all other determinations, Students' *t*-test or Welch's *t*-test was used. SAS®, version

9.2 was used for all statistical analyses. All *P* values correspond to two-sided hypothesis tests and $P < 0.05$ was regarded as significance.

4.3 Results

4.3.1 CpG methylation in the *Nrf2* promoter increases during prostate tumorigenesis in TRAMP mice

In the present study, we examined the methylation pattern of the first 5 CpG in the prostate of TRAMP and non-transgenic mice at different ages. In the prostate of TRAMP mice, the methylation of these CpG was significantly increased from 12 wk to 24 wk (Figure 4-1), while in the prostate of non-transgenic mice, the methylation remained unchanged (Figure 4-1). Age had a significant effect ($P = 0.015$) on increasing the methylation of the *Nrf2* promoter in the TRAMP mice.

4.3.2 Dietary feeding of 0.1% γ-TmT inhibits CpG hypermethylation in the *Nrf2* promoter in the prostate of TRAMP mice

The palpable tumor incidence (Table 1) was significantly lower in the γ-TmT group than the control group, which is consistent with the previous study [283]. The methylation of the first 5 CpG in the *Nrf2* promoter was significantly lower in the γ-TmT group than in the control group (Figure 4-2). The mean mRNA expression of *Nrf2* was higher in the γ-TmT group than the control group (Figure 4-2C), though the difference was not statistically significant due to the small size of experimental mice and variation between mice.

4.3.3 γ-TmT reverses CpG hypermethylation in the *Nrf2* promoter in TRAMP-C1 cells

From above *in vivo* study, which demonstrated that γ-TmT inhibited CpG methylation in the *Nrf2* promoter, we next investigated whether γ-TmT could reverse CpG hypermethylation in TRAMP-C1 cells. The methylation of the first 5 CpG in the

Nrf2 promoter was inhibited in the γ-TmT treated cells compared to the untreated cells at d 5 (Figure 4-3). Cell viability was not affected after treatment (data not shown).

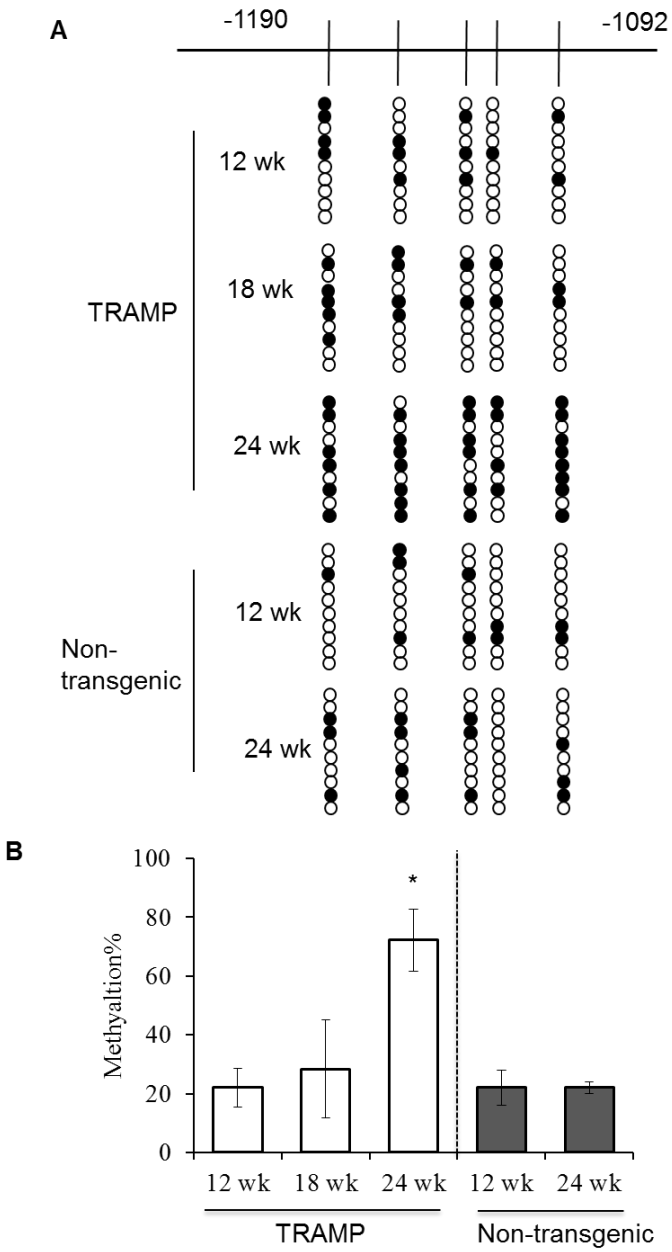

Figure 4-1. Methyaltion patterns of the first 5 CpG in the Nrf2 promoter in the prostate of TRAMP mice.

(A) Methylation patterns of the first 5 CpG in the Nrf2 promoter in prostate samples from TRAMP and non-transgenic mice. (B) Percentage of methylated CpG. In (B), data are mean ± SEM, n = 3-5 (TRAMP) or 2 (non-transgenic). *, $P < 0.05$.

Table 1. Palpable tumor incidence in TRAMP mice fed control or 0.1% γ-TmT diet for 16 wk

	Current study		Previous study[1]	
	n	Palpable tumor incidence	*n*	Palpable tumor incidence
Control	6	4/6	17	13/17
γ-TmT	7	0/7*	11	2/11*

* Differs from the control group, $P < 0.05$.

[1] Adapted from the reference [283].

4.3.4 γ-TmT induces mRNA and protein expressions of *Nrf2* and *Nqo1* in TRAMP-C1 cells

We examined the expression of *Nrf2* to see whether reduced promoter methylation could reactivate gene expression. The mRNA and protein expressions of *Nrf2* and *NQO1* was induced in TRAMP-C1 cells treated with 30 μmol/L of γ-TmT compared to the control cells in day 5.

4.3.5 γ-TmT suppresses the expression of DNMT in the prostate of TRAMP mice and TRAMP-C1 cells

In the prostate of TRAMP mice, the protein levels of DNMT, including DNMT1, DNMT3A and DNMT3B, were all lower in the γ-TmT group than in the control group (Fig. 5A). Interestingly, only DNMT3B was suppressed when TRAMP-C1 cells were treated with 30 μmol/L of γ-TmT for 5 d (Figure 4-5B). These results suggest the potential role of DNMT in CpG methylation and demethylation regulated by γ-TmT.

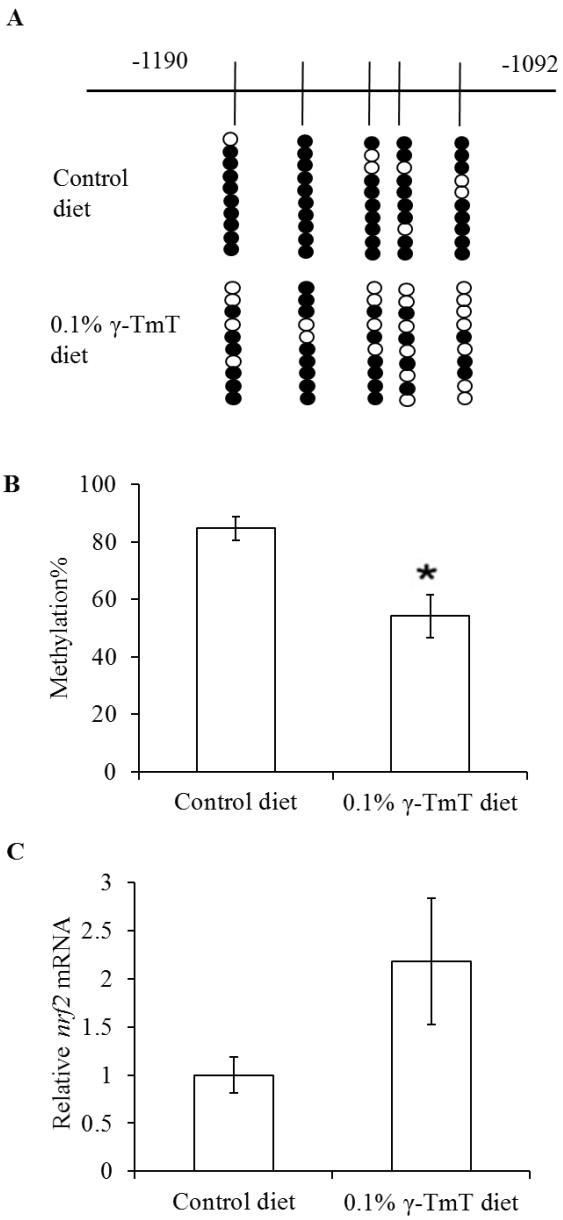

Figure 4-2. Methylation of the first 5 CpG in the Nrf2 promoter.

(A) Methylation patterns of the first 5 CpG in the Nrf2 promoter region. (B) Overall methylation percentage. (C) The mRNA expression of Nrf2 in the prostate of TRAMP mice fed control or 0.1% γ-TmT diet. Data are mean ± SEM, $n = 4$ (control) or 7 (γ-TmT). * Differs from the control, $P < 0.05$.

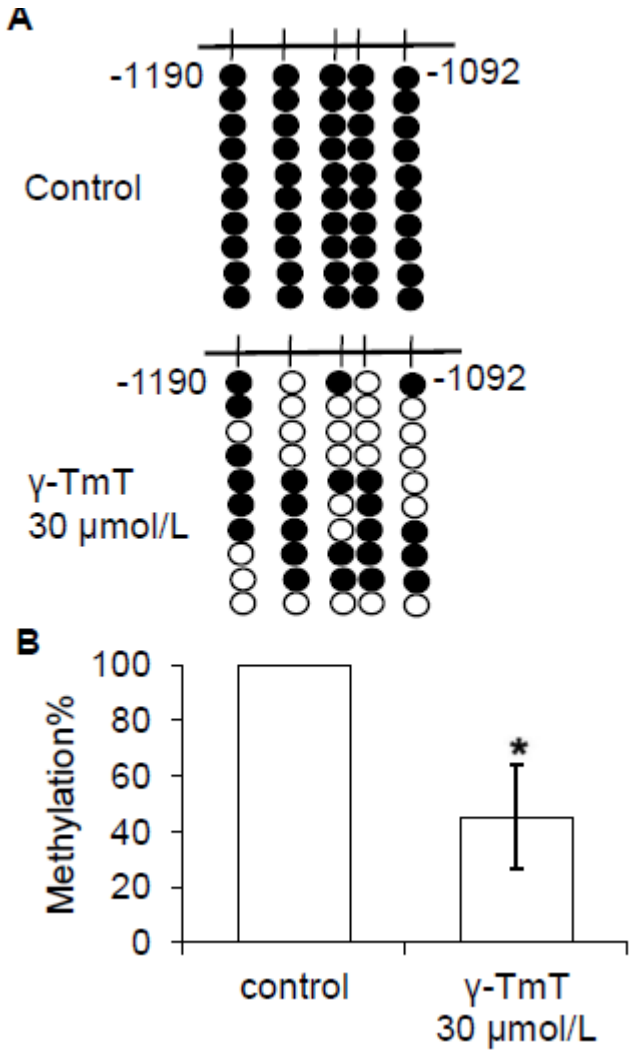

Figure 4-3. Methylation of the first 5 CpG in the Nrf2 promoter in TRAMP-C1 cells.

TRAMP-C1 cells were treated with control or 30 μmol/L of γ-TmT for 5 days. (A) Methylation pattern and (B) overall methylation percentage of the 5 CpGs in TRAMP-C1 cells. Data are mean ± SEM, $n = 3$. * Differs from the control, $P < 0.05$.

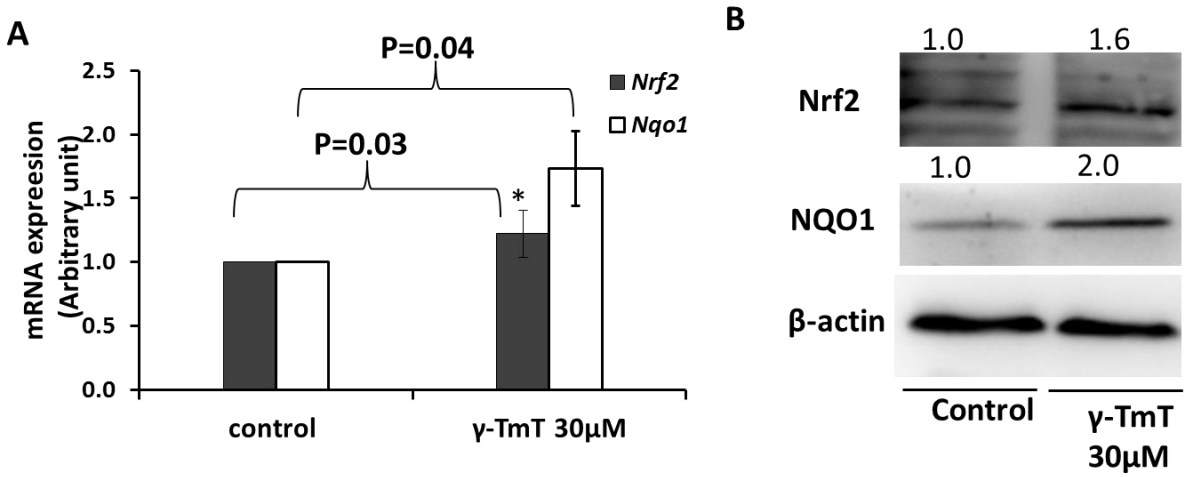

Figure 4-4. The mRNA and protein expression of Nrf2 and its target gene, NQO1, in TRAMP-C1 cells.

TRAMP-C1 cells were treated with control medium or 30 μmol/L of γ-TmT for 5 days, and then mRNA or protein were extracted. Three independent experiments were carried out. Data are mean ± SEM, $n = 3$. * Differs from the control, $P < 0.05$. C, control; T, γ-TmT.

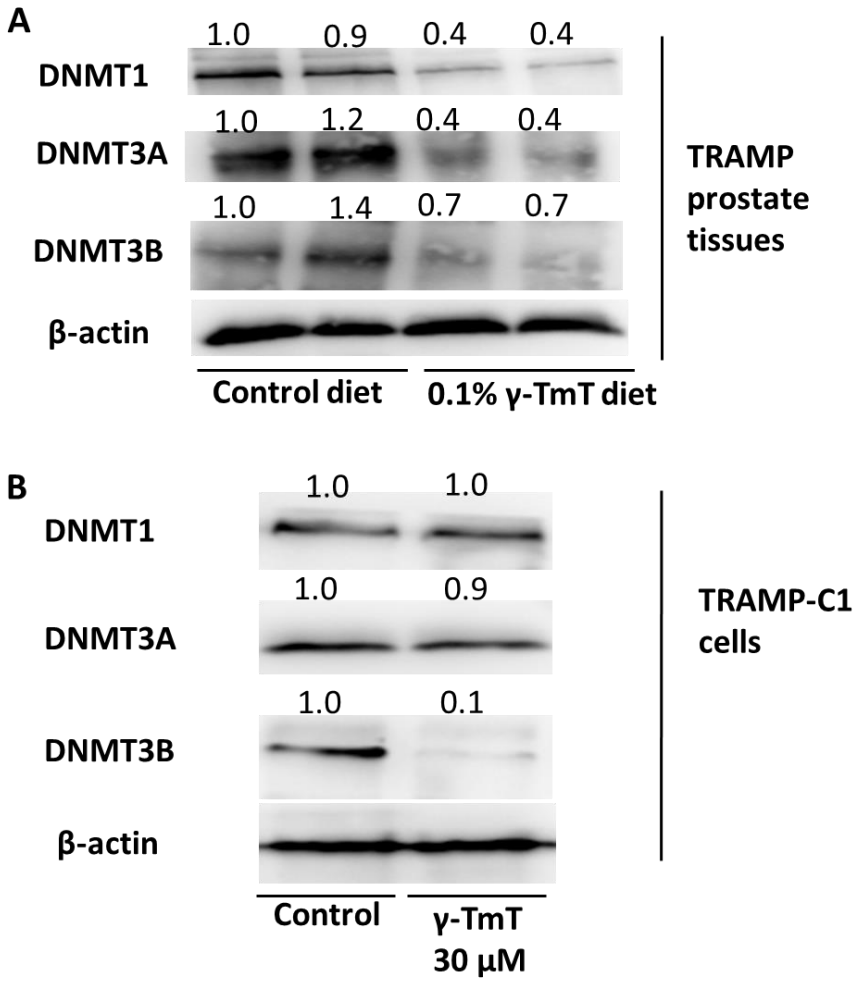

Figure 4-5. Protein levels of DNMT1, DNMT3A and DNMT3B in the prostate of TRAMP mice fed control or 0.1% γ-TMT diet.

TRAMP mice (n =4-7) were fed control or 0.1% γ-TMT diet from week 8 to week 24. Protein were extracted from prostate tissues and pooled for Western blotting. TRAMP-C1 cell were treated with control medium or 30 μmol/L of γ-TmT for 5 days. Cells were harvested and protein was extracted. Fold changes are mean ± SEM, *n* = 4-7 (TRAMP mice) or 3 (TRAMP-C1 cells). * Differs from the control, $P < 0.05$. C, control; T, γ-TmT.

4.4 Discussion

γ-TmT has been shown to inhibit prostate tumorigenesis in TRAMP mice associated with higher *Nrf2* expression [283], however the molecular mechanism remains unclear. In the present study, we show that γ-TmT treatment prevented CpG hypermethylation in the *Nrf2* promoter *in vivo* and reversed its hypermethylation *in vitro*, which might contribute to higher *Nrf2* expression. Tocopherols are extensively studied with respect to their anti-oxidative, anti-inflammatory, and anti-proliferative effects [287], yet to the best of our knowledge, their effects on epigenetic modification have not been reported.

The progression of prostate tumorigenesis in the TRAMP model is associated with abnormal DNA methylation events with both locus-specific hypermethylation and global genomic hypomethylation [288]. The present study demonstrated that methylation of the first 5 CpG in the *Nrf2* promoter increased during prostate cancer development in TRAMP mice, especially at the late stage (Figure 4-1A and C). These CpG are critical in regulating the expression of *Nrf2*, and the increased methylation may contribute to the lower *Nrf2* expression in prostate tumors of TRAMP mice as reported previously [52]. *NRF2* is also found to be repressed in human prostate cancer [251], however, future studies are warranted to investigate whether *NRF2* inactivation in human prostate cancer is caused by CpG hypermethylation.

Prostate cancer in the TRAMP model appears to be manifested with excessive oxidative stress, accompanied with increased damage to DNA, protein and lipid [273]. Since Nrf2 plays a central role in adapting the cells to environmental and endogenous stresses [204], the loss of *Nrf2* expression would potentially make the prostate of TRAMP mice more vulnerable to insults, as Nrf2-targeted enzymes such as SOD, UGT1A1, NQO1 and GST family are also lost during tumorigenesis [251, 283, 289].

γ-TmT inhibited CpG methylation (Figure 4-2A, B, and Figure 4-3) and elevated Nrf2 and its downstream antioxidant enzyme NQO1 in TRAMP-C1 cells (Fig. 4), which could potentially contribute to the prevention against prostate cancer.

Some natural phytochemicals have been shown to reactivate expression of silenced genes in tumor cells through epigenetic modifications [275, 290]. Possible mechanisms could be related to inhibition of DNMT and/or HDAC. For instance, green tea polyphenols, sulforaphane and curcumin have been reported to inhibit both DNMT and HDAC [193, 290, 291]. In the present study, we show that dietary γ-TmT feeding suppressed the expressions of all three DNMT in TRAMP mice (Fig. 5A). Lower expression of DNMT could prevent promoter CpG hypermethylation in the prostate of TRAMP mice, including the *Nrf2* promoter during early stages of tumorigenesis. Furthermore, metabolites of tocopherols are hypothetical HDAC inhibitors as predicted by molecular modeling [290]. It is speculative that histone modifications might also contribute to the reduced CpG methylation and higher *Nrf2* expression following γ-TmT treatment *in vivo*. Further study will be needed to explore the effect of γ-TmT on HDAC and histone modifications.

The human body preferentially retains α-tocopherol despite the high γ-tocopherol intake from the typical American diet [287]. This is achieved in part by the selectivity of the hepatic α-tocopherol transfer protein, which facilitates the entrance of α-tocopherol into the circulatory system, while the non-α-tocopherols undergo fast metabolism mediated by cytochrome P450s [292]. In immunodeficient mice fed 0.1% γ-TmT, α-tocopherol remained the most abundant form in the prostate, though its concentration did not increase compared to the control group [293]. The concentrations of γ- and δ-tocopherol in the prostate increased by 2- to 3-fold following 0.1% γ-TmT treatment. Another study showed that the urinary excretions of tocopherol metabolites

such as γ- and δ-carboxymethyl hydroxychromans were dramatically increased in immunodeficient mice following 0.17% to 0.3% of γ-TmT feeding [294]. These tocopherol levels reported in mice suggest that the observed epigenetic effect in the prostate of TRAMP mice in the present study may be attributed to single or combined effects of γ-, δ-tocopherol and or their metabolites.

As a proof-of-concept, we demonstrated that γ-TmT could reverse hypermethylation of the *Nrf2* promoter using TRAMP-C1 cells. However, DNMT3B, but not DNMT1 or DNMT3A, was suppressed in the γ-TmT treated cells at day 5. There are several possible explanations for the differences between the *in vivo* and *in vitro* results. First, the TRAMP study was primary prevention, in which γ-TmT could block the expression of DNMT proteins and the methylation of the *Nrf2* promoter during the prostate tumorigenesis. The *in vitro* study was carried out in a prostate cancer cell line, in which the *Nrf2* promoter is already hypermethylated [52], and the γ-TmT treatment would be to reverse the hypermethylation. Second, prostate tumors from TRAMP mice are of heterogeneous population [274] compared to the TRAMP-C1 cells which are relatively homogenous and therefore could result in different outcomes upon γ-TmT treatment. Third, the concentrations of different tocopherols and their metabolites existed in prostate tissues and TRAMP-C1 cells might be different. It is reported that only a small portion of tocopherols in cell culture medium can be metabolized by human prostate cancer cells [295]. Hence it is likely that TRAMP-C1 cells are mostly exposed to the parent tocopherols as they are supplemented in the medium. In contrast, mice can metabolize tocopherols extensively *in vivo*, generating high concentrations of carboxychromanol metabolites [294], some of which have been shown to possess superior biological activity as compared to the parent tocopherols [296-298].

4.5 Conclusions

In summary, in our present study we show that γ-TmT prevents CpG methylation in the *Nrf2* promoter *in vivo* in the prostate of TRAMP mice and reverses hypermethylation of *Nrf2* promoter *in vitro* in TRAMP-C1 cells, associated with lower protein expressions of DNMT. These epigenetic modifications might contribute to higher *Nrf2* expression, which potentially plays a role in the prevention against prostate tumorigenesis in TRAMP mice.

5 Chapter 5. Mechanisms of Prostate Carcinogenesis and its prevention by a γ-tocopherol-rich mixture of tocopherols in TRAMP mice

5.1 Introduction

Tocopherols belong to a subgroup of the vitamin E family that features a chromanol ring and a saturated side chain. Tocopherols exist in α, β, δ, and γ forms, depending on the number and position of the methyl groups on the chromanol ring [276]. They are the primary lipid-soluble antioxidant in cell membranes and protect the membranes from lipid peroxidation [299]. Tocopherols also exert many biological effects apart from their free radical-trapping properties. A number of studies have demonstrated that tocopherols, especially the δ and γ forms, and their metabolites inhibit inflammation and induce apoptosis in cancer cells [296, 297, 300, 301]. Treatment with either δ- or γ-tocopherol, as well as a mixture of tocopherols, prevents tumorigenesis in animal models of prostate, lung, colon, and breast cancer [53, 282, 283, 294, 302-306].

Prostate cancer is the most prevalent cancer in men in the United States [307]. Significant efforts have been made to identify effective strategies to prevent prostate cancer, including the use of supplements of consisting of dietary and natural agents, such as vitamin E. Many observational studies have shown an inverse association between prostate cancer and tocopherols, which have been quantified in either the blood or dietary intake [287], but the results from clinical trials are inconsistent and disappointing. The Alpha-Tocopherol, Beta-Carotene (ATBC) Cancer Prevention Study found that daily supplementation of 50 mg (approximately 75 IU) α-tocopherol significantly reduced prostate cancer risk in smokers [308]. However, no risk reduction was observed in either the Selenium and Vitamin E Cancer Prevention Trials (SELECT) or the Physicians' Health Study II, both of which used 400 IU of α-tocopherol [279]. Notably, all three studies used α-tocopherol to represent vitamin E. Although

tocopherols differ from each other solely in the methyl groups on their chromanol rings, they do not exhibit identical metabolic fates and biological activities [287, 309]. α-tocopherol is not as effective as δ- or γ-tocopherol in preventing carcinogenesis in animal studies [294, 303, 305].

In this study, we aimed to investigate the effects of a γ-tocopherol-rich mixture of tocopherols (γ-TmT) on global gene expression in the prostate of TRAMP (Transgenic Adenocarcinoma of the Mouse Prostate) and strain-matched C57BL/6 mice. The TRAMP mouse is a common preclinical model for evaluating the efficacy of various natural chemopreventive agents and therapeutic drugs [53, 55, 75, 310-314]. Spontaneous prostate tumorigenesis in this model is driven by the expression of oncogenic simian virus 40 (SV40) large tumor antigens [315]. γ-TmT is a byproduct of the refining of vegetable oils, consisting of 57%, 24%, 13% and 1.5% γ-, δ-, α-, and β-tocopherol, respectively. Twelve hours after oral gavage of either 600 mg/kg γ-TmT or the control vehicle, the gene expression profiles in the prostates of TRAMP and C57BL/6 mice were measured using whole mouse genome microarrays (Agilent, G4122F).

5.2 Materials and Methods

5.2.1 Animals and Dosing

Female TRAMP (line PB Tag 8347NG) and male C57BL/6 mice were purchased from the Jackson Laboratory (Bar Harbor, ME). The mice were housed and bred at the Animal Care Facility of Rutgers University in accordance with the NIH Guidelines for the Care and Use of Laboratory Animals. Their genotypes were identified using a PCR-based method. Eight-week-old TRAMP males and age-matched C57BL/6 males were used in this study. γ-TmT is comprised of 130, 15, 568, and 243 mg of α-, β-, γ-, and δ-tocopherol per gram, respectively (Cognis Corporation, Cincinnati, OH). γ-TmT was

dissolved in olive oil at concentration of 100 mg/mL. In groups 1 and 2, C57BL/6 mice were orally administered olive oil and 600 mg/kg γ-TmT, respectively. In groups 3 and 4, TRAMP mice were orally administered olive oil and 600 mg/kg γ-TmT, respectively. Three mice were used in each experimental group. The mice were given an AIN-76A diet from one week prior to the treatment until the day before the experiment, when they were fasted overnight before oral gavage. The mice were euthanized with CO_2 12 hours after dosing, and their prostates were collected and snap-frozen in liquid nitrogen. The study was conducted in accordance with a protocol approved by the Institutional Animal Use and Care Committee at Rutgers University.

5.2.2 Sample Preparation and Microarray Analysis

Total RNA was extracted using the RNeasy mini kit (Qiagen, Valencia, CA). An equal amount of RNA from three mice in each group was pooled. Quality control, cDNA synthesis, Cy3 dye labeling, hybridization, and scanning of the arrays were carried out at the Functional Genomics Core of Robert Wood Johnson Medical School, Rutgers University (New Brunswick, NJ) as previously described [72, 316, 317]. Agilent microarrays for the whole mouse genome (G4122F) containing 43379 biological features were used to examine the global gene expression profiles. After hybridization and washing, the intensity of the fluorescence signal was measured with an Agilent G2505C Scanner (Santa Clara, CA). Background subtraction was performed, and the expression values were determined using Agilent's standard protocol. The variation between the arrays was normalized using the quantile normalization method provided by preprocessCore, a Bioconductor package [318, 319]. Genes that were either induced or suppressed by at least two-fold between the treated versus the control group or the TRAMP versus the C57BL/6 (wild-type, WT) group were selected for analysis of biological functions using Ingenuity Pathway Analysis (IPA,

http://www.ingenuity.com). Venn diagrams and heat maps were generated using the VennDiagram and gplots R packages. The microarray data have been deposited in the NCBI GEO and the accession number is GSE61416.

5.2.3 Quantitative Real-Time PCR for Microarray Data Validation

One microgram of total RNA was converted to complementary DNA using TaqMan Reverse Transcription reagents (Applied Biosystems Inc., Foster City, CA). Quantitative real-time PCR was performed in the Applied Biosystems 7900HT system using SYBR Green PCR Master Mix. The ΔΔCt method was used for quantification, and *Actin* expression was employed as a loading control.

5.3 Results

5.3.1 Global view of gene expression changes in the prostate caused by γ -TmT treatment and the SV40 transgene

Quantile normalization removed the variance between the four microarrays, yielding the same median and density distribution of the signal intensity. The normalized datasets were used for subsequent analyses.

The SV40 transgene and γ-TmT treatment had significant effects on the obtained gene expression profiles. The effects of γ-TmT treatment on gene expression were genotype-dependent. In WT (C57BL/6) mice, the expression of 2861 genes was either elevated (1496) or inhibited (1365) by at least two-fold after γ-TmT treatment (group 2 vs. group 1). In TRAMP mice, the expression of 4886 genes was either increased (2474) or inhibited (2412) by at least two-fold after γ-TmT treatment (group 4 vs. group 3). The majority of the induced and inhibited genes were unique in each genotype, and only a small percentage of them overlapped (Figure 5-1). In addition, the basal gene expression profiles were dramatically different between the TRAMP and WT mice. There were 2614 and 2339 genes whose expression was either induced or suppressed

by at least two-fold, respectively, in the TRAMP mice compared to WT mice (group 3 vs. group 1).

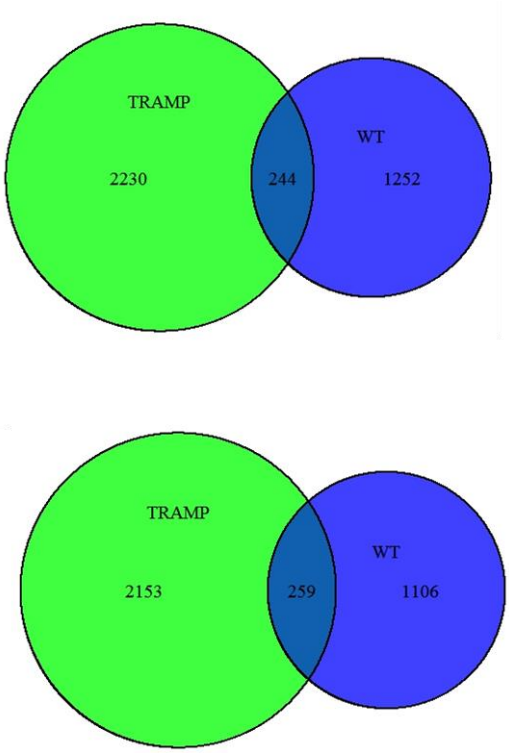

Figure 5-1. Comparison of γ-TmT regulated gene expression changes in the prostate of TRAMP and C57BL/6 (WT).

Venn diagrams showing the number and overlap of genes that were induced (the upper panel) and inhibited (the lower panel) 12 hours after oral administration of 600 mg/kg γ-TmT.

5.3.2 Gene annotation enrichment of differentially expressed genes

Gene ontology analysis was performed to gain insight into what biological functions might be significantly affected by the SV40 transgene and γ-TmT treatment. The top five functions that were significantly affected in TRAMP mice as a consequence of the expression SV40 were cellular growth and proliferation; the cell cycle; cellular assembly and organization; DNA replication, recombination and repair; and drug metabolism (Figure 5-2A). In C57BL/6 mice, the top five functions that were significantly altered by γ-TmT treatment were cell-to-cell signaling and interaction, cellular movement, protein synthesis, cellular functions and maintenance, and cell morphology (Figure 5-2B), whereas in TRAMP mice, the list of the top functions that were impacted included cellular movement, cell morphology, cell-to-cell signaling and interaction, cellular development, and cell death and survival (Figure 5-2C).

5.3.3 γ -TmT treatment inhibited genes involved in cell cycle progression in TRAMP mice

Figure 5-3 shows the list of genes that promote cell cycle progression. They were identified based on the criterion of either showing at least two-fold induction in the prostate of TRAMP mice compared to WT mice (group 3 vs. group 1) or exhibiting at least two-fold inhibition following γ-TmT treatment in TRAMP mice (group 4 vs. group 3). Detailed information on these genes is provided in Table 1. In addition, we observed that γ-TmT treatment had a minimal effect on altering the expression of these genes in the prostates of C57BL/6 mice.

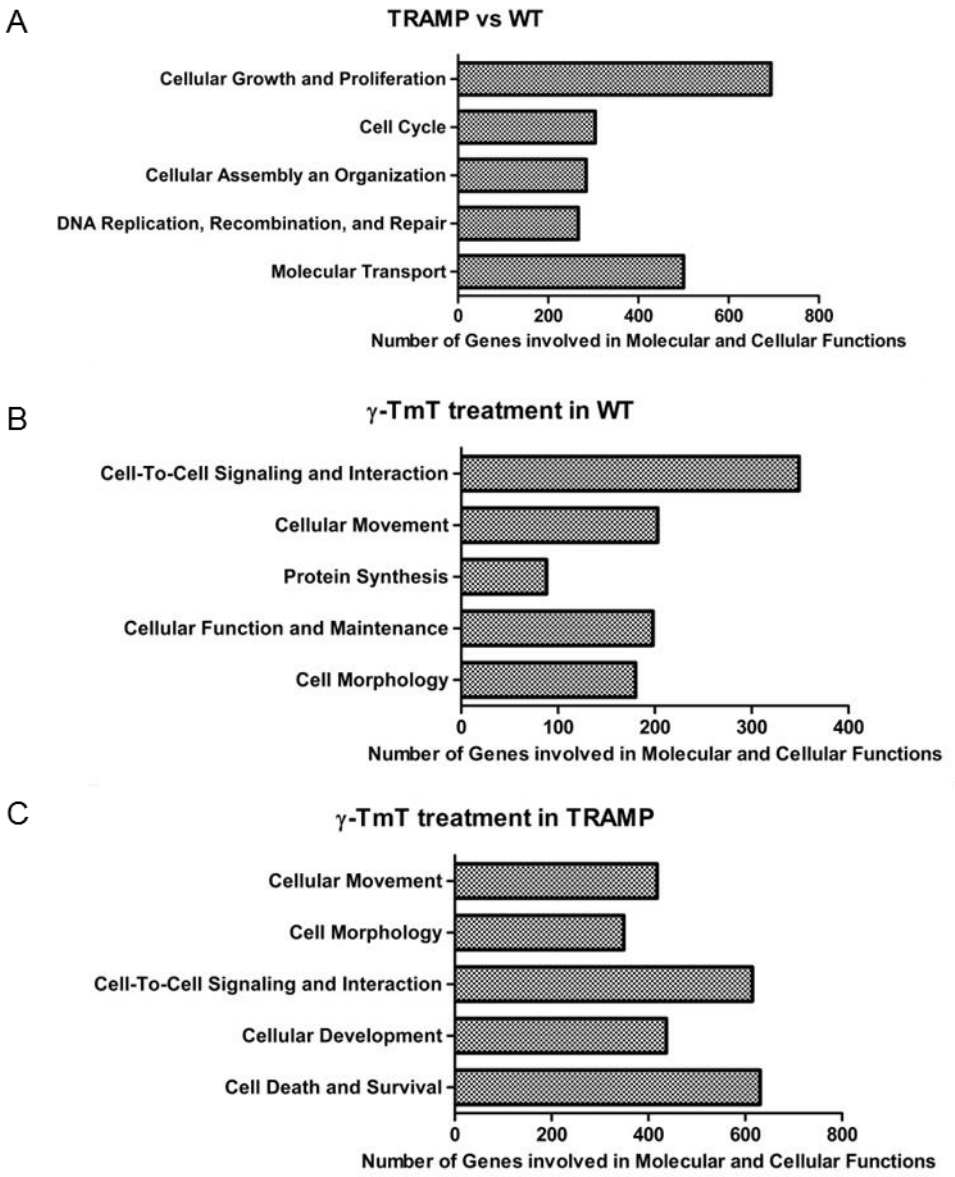

Figure 5-2. Top five functions that were significantly impacted.

Top five functions that were significantly impacted by the SV40 transgene (A) and by γ-TmT treatment in C57BL/6 (B) and TRAMP mice (C). Genes that were either induced or suppressed by at least two-fold between the treated versus the control group or the TRAMP versus the C57BL/6 (wild-type, WT) group were selected for analysis of biological functions using Ingenuity Pathway Analysis (IPA, http://www.ingenuity.com).

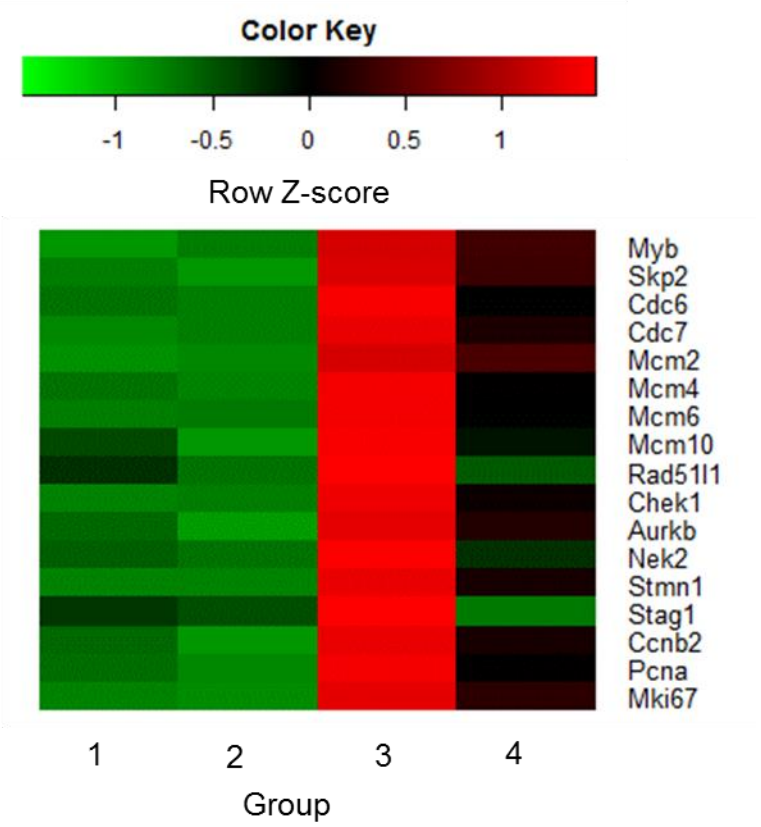

Figure 5-3. Expression of cell cycle-related genes that were highly expressed in the prostates of TRAMP mice and partially inhibited by γ-TmT treatment.

The colors represent the Z-score normalized signal intensity within each row. Group 1: WT mice treated with vehicle; Group 2: WT mice treated with 600 mg/kg γ-TmT; Group 3: TRAMP mice treated with vehicle; Group 4: TRAMP mice treated with 600 mg/kg γ-TmT.

5.3.4 γ -TmT treatment activated genes encoding antioxidant and phase II detoxification enzymes in TRAMP mice

Detoxification and phase II drug-metabolizing enzymes are critical in maintaining redox balance and inactivating toxic carcinogenic metabolites [320, 321]. Glutathione *S*-transferases (GST) are a family of enzymes that catalyze the conjugation of glutathione to electrophilic species, thereby diminishing their reactivity with cellular macromolecules [212]. In the prostates of TRAMP mice, the expression of GST family members, including mu, tau and alpha, was suppressed (Figure 5-4). γ-TmT treatment restored the expression of some of these genes to the levels observed in WT mice or even higher. Detailed information on these genes and the measured fold changes is provided in Table 1. Uridine 5'-diphospho-glucuronosyltransferase (Ugt) 2b34 and 3a1 were not suppressed in the TRAMP group, and their expression was induced by γ-TmT treatment in TRAMP but not WT mice. γ-TmT treatment also increased the expression of glutathione peroxidase 7 (Gpx7).

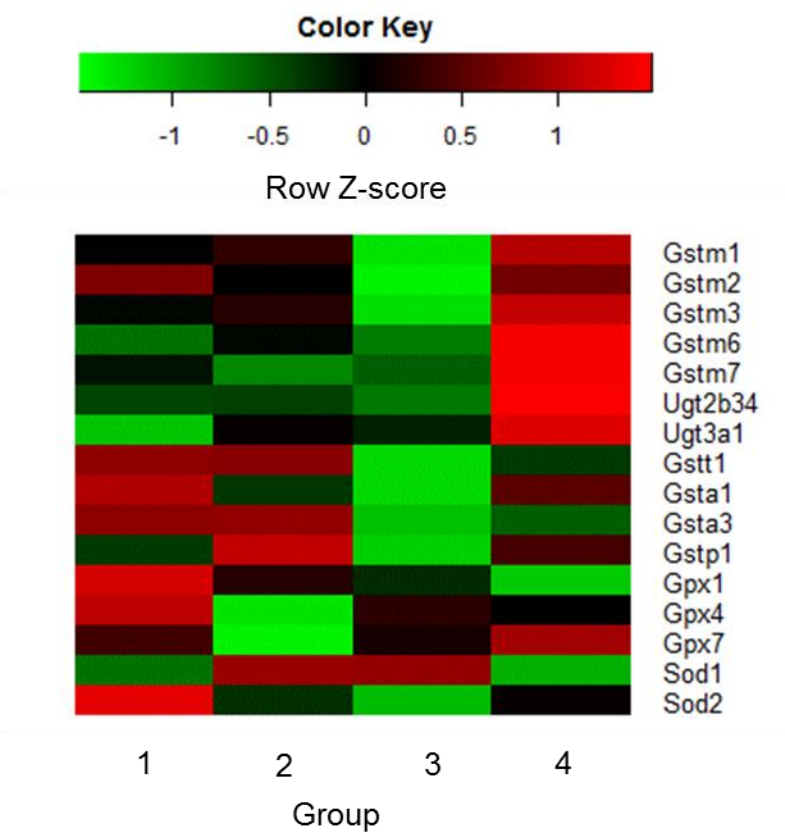

Figure 5-4. Expression of antioxidant and phase II detoxification genes.

The colors represent the Z-score normalized signal intensity within each row. Group 1: WT mice treated with vehicle; Group 2: WT mice treated with 600 mg/kg γ-TmT; Group 3: TRAMP mice treated with vehicle; Group 4: TRAMP mice treated with 600 mg/kg γ-TmT.

5.3.5 γ -TmT treatment suppressed metabolic genes in the prostate of TRAMP mice

Dysregulated energy metabolism is an emerging hallmark of cancer [184]. We identified four important genes (*Pfkl*, *Tkt*, *Acly* and *Prps2)* whose expression was markedly elevated in the prostates of TRAMP mice compared to WT mice (Figure 5-5). *Pfkl*, *Tkt*, *Acly* and *Prps2* encode key enzymes involved in glycolysis, the pentose phosphate pathway, fatty acid synthesis, and purine and pyrimidine synthesis, respectively [322-325]. γ-TmT treatment inhibited the expression of *Pfkl* and *Prps2* in the TRAMP mice, suggesting that this treatment might disrupt the synthesis of essential

molecules, such as nucleosides, required for cell proliferation and division. In addition, γ-TmT treatment suppressed the expression of *Idh3a/3b* and *Sdha/c/d* only in the TRAMP mice. These genes encode critical enzymes in the tricarboxylic acid cycle and the mitochondrial respiratory chain [326, 327].

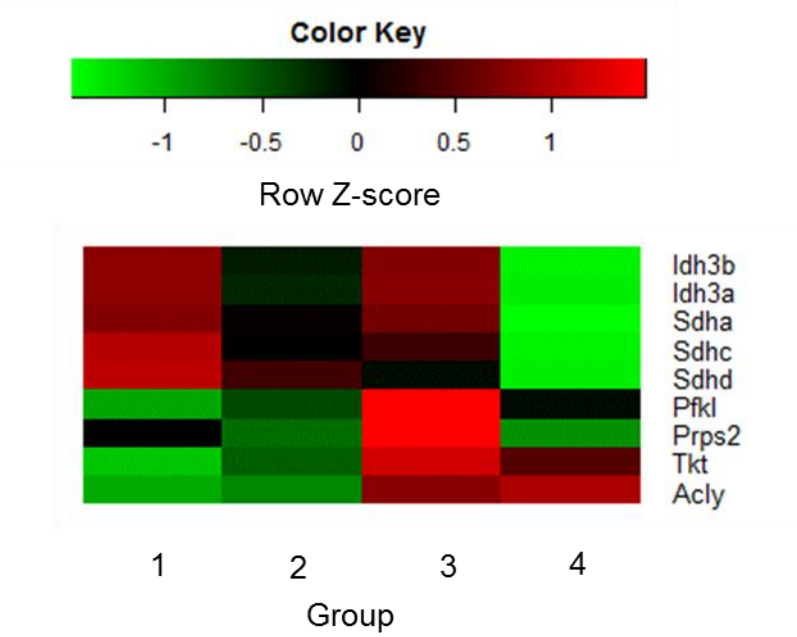

Figure 5-5. Expression of metabolic gene.

The colors represent the Z-score normalized signal intensity within each row. Group 1: WT mice treated with vehicle; Group 2: WT mice treated with 600 mg/kg γ-TmT; Group 3: TRAMP mice treated with vehicle; Group 4: TRAMP mice treated with 600 mg/kg γ-TmT.

5.3.6 Validation of selected genes via qPCR

mRNA samples from groups 3 and 4 were subjected to qPCR. *Chek1*, *Gstm2*, *Ugt2b3h* and *Idh3a* were selected as representatives of proliferative, phase II and metabolic genes. The qPCR results confirmed that the expression of *Gstm2* and *Ugt2b3h w*as elevated, whereas that of *Chek1* and *Idh3a* was suppressed in the prostates of TRAMP mice following γ-TmT treatment. The relative fold changes detected via microarray and qPCR analyses were consistent with each other (Figure 5-6).

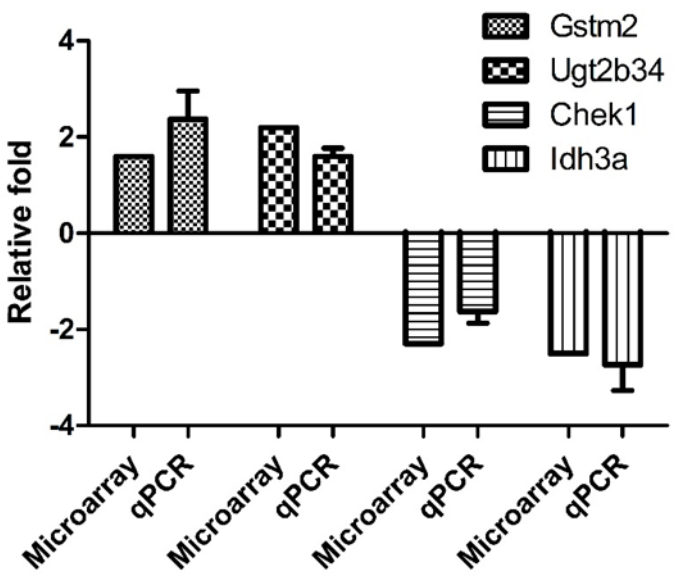

Figure 5-6. Relative expression of selected genes in the prostates of TRAMP mice after γ-TmT treatment.

Relative fold changes were calculated between vehicle- and γ-TmT-treated TRAMP mice. Error bars represent the standard deviation of three independent qPCR experiments.

Table 2. Information for the genes shown in Figure 5-3, Figure 5-4, Figure 5-5.

Gene Symbol	GenBank #	Description	Fold change Group 3 to 1	Fold change Group 4 to 3
Cell cycle				
Myb	NM_010848	Myeloblastosis oncogene	4.8	0.6
Skp2	NM_001243120	S-phase kinase-associated protein 2 (p45)	2	0.8
Cdc6	NM_011799	Cell division cycle 6	8.6	0.4
Cdc7	NM_009863	Cell division cycle 7	5.0	0.5
Mcm2	NM_008564	Minichromosome maintenance deficient 2	7.4	0.7
Mcm4	NM_008565	Minichromosome maintenance deficient 4	4.4	0.5
Mcm6	NM_008567	Minichromosome maintenance deficient 6	13.4	0.4
Mcm10	NM_027290	Minichromosome maintenance deficient 4	2.4	0.5
Rad51l1	NM_009014	RAD51-like 1	2.1	0.4
Chek1	NM_007691	Checkpoint kinase 1	9.3	0.4
Aurkb	NM_011496	Aurora kinase B	5.6	0.5
Nek2	NM_010892	NIMA-related expressed kinase 2	4.6	0.3
Stmn1	NM_019641	Stathmin 1	7.5	0.5
Stag1	NM_009282	Stromal antigen 1	2	0.6
Ccnb2	NM_007630	Cyclin B2	3.8	0.5
Pcna	NM_001353	Proliferating cell nuclear antigen	3.3	0.5

Mki67	NM_001512	Marker of proliferation Ki-67	10.2	0.6
Antioxidant and phase II detoxification enzymes				
Gstm1	NM_010358	Glutathione S-transferase mu 1	0.6	2.3
Gstm2	NM_008183	Glutathione S-transferase mu 2	0.6	1.6
Gstm3	NM_010359	Glutathione S-transferase mu 3	0.7	2.1
Gstm6	NM_008184	Glutathione S-transferase mu 6	1	2.0
Gstm7	NM_026672	Glutathione S-transferase mu 7	0.8	2.0
Ugt2b34	NM_153598	UDP glucuronosyltransferase 2 family, polypeptide B34	0.9	2.3
Ugt3a1	NM_207216	UDP glucuronosyltransferase 3 family, polypeptide A1	1.1	1.8
Gstt1	NM_008185	Glutathione S-transferase theta 1	0.3	2.0
Gsta1	NM_008181	Glutathione S-transferase alpha 1	0.6	1.5
Gsta3	NM_001077353	Glutathione S-transferase alpha 3	0.5	1.2
Gstp1	NM_013541	Glutathione S-transferase pi 1	0.9	1.3
Glucose metabolism				
Idh3b	NM_130884	Isocitrate dehydrogenase 3 (NAD+) beta	1.0	0.2

Idh3a	NM_029573	Isocitrate dehydrogenase 3 (NAD+) alpha	1.0	0.4
Sdha	NM_023281	Succinate dehydrogenase complex, subunit A	1.0	0.5
Sdhc	NM_025321	Succinate dehydrogenase complex, subunit C	0.8	0.4
Sdhd	NM_025848	Succinate dehydrogenase complex, subunit D	0.8	0.6
Pfkl	NM_008826	6-Phosphofructokinase	2.8	0.6
Prps2	NM_026662	Phosphoribosyl pyrophosphate synthetase 2	1.8	0.3
Tkt	NM_009388	Tkt transketolase	2.9	0.8
Acly	NM_001199296	ATP citrate lyase	2.8	1.0

5.4 Discussion

The present study shows that gene expression in the prostate can be significantly modulated *in vivo* by γ-TmT treatment. We focused on the proliferation, antioxidant and phase II detoxification, and metabolic pathways. These pathways are dysregulated during prostate tumorigenesis and are potential targets for tocopherols.

Defective cell cycle control leads to cellular transformation and tumorigenesis. The TRAMP model for prostate cancer is driven by the expression of the SV40 large T and small t antigens, which are regulated by a prostate-specific probasin promoter [315]. The large T antigen inactivates two important tumor suppressors (p53 and retinoblastoma protein) resulting in uncontrolled cell cycle progression. Using IPA, we observed that the top two gene lists affected in the TRAMP mice were cellular growth and proliferation and the cell cycle when compared to age- and strain-matched C57BL/6 mice (Figure 5-2). Many natural compounds exert promising anti-cancer effects by modulating regulatory cell cycle and apoptotic pathways in TRAMP mice [313, 314]. Several studies have reported that tocopherols and their derivatives inhibit prostate cancer cell growth *in vitro* by regulating cell cycle proteins such as cyclins and p27 [328-330]. In addition, treatment with tocopherols also induces apoptosis in human prostate cancer cells *in vitro* and in xenografted LNCaP tumors [300, 331, 332]. Short-term oral administration of γ-TmT suppressed a number of cell cycle-promoting genes (Figure 5-3), which can potentially contribute to prostate cancer prevention after long-term (16 weeks) treatment, as previously reported [53, 283].

Recent studies have shown that the development of prostate cancer in TRAMP mice is associated with elevated ROS levels and oxidative injury [251, 273]. We and others have demonstrated that the expression of antioxidant and phase II detoxification enzymes is suppressed in prostate tumors [251, 283, 289], possibly due to epigenetic

silencing of the upstream transcription factor Nrf2 [52, 53]. Deficiency of the anti-oxidative capacity can lead to elevated oxidative stress in the prostate, thereby promoting tumorigenesis through the activation of proliferative pathways [333]. Studies on polymorphisms in GSTs have revealed that some variants of GSTM1, GSTM3, GSTT1 and GSTP1 are associated with a higher risk of skin and lung cancer in humans, which further supports the protective role of phase II detoxification enzymes in cancer development [334, 335]. In this study, we found that the expression of the GST alpha, mu and tau families of genes as well as some UGT genes was suppressed in the prostates of TRAMP mice in the early stages of prostate cancer development. The induction of these protective genes through γ-TmT treatment appears to be an important mechanism that protects the prostate from oxidative damage and blocks tumorigenesis.

Metabolic reprogramming of multiple pathways from oxidative phosphorylation to aerobic glycolysis for energy production is a hallmark of cancer cells [184, 336]. This phenomenon is known as the Warburg effect, named after the researcher who first reported that cancer cells rapidly consume glucose and generate lactate [337]. We observed that the expression of *Pfkl*, *Tkt*, *Acly* and *Prps2* was markedly elevated in the prostates of 8-week-old TRAMP mice, suggesting an altered metabolism, including changes in glycolysis, the pentose phosphate pathway, fatty acid synthesis, and purine and pyrimidine synthesis. Future studies involving metabolic profiling will be necessary to characterize the metabolic changes during prostate tumorigenesis, which will help identify novel biomarkers and either therapeutic or preventive targets. Furthermore, γ-TmT treatment inhibited the expression of *Pfkl*, *Prps2*, *Idh3a/3b* and *Sdha/c/d*, indicating the potential impact of γ-TmT on the glucose metabolism pathway, although the detailed mechanisms of this modulation remain to be elucidated.

The negative results from the SELECT trial led the medical and scientific community to re-evaluate the potential of vitamin E supplementation. We speculate that supplementation with tocopherols benefits populations with low vitamin E intake as a source of antioxidants. However, for well-nourished populations, who intake sufficient levels of vitamin E, the beneficial effects of additional supplementation of tocopherols might occur through the modulation of signaling pathways such as inflammation, proliferation and apoptosis. Both *in vivo* and *in vitro* studies have demonstrated that γ- and δ-tocopherols are superior to α-tocopherol with regard to the inhibition of inflammation and proliferation as well as the induction of apoptosis [294, 303, 305, 309, 338]. In addition, a high oral dose of α-tocopherol has been observed to decrease the plasma concentration of γ-tocopherol [279]. These factors provide some explanations for the null results of the SELECT trial. Here, we used γ-TmT, which is inexpensive and can be obtained as a byproduct of the refinement of soybean oil. This mixture contains all four tocopherols and approximates the composition of γ-, α-, β-, and δ-tocopherol that can be digested from the diet. Administration of γ-TmT prevents prostate, breast, lung and colon cancer in animal models [53, 282, 283, 294, 302-306].

5.5 Conclusions

In summary, we have demonstrated that thousands of genes and various pathways are altered in the prostates of TRAMP mice. In particular, we observed enhanced proliferation, suppressed phase II detoxification and metabolic reprogramming in the TRAMP model. As a naturally occurring vitamin E, γ-TmT can modulate multiple signaling cascades *in vivo*, which might delay the progression of prostate cancer.

6 Chapter 6. A naturally occurring mixture of tocotrienols inhibits the growth of human prostate tumor *in vivo* and *in vitro*

6.1 Introduction

The biological functions of tocotrienols (T3s), a sub-group of the vitamin E family, have been not fully recognized over the decades of the vitamin E research, which predominately focused on tocopherols (Ts), especially α-T. T3s are similar to Ts except the three unsaturated bonds in the side chain that distinguish T3s and Ts (Figure 6-1). The biological role of T3s is underestimated probably because of their low blood levels in humans, resulting from low ingestion from typical Western diets. In addition, the hepatic α-T transfer protein preferentially transports α-T from hepatocytes to blood, while the majority of other vitamin E homologs get metabolized in the liver and thus their blood levels are low [276]. Nevertheless, T3s are abundant in a variety of natural sources such as palm oil and rice bran, which contain about 50-70 mg total tocotrienols in 100 g of product [339].

T3s, particularly the γ and δ homologs, have been shown to inhibit the growth of various types of tumor in mouse models, including prostate cancer [340-345]. It has been reported that intraperitoneal or oral administration of γ-T3 suppressed the growth of PC3 and LNCaP human prostate tumors in nude mice [344, 345]. In addition, dietary feeding of mixed tocotrienols inhibits prostate tumorigenesis in the transgenic adenocarcinoma mouse prostate (TRAMP) model [346]. γ-T3 treatment also sensitizes tumors to chemotherapeutic drugs such as gemcitabine, docetaxel and capecitabine [340, 342, 345]. T3s suppress proliferation and induce apoptosis by modulating multiple targets such as inhibition of NF-κB, phosphoinositide 3-kinase (PI3K)/Akt and STAT3, induction of p53, p27 and PARP-γ, and modulating metabolism of endogenous substances such as cholesterol, dihydroceramide and dihydrosphingosine [340-342, 344,

347, 348]. Notably, *in vitro* studies have shown that different forms of T3s possess differential anti-cancer activities, although they differ from each other solely by the location of methyl groups on their chromanol rings. The order of growth inhibitory effects is δ, γ, β, and α, from high to low, in LNCaP and PC3 cells [349].

In this study, we aimed to evaluate the effects of a naturally occurring mixture of tocotrienols on the growth of VCaP human prostate tumor in a nude mouse xenograft model. We also measured the blood and tissue levels of different T3s to evaluate the exposure after oral administration. In addition, we examined effects of α-, δ-, γ-T3 on the growth of VCaP cells *in vitro* and their effects on regulating cell cycle.

6.2 Materials and Methods

6.2.1 Cell culture and reagents

Human prostate cancer VCaP cells were originally purchased from the American Type Tissue Collection (ATCC, Rockville, MD). This cell line was derived from vertebral bone metastasis of hormone refractory prostate cancer [350]. VCaP cells were transfected with a luciferase construct, a single clone VCaP-luc was obtained and used for subcutaneous implantation in nude mice. Cells were cultured in RPMI medium containing 10% FBS, 50 units/mL penicillin, and 50 μg/mL streptomycin. Antibodies against cyclin A, cyclin D1, p21, p27 and β-actin were purchased from Santa Cruz Biotechnology (Santa Cruz, CA). α-, δ-, γ-T3 and a naturally occurring mixture of T3s were provided by Carotech (Perak, Malaysia).The mixture of T3s (mixed T3) contains 8.3, 1.5, 4.6, 11.4 and 6.0 g of α-, β-, δ-, γ-T3 and α-T per 100 g of product, respectively. The mixed T3 is water-dispersible.

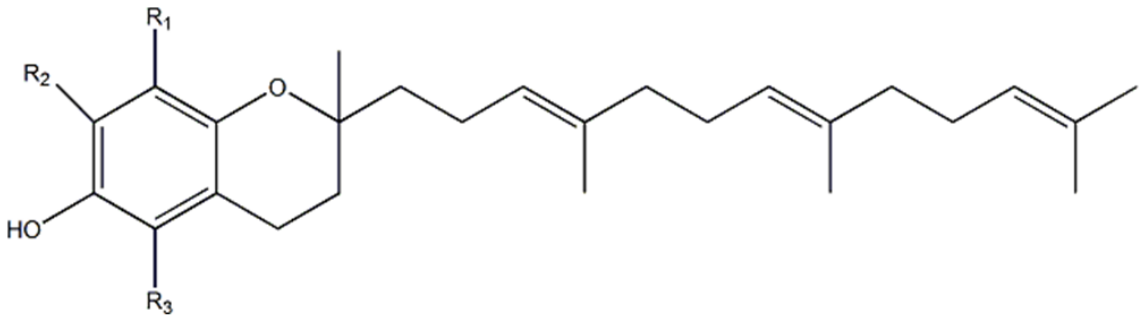

$R_1 = R_2 = R_3 = CH3$ α-tocotrienol
$R_1 = R_3 = CH3, R_2 = H$ β-tocotrienol
$R_1 = R_2 = H, R_3 = CH3$ δ-tocotrienol
$R_1 = H, R_2 = R_3 = CH3$ γ-tocotrienol

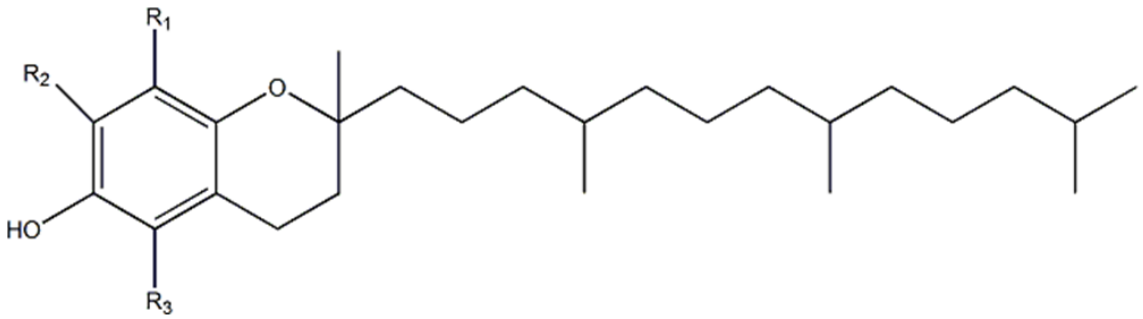

$R_1 = R_2 = R_3 = CH3$ α-tocopherol
$R_1 = R_3 = CH3, R_2 = H$ β-tocopherol
$R_1 = R_2 = H, R_3 = CH3$ δ-tocopherol
$R_1 = H, R_2 = R_3 = CH3$ γ-tocopherol

Figure 6-1. Structure of different homologs of tocotrienols and tocopherols.

6.2.2 Xenograft human prostate VCaP tumors in immunodeficient mice

Eight-week-old male NCr immunodeficient mice were purchased from Taconic Farms and housed in Rutgers Animal Care Facility. The mice had free access to sterilized AIN76A diet (Research Diet, New Brunswick, NJ) and water. VCaP-luc cells (5×10^6/0.1mL) were suspended in 50% Matrigel in RPMI 1640 medium and injected subcutaneously in the right flank of mice. Mixed T3 was suspended in saline with final concentrations such that oral administration of 0.1 mL will provide 200 mg/kg or 400 mg/kg of total T3s and α-T in the low (n=12) and high dose (n = 12) groups. The control mice (n = 10) were given 0.1 mL of saline. Oral gavage were performed three

times a week for eight weeks. Tumor volume was measured every other week by bioluminescence imaging using IVIS system. Before imaging, mice were anesthetized with isoflurane and then injected 3 mg/mouse of D-luciferin by i.p.. Images were taken in prone position for 1 min, beginning at 8 min after the luciferin injection; and luminescent signal was reported as the photon flux (ph/s). Tumors, plasma, and prostate were collected at week 8 when mice were euthanized by CO2 asphyxiation. The study was carried out under an IACUC-approved protocol at Rutgers University.

6.2.3 Analysis of tocotrienols and α-tocopherol levels by high-performance liquid chromatography (HPLC)

The levels of T3s and α-T in plasma, tumors and prostates were measured by an establish method using HPLC [294]. Briefly, plasma samples (20 μL) was mixed with 130 μL deionized water and 150 μL ethanol and then the mixture was extracted twice with 1 mL hexane each time. Tissue samples were homogenized in 50% ethanol containing 0.05% ascorbic acid and the supernatant was extracted twice with hexane. The hexane extracts were dried under nitrogen gas and then resolved in 100 μL ethanol. The analytes were separated using HPLC with a Supelcosil C18 column (150 X 4.6 mm). The mobile phase was 82% ethanol in water containing 20 mmol/L ammonium acetate. The analytes were detected using an ESA 5600A Coulochem electrode array system with potential set at 200, 300, 500 and 700 mV.

6.2.4 *In vitro* cell viability and proliferation assay

VCaP cells were seeded at a density of 5000 cells/well in 96-well plates overnight and treated with T3s in triplicate at concentrations of 0-100 μM for 24 hours to measure cell viability. Cells were treated with 20 μM, 10 μM and 20 μM of α-, δ- and γ-T3 in triplicate for 1, 2, and 3 days. After treatment, T3-containing medium was aspirated, and 100 μL fresh culture medium containing 20 μL CellTiter 96® AQueous One

Solution (Promega, Madison, MI) was added into each well. After 1 hour at 37 ℃ in a humidified and 5% CO_2 atmosphere, absorbance at 490 nm was measured using a plate reader (Infinite M200 Pro, Tecan, San Jose, CA).

6.2.5 Flow cytometry analysis of cell cycle

VCaP cells were seeded at 70-80% confluency in 10 mm culture dishes overnight and treated with 20 μM α-T3, 10 μM δ-T3 and 20 μM γ-T3 for 24 hours. After treatment, cells were trypsinized, washed with PBS, and re-suspended in 0.5 mL PBS. Cells were fixed by slowly adding 4.5 mL of cold 70% ethanol and kept at 4 ℃ for at least 2 hours. The ethanol-suspended cells were centrifuged at 300 g for 5 min, and ethanol was removed carefully. Cells were washed by 5 mL PBS, re-suspended in 500 μL PBS with 5 μL propidium iodide (1 mg/mL) and 5 uL RNAse A (10 mg/mL), and then kept in dark at room temperature for 30 min. Cells were transferred to the Beckman Coulter Gallior Flow Cytometer for analysis of cell cycle.

6.2.6 Preparation of protein lysate and Western blotting

VCaP cells were seeded in 6-well plates overnight and treated with 20 μM α-T3, 10 μM δ-T3 and 20 μM γ-T3 for 24 hours. After treatment, cells were washed with cold PBS and harvested. Cells were lysed with RIPA buffer containing protease inhibitor cocktail. Protein concentration was determined using the bicinchoninic acid assay (Thermo Fisher Scientific, Rockford, IL). Protein (15 μg) was loaded on to Criterion™ Tris-HCL 4-15% gel (Biorad, Hercules, CA) and transferred to PVDF membrane. The membrane was incubated with 5% bovine serum albumin (BSA) in 0.1% TBST buffer for 1 h, and then incubated with primary and horseradish peroxidase-conjugated secondary antibodies overnight and 1 h, respectively. The membrane was washed four times, 10 min per wash, with 0.1% TBST after antibody incubation. The protein bands were visualized with the Super Signal chemiluminescent substrate (Thermo Fisher

Scientific) in the BioRad ChemiDoc XRS system and semiquantified using ImageJ program.

6.2.7 RNA extraction and reverse transcription quantitative-PCR

VCaP cells were seeded in 6-well plates overnight and treated with 20 μM α-T3, 10 μM δ-T3 and 20 μM γ-T3 for 6 hours. After treatment, cells were washed with cold PBS and harvested. Total RNA was extracted using RNeasy kit (Qiagen, Valencia, CA) according to the manufacturer's instructions. Reverse transcription (RT) was carried out using TapMan® RT reagents (Applied Biosystems). The cDNA was used as the template for PCR reaction performed using Power SYBR Green PCR Master Mix. Relative mRNA expression levels were determined by quantitative real-time PCR (ABI7900HT) using the ΔΔCt method.

6.2.8 Statistical Analysis

Cell viability, cell growth (day 3), tumor volume (week 8), tumor weight and mRNA expression were analyzed using one-way ANOVA, in which treatment was regarded as the main effect, followed by t-test. Distribution of cell cycle was analyzed using Chi-square test, in which original count of cells in each phase was used for analysis. Type-I error of multiple comparison was adjusted by the Sidak method, assuming each comparison was independent.

6.3 Results

6.3.1 Mixed T3 inhibits the growth of human prostate cancer in nude mice

Oral gavage of saline, 200 mg/kg, and 400 mg/kg three times a week did not affect the overall health of nude mice. Body, liver and kidney weights did not differ significantly among the three groups. The luminescence images (Figure 6-2A) showed a gradual increase in tumor volume in all three groups, with the strongest signal in the control group. In week 8, mice were euthanized, and tumors were collected and weighed.

The tumor weight and luminescent signal were highly correlated with each other (R^2=0.85, data not shown). Both measurement demonstrated mixed T3 inhibited the growth of subcutaneously implanted human prostate cancer VCaP cells in nude mice in a dose-dependent manner (Figure 6-2B and C). The high dose group (400 mg/kg of total tocotrienols and α-tocopherol) had significantly lower tumor volume and tumor weight at week 8 than the control group.

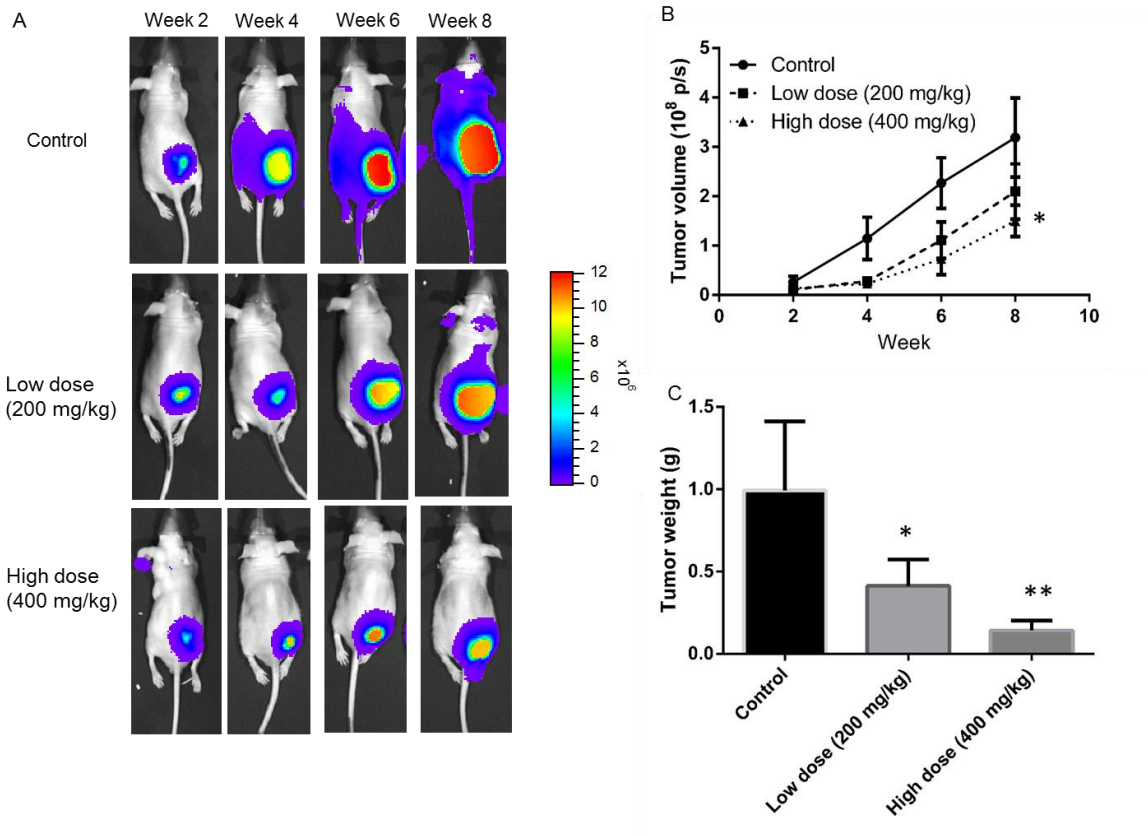

Figure 6-2. Oral administration of the mixture of tocotrienols suppresses the growth of human prostate tumor in nude mice.

The control (n = 10), low dose (n = 12) and high dose (n = 12) group were orally given saline, 200 mg/kg, and 400 mg/kg of total T3 and α-tocopherol three times/week for eight weeks. (A) Bioluminescence IVIS images of subcutaneously implanted prostate tumors. (B) Strength of bioluminescence signal (photons/second) at week 2, 4, 6, and 8. (C) Tumor weight measured on the last day (week 8) when mice were euthanized. Data are represented as mean ± SD. *, p-value < 0.05.

6.3.2 Distribution of tocotrienols (T3) and tocopherols (T) in tumors, prostates and plasma in nude mice treated with the mixed T3

All mice were fed AIN76A diet containing 0.1g/kg α-T. In the control group given saline as the vehicle control, α-T was the predominant form of vitamin E (Table 3). Oral administration of 200 and 400 mg/kg mixed T3 three times a week for 8 weeks

markedly increased the concentration of α-, δ-, and γ-T3 in tumors, prostates and plasma (Table 3). In the low dose group, the average level of total T3 (α, δ and γ combined) were 19.74 μmol/kg, 27.57 μmol/kg and 4.96 μmol/L in tumors, prostates and plasma, respectively. In the high dose group, the average level of total T3 were 26.07 μmol/kg, 76.12 μmol/kg and 4.74 μmol/L in tumors, prostates and plasma, respectively. Notably, prostates and tumors had much higher accumulation of T3 than plasma, indicating excellent exposure to T3 in these target tissues after oral administration. Meanwhile, the level of α-T was only increased slightly after the mixed T3 treatment, and δ- and γ-T almost remained the same.

Table 3. Concentrations of different tocotrienols (T3) and tocopherols (T) in tumors, prostates, brains and plasma in nude mice.

	Prostate (μmol/kg, mean ± SD)					
	α-T3	δ-T3	γ-T3	α-T	δ-T	γ-T
Control	0.51 ± 0.20	0.33 ± 0.24	0.92 ± 0.20	28.23 ± 8.37	0.14 ± 0.02	1.20 ± 0.31
200 mg/kg mixed T3	8.91 ± 7.80	5.39 ± 1.32	13.27 ± 3.66	30.02 ± 8.01	0.11 ± 0.01	0.65 ± 0.09
400 mg/kg mixed T3	34.91 ± 17.10	9.89 ± 2.67	31.32 ± 11.63	43.95 ± 11.94	0.16 ± 0.04	0.81 ± 0.26

	Tumor (μmol/kg, mean ± SD)					
	α-T3	δ-T3	γ-T3	α-T	δ-T	γ-T
Control	0.35 ± 0.19	0.00 ± 0.00	0.43 ± 0.19	18.26 ± 4.75	0.04 ± 0.02	0.42 ± 0.12
200 mg/kg mixed T3	6.87 ± 3.94	2.64 ± 2.08	10.23 ± 10.79	24.14 ± 4.23	0.08 ± 0.02	0.45 ± 0.16
400 mg/kg mixed T3	10.59 ± 0.79	4.41 ± 0.42	11.07 ± 0.39	15.88 ± 2.76	0.05 ± 0.01	0.41 ± 0.26

	Brain (μmol/kg, mean ± SD)					
	α-T3	δ-T3	γ-T3	α-T	δ-T	γ-T
Control	0.10 ± 0.11	0.02 ± 0.03	0.11 ± 0.13	11.76 ± 0.77	0.06 ± 0.03	1.40 ± 0.47
200 mg/kg mixed T3	2.55 ± 0.47	0.14 ± 0.05	0.64 ± 1.32	44.15 ± 8.98	0.49 ± 0.09	0.40 ± 0.15
400 mg/kg mixed T3	4.05 ± 0.18	0.37 ± 0.11	1.91 ± 0.61	49.24 ± 5.09	0.64 ± 0.05	0.22 ± 0.02

	Plasma (μmol/L, mean ± SD)					
	α-T3	δ-T3	γ-T3	α-T	δ-T	γ-T
Control	0.06 ± 0.07	0.07 ± 0.08	0.17 ± 0.20	4.76 ± 0.36	0.02 ± 0.01	0.08 ± 0.02
200 mg/kg mixed T3	1.49 ± 0.13	0.65 ± 0.15	2.82 ± 1.10	6.19 ± 2.47	0.04 ± 0.02	0.08 ± 0.02
400 mg/kg mixed T3	1.59 ± 1.22	0.60 ± 0.36	2.55 ± 1.81	5.89 ± 1.06	0.03 ± 0.01	0.06 ± 0.02

6.3.3 Effects of tocotrienol (T3) on cell growth and cell cycle in VCaP cells

All three T3 inhibited the viability of VCaP cells in a dose-dependent manner (Figure 6-3A). The order of *in vitro* cytotoxicity was δ- > γ- > α-tocotrienol. The IC_{50} (concentration caused 50% cell death) was estimated to be >100, 24 ± 8, and 49 ± 15 μM for α-, δ- and γ-T3, respectively. The effective concentrations of δ- and γ-T3 *in vitro* appears to be achievable in the prostate by oral administration of mixed T3, based on tissue levels shown in the Table 3. VCaP cells were treated with T3 at concentration lower than IC_{50} to examine the effects of T3 on cell growth and cell cycle. Treatment of 10 μM δ-T3 and 20 μM γ-T3 significantly inhibited the growth of VCaP cells *in vitro* (Figure 6-3B). In agreement with the cytotoxicity effect, δ-T3 was the most effective homologs among different homologs of T3 in inhibiting cell grown. In addition, cells treated with 10 μM δ-T3 had significantly higher percentage in G1 phase and lower percentage in S phase than the control cells; 20 μM γ-T3 treated cells also had significantly higher percentage in G1 phase than the control cell, although the accumulation was not so strong compared to 10 μM δ-T3 treated cells (Figure 6-3 C and D).

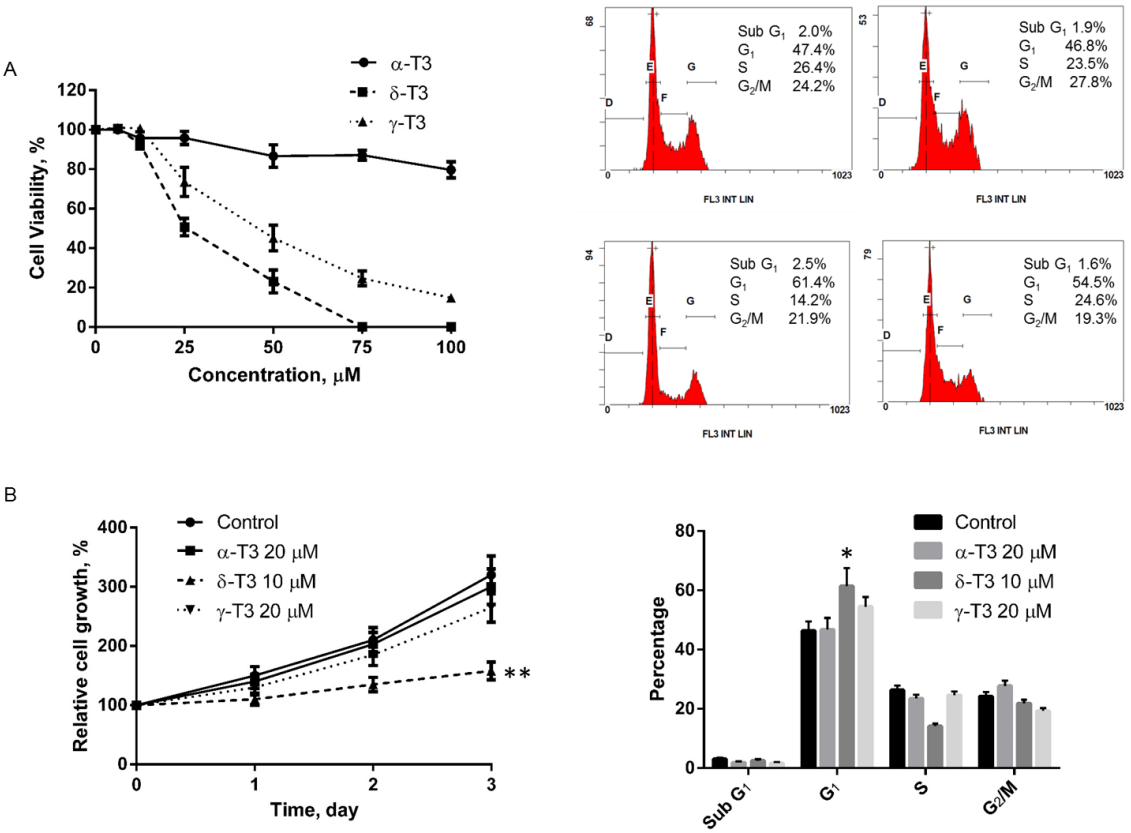

Figure 6-3. Effects of α-, δ- and γ-tocotrienol (T3) on cell growth and cell cycle *in vitro.*

(A) T3s inhibited cell viability in dose-dependent manner. VCaP cells were treated with T3sat concentration of 0-100 μM for 24 hours. Cell viability was measured as described in Materials and Methods. (B) Effects of T3 on cell growth. VCaP cells were cultured with or without 20, 10, and 20 α-, δ- and γ-T3 for 1 to 3 days. (C) Representative results from flow cytometry analysis. (D) Percentage of VCaP cells in different phases of cell cycle. VCaP cells were culture with or without 20, 10, and 20 α-, δ- and γ-T3 for 24 hours and then stained with propidium iodide as described. Bars represent standard deviation of at least three independent experiments. *, p-value < 0.05; **, p-value < 0.01.

6.3.4 Effects of tocotrienol (T3) on expression cyclins D1 and cyclin A

It is known that D-type cyclins serve to convey extracellular signals to the cell cycle controlling system, which is responsible for advancing cell cycle from early G1 phase to late G1 phase. In the S phase, the level cyclin A and E dramatically increases, and they drive cell through S the phase to enter the M phase. We measured these key proteins involved in cell cycle control. As shown in Figure 6-4A, δ- and γ-T3 inhibited the expression of cyclin D1 in the protein and mRNA levels (Figure 6-4), which was consistent with the observed cell cycle arrest in the G1 phase. Only δ-T3 reduced the protein expression cyclin A. The mRNA expression of cylin A was not altered by any of T3s. The expression of cyclin E did not change either (data not shown).

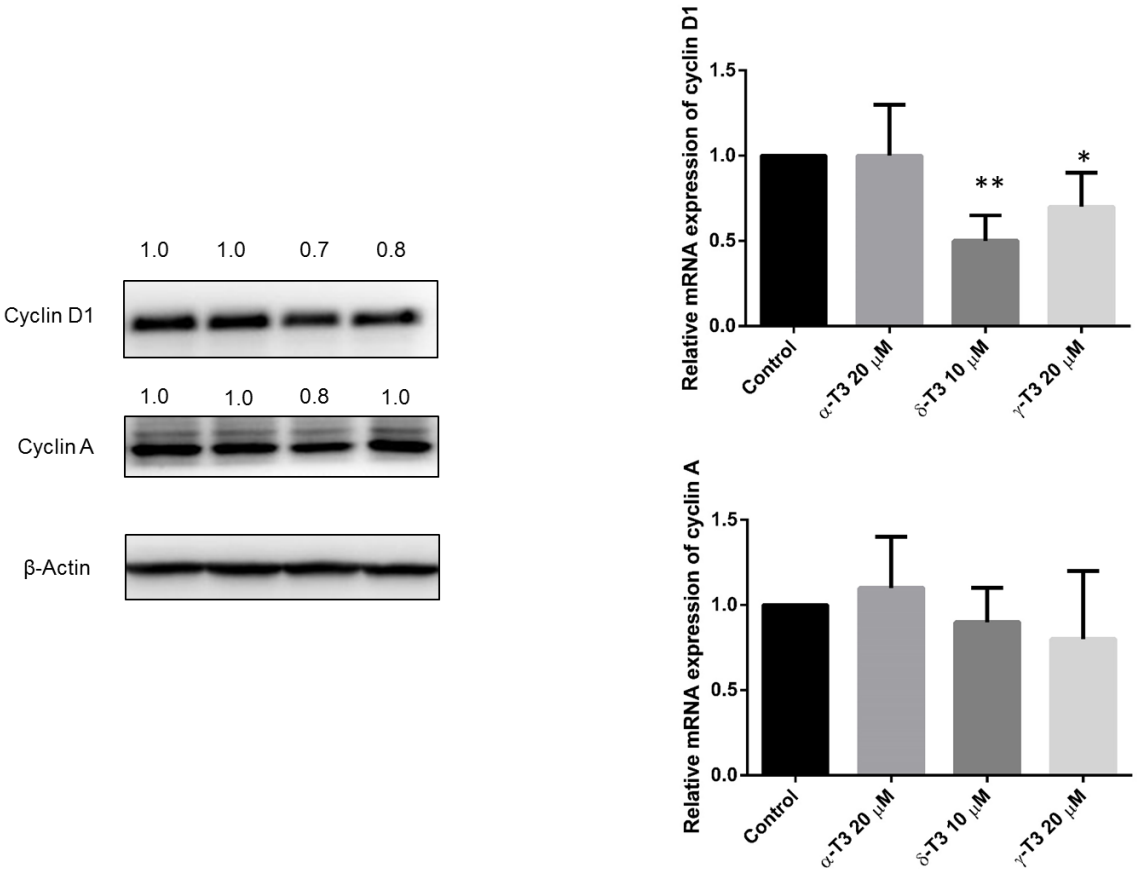

Figure 6-4. Expression of cyclin D1 and cyclin A in VCaP cells.

VCaP cells were treated with 20, 10, and 20 μM α-, δ- and γ-T3 for 24 hours. Protein or mRNA were extracted. (A) Western blotting for cyclin D1 and cyclin A. β-actin was used to normalize difference in protein loading. Numbers on top of the bands represent changes in protein levels relative to control, determined by densitometric analysis using ImageJ. (B) Relative mRNA expression of cyclin D1 and cyclin A. Bars represent standard deviation of at least three independent experiments. *, p-value < 0.05; **, p-value < 0.01.

6.3.5 Effects of tocotrienol (T3) on expression cyclin-dependent kinases p21 and p27

Next, we examined whether cyclin-dependent kinases were altered by T3 treatment. In agreement with the effects of cell growth inhibition, α-T3 treatment did not alter the expression of p21 or p27 in the protein and mRNA level. Both δ- and γ-T3 induced the protein and mRNA level of p21, and δ-T3 exhibited stronger effect. In addition, δ- and γ-T3 induced the protein and mRNA level of p27, and and γ-T3 showed strong effect.

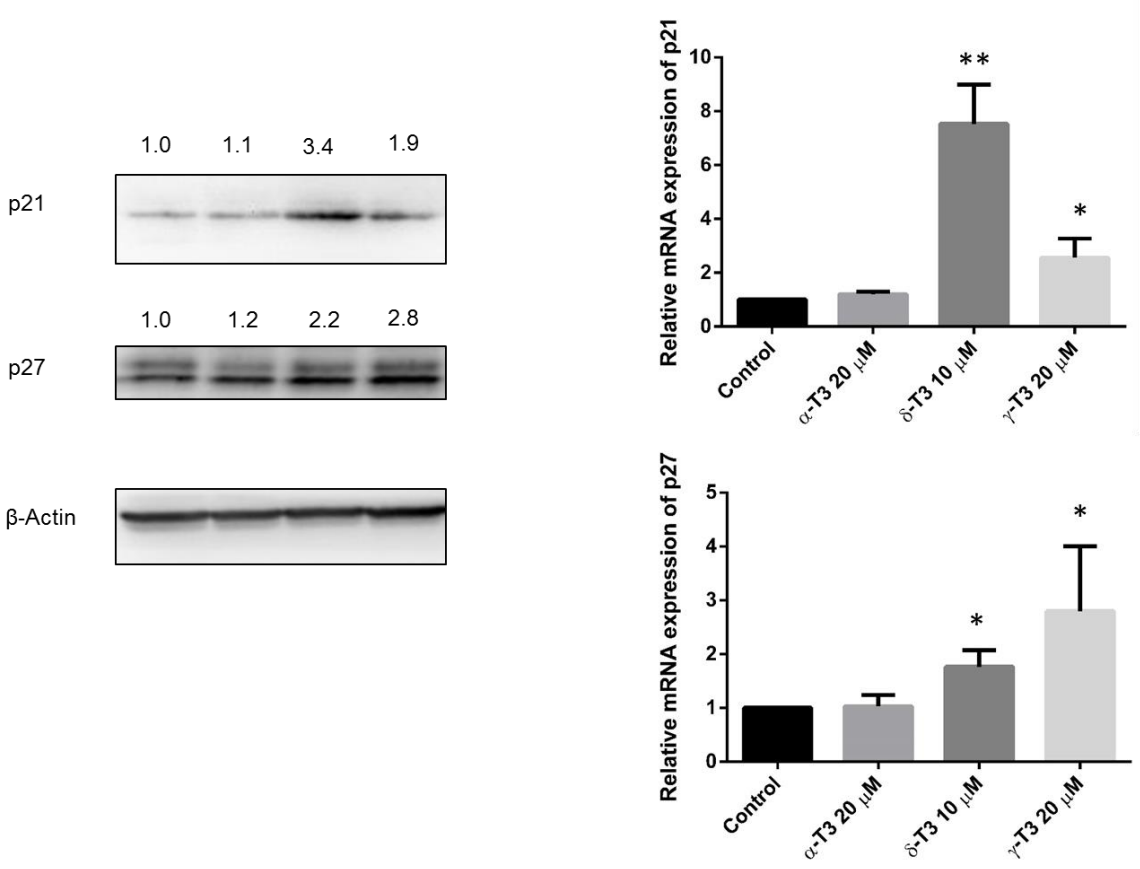

Figure 6-5. Expression of p21 and p27 in VCaP cells.

VCaP cells were treated with 20, 10, and 20 μM α-, δ- and γ-T3 for 24 hours. Protein or mRNA were extracted. (A) Western blotting for p21 and p27. β-actin was used to normalize difference in protein loading. Numbers on top of the bands represent changes in protein levels relative to control, determined by densitometric analysis using ImageJ. (B) Relative mRNA expression of p21 and p27. Bars represent

standard deviation of at least three independent experiments. *, p-value < 0.05; **, p-value < 0.01.

6.4 Discussion

In this study, we demonstrate that the effects of tocotrienols (T3) on inhibiting the growth of human prostate cancer *in vivo* and *in vitro* and their effects on cell cycle regulation. Our results show that (i) oral administration of mixed T3 inhibits the growth of xenografted human VCaP prostate tumors in nude mice; (ii) tumors and prostates are good target tissues for T3 accumulation after oral administration; (iii) *in vitro* T3 treatment at physiologically achievable concentration causes cell cycle arrest at the G1 phase, associated with inhibition of cyclin D1 and cyclin A and induction of p21 and p27.

Oral administration of 200 and 400 mg/kg mixed T3 markedly increased α-, δ- and γ-T3 levels in the body, especially in the tumor and prostate. A dose of 200 mg/kg in mice is equivalent to 1138 mg for 70 kg humans [351]. This dosage can be obtained by taking commercially available supplementation, which typically contain 500 mg or 1000 mg of T3 per capsule. Furthermore, we found that total level of T3 were much higher in prostate and tumor tissues than in plasma (Table 1). This result was consistent with previously studies showing high accumulation of δ-T3 in breast and pancreas tissues after oral administration of δ-T3 [343, 352]. The level γ-T3 is also found to be higher in the xenografted PC3 tumor than plasma after intraperitoneal injection of γ-T3 [345]. Therefore, T3 can successfully accumulate in target organs to block tumor growth, which is critical to be used as preventive or therapeutic agents.

Treatment of δ- and γ-T3 at physiologically relevant concentration led to cell cycle arrest at the G_1 phase, associated with inhibition of cyclin D1 and cyclin A and induction of cyclin-dependent kinase (CDK) inhibitors p21 and p27 (Figure 6-3 and

Figure 6-4). Previous studies have shown that δ-T3 and T3-rich fraction induce cell cycle arrest in pancreatic cancer cells, melanoma cells, diploid fibroblasts and adipocytes [341, 353-355]. Cell cycle progression is tightly controlled by cooperation of a group of cyclin proteins and CDK. Among cyclin proteins, cyclin D is found to drive cells to enter G_1 phase and progress to pass the checkpoint in late G1. Cyclin A is responsible to promote passage through S phase. In addition, cyclin-CDK complexes are also regulated by CDK inhibitors. The cip family of CDK inhibitors such as p21 and p27 are found to inhibit cyclin-CDK complexes that forms after G_1 phase. Together, the growth inhibitory effect of mixed T3, mainly δ- and γ-T3, could be the results of cell cycle arrest through modulation of cyclins and CDK inhibitors.

Use of vitamin E as a strategy to prevent prostate cancer has been extensively examined in clinical and preclinical studies. However, most of studies focused on α-tocopherol (T). For example, the Selenium and Vitamin E Cancer Prevention Trials (SELECT) and the Physicians' Health Study II tested daily supplementation of 400 IU α-tocopherol in healthy men, but did not show efficacy in preventing prostate cancer after 7-12 years of follow-up [279, 356]. The biological activity of T3 differs dramatically from T. Especially, T3 has superior anti-cancer effects than T, as shown in both *in vitro* and *in vivo* studies [344, 349]. Our present study as well as other studies have demonstrated that T3 treatment inhibits prostate cancer including LNCaP, VCaP and PC3 in xenograft models and in TRAMP mice [344-346]. These findings would support future studies in humans using more effective vitamin E homologs such as δ- and γ-T3.

6.5 Conclusions

In this study, we showed that a naturally occurring mixture of tocotrienols inhibited the growth of VCaP prostate tumors in nude mice. The antitumor effect of the

tocotrienol mixture might be related to the cell cycle arrest, especially due to the effect of δ-tocotrienols. Since our study demonstrated a strong inhibitory effect of the tocotrienol mixture without apparent toxicity at tested dose, clinical studies in men with a high risk of prostate cancer are warranted to examine the potential preventive effect of this agent.

7 Summary

In this dissertation, we have shown that the transcription factor Nrf2 plays a critical role in cellular defensive response against the peroxidation product of lipid, 4-HNE, through induction of antioxidant and phase II detoxifying enzymes. Increased serum lipid peroxidation has been observed in patients with advanced prostate cancer [357]. It has been suggested that prostate cancer, especially the aggressive stage, is associated with elevated oxidative stress [357-360]. Various molecular events can lead to increased production of ROS, including metabolic alteration, androgen receptor activation, mitochondrial dysfunctions, inflammation, xenobiotic metabolism and hypoxia [361]. In addition, reduced expression of Nrf2 and GSTP1 due to promoter hypermethylation might also exacerbate oxidative stress [362, 363]. Given the important role of Nrf2 in modulating cellular defense against oxidative stress and carcinogens, it is rational to target Nrf2 as a strategy for prostate cancer prevention. Many phytochemicals have been shown to activate the Nrf2 pathway and induce the expression of Nrf2-regulated genes [13, 320]. We show in this dissertation that curcumin and γTmT can epigenetically restore Nrf2 expression via demethylation of CpG islands in the TRAMP model. Both curcumin and γTmT are effective in inhibiting prostate cancer in the TRAMP model. The TRAMP model is a commonly used mouse model for prostate cancer. Here we have demonstrated that a number of functions are altered in the prostate of TRAMP mice, compared to non-transgenic mice, including proliferation and phase II/antioxidant functions. Furthermore, we have shown that a naturally occurring mixture of tocotrienols inhibits the growth of human prostate tumor in nude mice by cell cycle arrest in G1 phase. Taken together, we have provided convincing data to demonstrate the chemopreventive potential of phytochemicals in mouse prostate cancer models. The ultimate proof of efficacy of

phytochemicals in prostate cancer prevention require well-designed long-term phase III clinical trials.

8 References

1. Center, M.M., et al., International variation in prostate cancer incidence and mortality rates. Eur Urol, 2012. **61**(6): p. 1079-92.
2. Siegel, R., et al., Cancer statistics, 2014. CA Cancer J Clin, 2014. **64**(1): p. 9-29.
3. Shen, M.M. and C. Abate-Shen, Molecular genetics of prostate cancer: new prospects for old challenges. Genes Dev, 2010. **24**(18): p. 1967-2000.
4. Li, L.C., P.R. Carroll, and R. Dahiya, Epigenetic changes in prostate cancer: implication for diagnosis and treatment. J Natl Cancer Inst, 2005. **97**(2): p. 103-15.
5. Sporn, M.B., Approaches to prevention of epithelial cancer during the preneoplastic period. Cancer Res, 1976. **36**(7 PT 2): p. 2699-702.
6. Surh, Y.J., Cancer chemoprevention with dietary phytochemicals. Nat Rev Cancer, 2003. **3**(10): p. 768-80.
7. Prevention of cancer in the next millennium: Report of the Chemoprevention Working Group to the American Association for Cancer Research. Cancer Res, 1999. **59**(19): p. 4743-58.
8. Chen, C. and A.N. Kong, Dietary cancer-chemopreventive compounds: from signaling and gene expression to pharmacological effects. Trends Pharmacol Sci, 2005. **26**(6): p. 318-26.
9. Itoh, K., et al., An Nrf2/small Maf heterodimer mediates the induction of phase II detoxifying enzyme genes through antioxidant response elements. Biochem Biophys Res Commun, 1997. **236**(2): p. 313-22.
10. McMahon, M., et al., The Cap'n'Collar basic leucine zipper transcription factor Nrf2 (NF-E2 p45-related factor 2) controls both constitutive and inducible expression of intestinal detoxification and glutathione biosynthetic enzymes. Cancer Res, 2001. **61**(8): p. 3299-307.
11. Iida, K., et al., Nrf2 is essential for the chemopreventive efficacy of oltipraz against urinary bladder carcinogenesis. Cancer Res, 2004. **64**(18): p. 6424-31.
12. Ramos-Gomez, M., et al., Sensitivity to carcinogenesis is increased and chemoprotective efficacy of enzyme inducers is lost in nrf2 transcription factor-deficient mice. Proc Natl Acad Sci U S A, 2001. **98**(6): p. 3410-5.
13. Kwak, M.K. and T.W. Kensler, Targeting NRF2 signaling for cancer chemoprevention. Toxicol Appl Pharmacol, 2010. **244**(1): p. 66-76.
14. Itoh, K., et al., Keap1 represses nuclear activation of antioxidant responsive elements by Nrf2 through binding to the amino-terminal Neh2 domain. Genes Dev, 1999. **13**(1): p. 76-86.
15. McMahon, M., et al., Keap1-dependent proteasomal degradation of transcription factor Nrf2 contributes to the negative regulation of antioxidant response element-driven gene expression. J Biol Chem, 2003. **278**(24): p. 21592-600.
16. Dhakshinamoorthy, S. and A.K. Jaiswal, Functional characterization and role of INrf2 in antioxidant response element-mediated expression and antioxidant induction of NAD(P)H:quinone oxidoreductase1 gene. Oncogene, 2001. **20**(29): p. 3906-17.
17. Kobayashi, A., et al., Oxidative stress sensor Keap1 functions as an adaptor for Cul3-based E3 ligase to regulate proteasomal degradation of Nrf2. Mol Cell Biol, 2004. **24**(16): p. 7130-9.

18. McMahon, M., et al., Dimerization of substrate adaptors can facilitate cullin-mediated ubiquitylation of proteins by a "tethering" mechanism: a two-site interaction model for the Nrf2-Keap1 complex. J Biol Chem, 2006. **281**(34): p. 24756-68.
19. Tong, K.I., et al., Keap1 recruits Neh2 through binding to ETGE and DLG motifs: characterization of the two-site molecular recognition model. Mol Cell Biol, 2006. **26**(8): p. 2887-900.
20. Zhang, D.D., et al., Keap1 is a redox-regulated substrate adaptor protein for a Cul3-dependent ubiquitin ligase complex. Mol Cell Biol, 2004. **24**(24): p. 10941-53.
21. Furukawa, M. and Y. Xiong, BTB protein Keap1 targets antioxidant transcription factor Nrf2 for ubiquitination by the Cullin 3-Roc1 ligase. Mol Cell Biol, 2005. **25**(1): p. 162-71.
22. Wakabayashi, N., et al., Keap1-null mutation leads to postnatal lethality due to constitutive Nrf2 activation. Nat Genet, 2003. **35**(3): p. 238-45.
23. Suzuki, T., J. Maher, and M. Yamamoto, Select heterozygous Keap1 mutations have a dominant-negative effect on wild-type Keap1 in vivo. Cancer Res, 2011. **71**(5): p. 1700-9.
24. Dinkova-Kostova, A.T., et al., Direct evidence that sulfhydryl groups of Keap1 are the sensors regulating induction of phase 2 enzymes that protect against carcinogens and oxidants. Proc Natl Acad Sci U S A, 2002. **99**(18): p. 11908-13.
25. Suzuki, T., H. Motohashi, and M. Yamamoto, Toward clinical application of the Keap1-Nrf2 pathway. Trends Pharmacol Sci, 2013. **34**(6): p. 340-6.
26. McMahon, M., et al., Keap1 perceives stress via three sensors for the endogenous signaling molecules nitric oxide, zinc, and alkenals. Proc Natl Acad Sci U S A, 2010. **107**(44): p. 18838-43.
27. Zhang, D.D. and M. Hannink, Distinct cysteine residues in Keap1 are required for Keap1-dependent ubiquitination of Nrf2 and for stabilization of Nrf2 by chemopreventive agents and oxidative stress. Mol Cell Biol, 2003. **23**(22): p. 8137-51.
28. Takaya, K., et al., Validation of the multiple sensor mechanism of the Keap1-Nrf2 system. Free Radic Biol Med, 2012. **53**(4): p. 817-27.
29. Eggler, A.L., et al., Modifying specific cysteines of the electrophile-sensing human Keap1 protein is insufficient to disrupt binding to the Nrf2 domain Neh2. Proc Natl Acad Sci U S A, 2005. **102**(29): p. 10070-5.
30. Nguyen, T., et al., Nrf2 controls constitutive and inducible expression of ARE-driven genes through a dynamic pathway involving nucleocytoplasmic shuttling by Keap1. J Biol Chem, 2005. **280**(37): p. 32485-92.
31. Hayes, J.D., et al., Cancer chemoprevention mechanisms mediated through the Keap1-Nrf2 pathway. Antioxid Redox Signal, 2010. **13**(11): p. 1713-48.
32. Huang, H.C., T. Nguyen, and C.B. Pickett, Regulation of the antioxidant response element by protein kinase C-mediated phosphorylation of NF-E2-related factor 2. Proc Natl Acad Sci U S A, 2000. **97**(23): p. 12475-80.
33. Sun, Z., Z. Huang, and D.D. Zhang, Phosphorylation of Nrf2 at multiple sites by MAP kinases has a limited contribution in modulating the Nrf2-dependent antioxidant response. PLoS One, 2009. **4**(8): p. e6588.
34. Numazawa, S., et al., Atypical protein kinase C mediates activation of NF-E2-related factor 2 in response to oxidative stress. Am J Physiol Cell Physiol, 2003. **285**(2): p. C334-42.

35. Bloom, D.A. and A.K. Jaiswal, Phosphorylation of Nrf2 at Ser40 by protein kinase C in response to antioxidants leads to the release of Nrf2 from INrf2, but is not required for Nrf2 stabilization/accumulation in the nucleus and transcriptional activation of antioxidant response element-mediated NAD(P)H:quinone oxidoreductase-1 gene expression. J Biol Chem, 2003. **278**(45): p. 44675-82.
36. Lee, J.H., et al., Dietary phytochemicals and cancer prevention: Nrf2 signaling, epigenetics, and cell death mechanisms in blocking cancer initiation and progression. Pharmacol Ther, 2013. **137**(2): p. 153-71.
37. Cullinan, S.B. and J.A. Diehl, PERK-dependent activation of Nrf2 contributes to redox homeostasis and cell survival following endoplasmic reticulum stress. J Biol Chem, 2004. **279**(19): p. 20108-17.
38. Kang, K.W., et al., Phosphatidylinositol 3-kinase regulates nuclear translocation of NF-E2-related factor 2 through actin rearrangement in response to oxidative stress. Mol Pharmacol, 2002. **62**(5): p. 1001-10.
39. Jain, A.K. and A.K. Jaiswal, GSK-3beta acts upstream of Fyn kinase in regulation of nuclear export and degradation of NF-E2 related factor 2. J Biol Chem, 2007. **282**(22): p. 16502-10.
40. Rada, P., et al., SCF/{beta}-TrCP promotes glycogen synthase kinase 3-dependent degradation of the Nrf2 transcription factor in a Keap1-independent manner. Mol Cell Biol, 2011. **31**(6): p. 1121-33.
41. Chowdhry, S., et al., Nrf2 is controlled by two distinct beta-TrCP recognition motifs in its Neh6 domain, one of which can be modulated by GSK-3 activity. Oncogene, 2013. **32**(32): p. 3765-81.
42. Rojo, A.I., M.R. Sagarra, and A. Cuadrado, GSK-3beta down-regulates the transcription factor Nrf2 after oxidant damage: relevance to exposure of neuronal cells to oxidative stress. J Neurochem, 2008. **105**(1): p. 192-202.
43. DeNicola, G.M., et al., Oncogene-induced Nrf2 transcription promotes ROS detoxification and tumorigenesis. Nature, 2011. **475**(7354): p. 106-9.
44. Li, W., et al., An internal ribosomal entry site mediates redox-sensitive translation of Nrf2. Nucleic Acids Res, 2010. **38**(3): p. 778-88.
45. Ghavifekr Fakhr, M., et al., DNA Methylation Pattern as Important Epigenetic Criterion in Cancer. Genet Res Int, 2013. **2013**: p. 317569.
46. Esteller, M., CpG island hypermethylation and tumor suppressor genes: a booming present, a brighter future. Oncogene, 2002. **21**(35): p. 5427-40.
47. Issa, J.P. and H.M. Kantarjian, Targeting DNA methylation. Clin Cancer Res, 2009. **15**(12): p. 3938-46.
48. Feinberg, A.P. and B. Tycko, The history of cancer epigenetics. Nat Rev Cancer, 2004. **4**(2): p. 143-53.
49. Arasaradnam, R.P., et al., A review of dietary factors and its influence on DNA methylation in colorectal carcinogenesis. Epigenetics, 2008. **3**(4): p. 193-8.
50. Egger, G., et al., Epigenetics in human disease and prospects for epigenetic therapy. Nature, 2004. **429**(6990): p. 457-63.
51. Esteller, M., Epigenetics in cancer. N Engl J Med, 2008. **358**(11): p. 1148-59.
52. Yu, S., et al., Nrf2 expression is regulated by epigenetic mechanisms in prostate cancer of TRAMP mice. PLoS One, 2010. **5**(1): p. e8579.
53. Huang, Y., et al., A gamma-tocopherol-rich mixture of tocopherols maintains Nrf2 expression in prostate tumors of TRAMP mice via epigenetic inhibition of CpG methylation. J Nutr, 2012. **142**(5): p. 818-23.

54. Zhang, C., et al., Sulforaphane enhances Nrf2 expression in prostate cancer TRAMP C1 cells through epigenetic regulation. Biochem Pharmacol, 2013. **85**(9): p. 1398-404.
55. Wu, T.Y., et al., Epigenetic modifications of Nrf2 by 3,3'-diindolylmethane in vitro in TRAMP C1 cell line and in vivo TRAMP prostate tumors. AAPS J, 2013. **15**(3): p. 864-74.
56. Su, Z.Y., et al., Requirement and Epigenetics Reprogramming of Nrf2 in Suppression of Tumor Promoter TPA-Induced Mouse Skin Cell Transformation by Sulforaphane. Cancer Prev Res (Phila), 2014. **7**(3): p. 319-29.
57. Croce, C.M., Causes and consequences of microRNA dysregulation in cancer. Nat Rev Genet, 2009. **10**(10): p. 704-14.
58. Narasimhan, M., et al., Identification of novel microRNAs in post-transcriptional control of Nrf2 expression and redox homeostasis in neuronal, SH-SY5Y cells. PLoS One, 2012. **7**(12): p. e51111.
59. Sangokoya, C., M.J. Telen, and J.T. Chi, microRNA miR-144 modulates oxidative stress tolerance and associates with anemia severity in sickle cell disease. Blood, 2010. **116**(20): p. 4338-48.
60. Yang, M., et al., MiR-28 regulates Nrf2 expression through a Keap1-independent mechanism. Breast Cancer Res Treat, 2011. **129**(3): p. 983-91.
61. Li, N., et al., Increased expression of miR-34a and miR-93 in rat liver during aging, and their impact on the expression of Mgst1 and Sirt1. Mech Ageing Dev, 2011. **132**(3): p. 75-85.
62. Eades, G., et al., miR-200a regulates Nrf2 activation by targeting Keap1 mRNA in breast cancer cells. J Biol Chem, 2011. **286**(47): p. 40725-33.
63. Prestera, T., et al., Chemical and molecular regulation of enzymes that detoxify carcinogens. Proc Natl Acad Sci U S A, 1993. **90**(7): p. 2965-9.
64. Bryan, H.K., et al., The Nrf2 cell defence pathway: Keap1-dependent and -independent mechanisms of regulation. Biochem Pharmacol, 2013. **85**(6): p. 705-17.
65. Eggler, A.L., et al., Identification of the highly reactive cysteine 151 in the chemopreventive agent-sensor Keap1 protein is method-dependent. Chem Res Toxicol, 2007. **20**(12): p. 1878-84.
66. Wakabayashi, N., et al., Protection against electrophile and oxidant stress by induction of the phase 2 response: fate of cysteines of the Keap1 sensor modified by inducers. Proc Natl Acad Sci U S A, 2004. **101**(7): p. 2040-5.
67. Abiko, Y., et al., Participation of covalent modification of Keap1 in the activation of Nrf2 by tert-butylbenzoquinone, an electrophilic metabolite of butylated hydroxyanisole. Toxicol Appl Pharmacol, 2011. **255**(1): p. 32-9.
68. Hu, C., et al., Modification of keap1 cysteine residues by sulforaphane. Chem Res Toxicol, 2011. **24**(4): p. 515-21.
69. Kobayashi, M., et al., The antioxidant defense system Keap1-Nrf2 comprises a multiple sensing mechanism for responding to a wide range of chemical compounds. Mol Cell Biol, 2009. **29**(2): p. 493-502.
70. Hu, R., et al., Gene expression profiles induced by cancer chemopreventive isothiocyanate sulforaphane in the liver of C57BL/6J mice and C57BL/6J/Nrf2 (-/-) mice. Cancer Lett, 2006. **243**(2): p. 170-92.
71. Thimmulappa, R.K., et al., Identification of Nrf2-regulated genes induced by the chemopreventive agent sulforaphane by oligonucleotide microarray. Cancer Res, 2002. **62**(18): p. 5196-203.

72. Khor, T.O., et al., Pharmacogenomics of cancer chemopreventive isothiocyanate compound sulforaphane in the intestinal polyps of ApcMin/+ mice. Biopharm Drug Dispos, 2006. **27**(9): p. 407-20.
73. Xu, C., et al., Inhibition of 7,12-dimethylbenz(a)anthracene-induced skin tumorigenesis in C57BL/6 mice by sulforaphane is mediated by nuclear factor E2-related factor 2. Cancer Res, 2006. **66**(16): p. 8293-6.
74. Nair, S., et al., Regulation of Nrf2- and AP-1-mediated gene expression by epigallocatechin-3-gallate and sulforaphane in prostate of Nrf2-knockout or C57BL/6J mice and PC-3 AP-1 human prostate cancer cells. Acta Pharmacol Sin, 2010. **31**(9): p. 1223-40.
75. Keum, Y.S., et al., Pharmacokinetics and pharmacodynamics of broccoli sprouts on the suppression of prostate cancer in transgenic adenocarcinoma of mouse prostate (TRAMP) mice: implication of induction of Nrf2, HO-1 and apoptosis and the suppression of Akt-dependent kinase pathway. Pharm Res, 2009. **26**(10): p. 2324-31.
76. Wang, H., et al., Pharmacokinetics and pharmacodynamics of phase II drug metabolizing/antioxidant enzymes gene response by anticancer agent sulforaphane in rat lymphocytes. Mol Pharm, 2012. **9**(10): p. 2819-27.
77. Kensler, T.W., et al., Keap1-nrf2 signaling: a target for cancer prevention by sulforaphane. Top Curr Chem, 2013. **329**: p. 163-77.
78. Shapiro, T.A., et al., Safety, tolerance, and metabolism of broccoli sprout glucosinolates and isothiocyanates: a clinical phase I study. Nutr Cancer, 2006. **55**(1): p. 53-62.
79. Egner, P.A., et al., Bioavailability of Sulforaphane from two broccoli sprout beverages: results of a short-term, cross-over clinical trial in Qidong, China. Cancer Prev Res (Phila), 2011. **4**(3): p. 384-95.
80. Kensler, T.W., et al., Modulation of the metabolism of airborne pollutants by glucoraphanin-rich and sulforaphane-rich broccoli sprout beverages in Qidong, China. Carcinogenesis, 2012. **33**(1): p. 101-7.
81. Liby, K., et al., The synthetic triterpenoids, CDDO and CDDO-imidazolide, are potent inducers of heme oxygenase-1 and Nrf2/ARE signaling. Cancer Res, 2005. **65**(11): p. 4789-98.
82. Thimmulappa, R.K., et al., Preclinical evaluation of targeting the Nrf2 pathway by triterpenoids (CDDO-Im and CDDO-Me) for protection from LPS-induced inflammatory response and reactive oxygen species in human peripheral blood mononuclear cells and neutrophils. Antioxid Redox Signal, 2007. **9**(11): p. 1963-70.
83. Liby, K.T., M.M. Yore, and M.B. Sporn, Triterpenoids and rexinoids as multifunctional agents for the prevention and treatment of cancer. Nat Rev Cancer, 2007. **7**(5): p. 357-69.
84. Eggler, A.L., et al., Cul3-mediated Nrf2 ubiquitination and antioxidant response element (ARE) activation are dependent on the partial molar volume at position 151 of Keap1. Biochem J, 2009. **422**(1): p. 171-80.
85. Yates, M.S., et al., Genetic versus chemoprotective activation of Nrf2 signaling: overlapping yet distinct gene expression profiles between Keap1 knockout and triterpenoid-treated mice. Carcinogenesis, 2009. **30**(6): p. 1024-31.
86. Liby, K.T. and M.B. Sporn, Synthetic oleanane triterpenoids: multifunctional drugs with a broad range of applications for prevention and treatment of chronic disease. Pharmacol Rev, 2012. **64**(4): p. 972-1003.

87. Sussan, T.E., et al., Targeting Nrf2 with the triterpenoid CDDO-imidazolide attenuates cigarette smoke-induced emphysema and cardiac dysfunction in mice. Proc Natl Acad Sci U S A, 2009. **106**(1): p. 250-5.
88. Liu, M., et al., The Nrf2 triterpenoid activator, CDDO-imidazolide, protects kidneys from ischemia-reperfusion injury in mice. Kidney Int, 2014. **85**(1): p. 134-41.
89. Kensler, T.W., et al., Development of cancer chemopreventive agents: oltipraz as a paradigm. Chem Res Toxicol, 1999. **12**(2): p. 113-26.
90. Jia, Z., et al., Generation of superoxide from reaction of 3H-1,2-dithiole-3-thione with thiols: implications for dithiolethione chemoprotection. Mol Cell Biochem, 2008. **307**(1-2): p. 185-91.
91. Velayutham, M., et al., Glutathione-mediated formation of oxygen free radicals by the major metabolite of oltipraz. Chem Res Toxicol, 2005. **18**(6): p. 970-5.
92. Holland, R., et al., Hydrogen peroxide is a second messenger in phase 2 enzyme induction by cancer chemopreventive dithiolethiones. Chem Res Toxicol, 2009. **22**(8): p. 1427-34.
93. Ramos-Gomez, M., et al., Interactive effects of nrf2 genotype and oltipraz on benzo[a]pyrene-DNA adducts and tumor yield in mice. Carcinogenesis, 2003. **24**(3): p. 461-7.
94. Buetler, T.M., et al., Induction of phase I and phase II drug-metabolizing enzyme mRNA, protein, and activity by BHA, ethoxyquin, and oltipraz. Toxicol Appl Pharmacol, 1995. **135**(1): p. 45-57.
95. Wattenberg, L.W. and E. Bueding, Inhibitory effects of 5-(2-pyrazinyl)-4-methyl-1,2-dithiol-3-thione (Oltipraz) on carcinogenesis induced by benzo[a]pyrene, diethylnitrosamine and uracil mustard. Carcinogenesis, 1986. **7**(8): p. 1379-81.
96. Kensler, T.W., et al., Modification of aflatoxin B1 binding to DNA in vivo in rats fed phenolic antioxidants, ethoxyquin and a dithiothione. Carcinogenesis, 1985. **6**(5): p. 759-63.
97. Helzlsouer, K.J. and T.W. Kensler, Cancer chemoprotection by oltipraz: experimental and clinical considerations. Prev Med, 1993. **22**(5): p. 783-95.
98. Kensler, T.W., et al., Mechanism of protection against aflatoxin tumorigenicity in rats fed 5-(2-pyrazinyl)-4-methyl-1,2-dithiol-3-thione (oltipraz) and related 1,2-dithiol-3-thiones and 1,2-dithiol-3-ones. Cancer Res, 1987. **47**(16): p. 4271-7.
99. Zhang, Y. and R. Munday, Dithiolethiones for cancer chemoprevention: where do we stand? Mol Cancer Ther, 2008. **7**(11): p. 3470-9.
100. Wang, J.S., et al., Protective alterations in phase 1 and 2 metabolism of aflatoxin B1 by oltipraz in residents of Qidong, People's Republic of China. J Natl Cancer Inst, 1999. **91**(4): p. 347-54.
101. Yamamoto, T., et al., Physiological significance of reactive cysteine residues of Keap1 in determining Nrf2 activity. Mol Cell Biol, 2008. **28**(8): p. 2758-70.
102. Hong, F., et al., Specific patterns of electrophile adduction trigger Keap1 ubiquitination and Nrf2 activation. J Biol Chem, 2005. **280**(36): p. 31768-75.
103. Yu, R., T.H. Tan, and A.N. Kong, Butylated hydroxyanisole and its metabolite tert-butylhydroquinone differentially regulate mitogen-activated protein kinases. The role of oxidative stress in the activation of mitogen-activated protein kinases by phenolic antioxidants. J Biol Chem, 1997. **272**(46): p. 28962-70.

104. Nair, S., et al., Pharmacogenomics of phenolic antioxidant butylated hydroxyanisole (BHA) in the small intestine and liver of Nrf2 knockout and C57BL/6J mice. Pharm Res, 2006. **23**(11): p. 2621-37.
105. Wang, X.J., et al., Activation of the NRF2 signaling pathway by copper-mediated redox cycling of para- and ortho-hydroquinones. Chem Biol, 2010. **17**(1): p. 75-85.
106. Dinkova-Kostova, A.T. and X.J. Wang, Induction of the Keap1/Nrf2/ARE pathway by oxidizable diphenols. Chem Biol Interact, 2011. **192**(1-2): p. 101-6.
107. Rao, M.S., et al., Inhibitory effect of antioxidants ethoxyquin and 2(3)-tert-butyl-4-hydroxyanisole on hepatic tumorigenesis in rats fed ciprofibrate, a peroxisome proliferator. Cancer Res, 1984. **44**(3): p. 1072-6.
108. Kahl, R., Synthetic antioxidants: biochemical actions and interference with radiation, toxic compounds, chemical mutagens and chemical carcinogens. Toxicology, 1984. **33**(3-4): p. 185-228.
109. Hirose, M., et al., Carcinogenicity of antioxidants BHA, caffeic acid, sesamol, 4-methoxyphenol and catechol at low doses, either alone or in combination, and modulation of their effects in a rat medium-term multi-organ carcinogenesis model. Carcinogenesis, 1998. **19**(1): p. 207-12.
110. He, X., et al., Arsenic induces NAD(P)H-quinone oxidoreductase I by disrupting the Nrf2 x Keap1 x Cul3 complex and recruiting Nrf2 x Maf to the antioxidant response element enhancer. J Biol Chem, 2006. **281**(33): p. 23620-31.
111. Lau, A., et al., Arsenic inhibits autophagic flux, activating the Nrf2-Keap1 pathway in a p62-dependent manner. Mol Cell Biol, 2013. **33**(12): p. 2436-46.
112. Lau, A., et al., A noncanonical mechanism of Nrf2 activation by autophagy deficiency: direct interaction between Keap1 and p62. Mol Cell Biol, 2010. **30**(13): p. 3275-85.
113. Jiang, T., et al., Nrf2 protects against As(III)-induced damage in mouse liver and bladder. Toxicol Appl Pharmacol, 2009. **240**(1): p. 8-14.
114. Valko, M., et al., Free radicals and antioxidants in normal physiological functions and human disease. Int J Biochem Cell Biol, 2007. **39**(1): p. 44-84.
115. Hayes, J.D. and M. McMahon, NRF2 and KEAP1 mutations: permanent activation of an adaptive response in cancer. Trends Biochem Sci, 2009. **34**(4): p. 176-88.
116. Xu, C., C.Y. Li, and A.N. Kong, Induction of phase I, II and III drug metabolism/transport by xenobiotics. Arch Pharm Res, 2005. **28**(3): p. 249-68.
117. Nebert, D.W., et al., Oral benzo[a]pyrene: understanding pharmacokinetics, detoxication, and consequences--Cyp1 knockout mouse lines as a paradigm. Mol Pharmacol, 2013. **84**(3): p. 304-13.
118. Eaton, D.L. and E.P. Gallagher, Mechanisms of aflatoxin carcinogenesis. Annu Rev Pharmacol Toxicol, 1994. **34**: p. 135-72.
119. Bosma-den Boer, M.M., M.L. van Wetten, and L. Pruimboom, Chronic inflammatory diseases are stimulated by current lifestyle: how diet, stress levels and medication prevent our body from recovering. Nutr Metab (Lond), 2012. **9**(1): p. 32.
120. Berk, M., et al., So depression is an inflammatory disease, but where does the inflammation come from? BMC Med, 2013. **11**: p. 200.
121. Chen, X.L. and C. Kunsch, Induction of cytoprotective genes through Nrf2/antioxidant response element pathway: a new therapeutic approach for

the treatment of inflammatory diseases. Current pharmaceutical design, 2004. **10**(8): p. 879-91.
122. Yang, H., et al., Tumour necrosis factor alpha induces co-ordinated activation of rat GSH synthetic enzymes via nuclear factor kappaB and activator protein-1. The Biochemical journal, 2005. **391**(Pt 2): p. 399-408.
123. Chen, X.L., et al., Activation of Nrf2/ARE pathway protects endothelial cells from oxidant injury and inhibits inflammatory gene expression. American journal of physiology. Heart and circulatory physiology, 2006. **290**(5): p. H1862-70.
124. Khor, T.O., et al., Nrf2-deficient mice have an increased susceptibility to dextran sulfate sodium-induced colitis. Cancer Res, 2006. **66**(24): p. 11580-4.
125. Singh, A., et al., Dysfunctional KEAP1-NRF2 interaction in non-small-cell lung cancer. PLoS Med, 2006. **3**(10): p. e420.
126. Rahman, I., S.K. Biswas, and P.A. Kirkham, Regulation of inflammation and redox signaling by dietary polyphenols. Biochemical pharmacology, 2006. **72**(11): p. 1439-52.
127. Yates, M.S. and T.W. Kensler, Chemopreventive promise of targeting the Nrf2 pathway. Drug news & perspectives, 2007. **20**(2): p. 109-17.
128. Cho, H.Y., et al., The transcription factor NRF2 protects against pulmonary fibrosis. The FASEB journal : official publication of the Federation of American Societies for Experimental Biology, 2004. **18**(11): p. 1258-60.
129. Ishii, Y., et al., Transcription factor Nrf2 plays a pivotal role in protection against elastase-induced pulmonary inflammation and emphysema. Journal of immunology, 2005. **175**(10): p. 6968-75.
130. Rangasamy, T., et al., Genetic ablation of Nrf2 enhances susceptibility to cigarette smoke-induced emphysema in mice. The Journal of clinical investigation, 2004. **114**(9): p. 1248-59.
131. Rangasamy, T., et al., Disruption of Nrf2 enhances susceptibility to severe airway inflammation and asthma in mice. The Journal of experimental medicine, 2005. **202**(1): p. 47-59.
132. Thimmulappa, R.K., et al., Nrf2 is a critical regulator of the innate immune response and survival during experimental sepsis. The Journal of clinical investigation, 2006. **116**(4): p. 984-95.
133. Thimmulappa, R.K., et al., Nrf2-dependent protection from LPS induced inflammatory response and mortality by CDDO-Imidazolide. Biochemical and biophysical research communications, 2006. **351**(4): p. 883-9.
134. Lin, W., et al., Sulforaphane suppressed LPS-induced inflammation in mouse peritoneal macrophages through Nrf2 dependent pathway. Biochem Pharmacol, 2008. **76**(8): p. 967-73.
135. Heiss, E., et al., Nuclear factor kappa B is a molecular target for sulforaphane-mediated anti-inflammatory mechanisms. J Biol Chem, 2001. **276**(34): p. 32008-15.
136. Khor, T.O., S. Yu, and A.N. Kong, Dietary cancer chemopreventive agents - targeting inflammation and Nrf2 signaling pathway. Planta medica, 2008. **74**(13): p. 1540-7.
137. Sen, R. and D. Baltimore, Inducibility of kappa immunoglobulin enhancer-binding protein Nf-kappa B by a posttranslational mechanism. Cell, 1986. **47**(6): p. 921-8.
138. Lawrence, T., The nuclear factor NF-kappaB pathway in inflammation. Cold Spring Harb Perspect Biol, 2009. **1**(6): p. a001651.

139. Inoue, J., et al., I kappa B gamma, a 70 kd protein identical to the C-terminal half of p110 NF-kappa B: a new member of the I kappa B family. Cell, 1992. **68**(6): p. 1109-20.
140. Pahl, H.L., Activators and target genes of Rel/NF-kappaB transcription factors. Oncogene, 1999. **18**(49): p. 6853-66.
141. Karin, M. and Y. Ben-Neriah, Phosphorylation meets ubiquitination: the control of NF-[kappa]B activity. Annu Rev Immunol, 2000. **18**: p. 621-63.
142. Bonizzi, G. and M. Karin, The two NF-kappaB activation pathways and their role in innate and adaptive immunity. Trends Immunol, 2004. **25**(6): p. 280-8.
143. Traenckner, E.B., et al., Phosphorylation of human I kappa B-alpha on serines 32 and 36 controls I kappa B-alpha proteolysis and NF-kappa B activation in response to diverse stimuli. EMBO J, 1995. **14**(12): p. 2876-83.
144. Reuter, S., et al., Oxidative stress, inflammation, and cancer: how are they linked? Free radical biology & medicine, 2010. **49**(11): p. 1603-16.
145. Liu, G.H., J. Qu, and X. Shen, NF-kappaB/p65 antagonizes Nrf2-ARE pathway by depriving CBP from Nrf2 and facilitating recruitment of HDAC3 to MafK. Biochimica et biophysica acta, 2008. **1783**(5): p. 713-27.
146. Hirota, K., et al., Distinct roles of thioredoxin in the cytoplasm and in the nucleus. A two-step mechanism of redox regulation of transcription factor NF-kappaB. J Biol Chem, 1999. **274**(39): p. 27891-7.
147. Jun, C.D., et al., Gliotoxin reduces the severity of trinitrobenzene sulfonic acid-induced colitis in mice: evidence of the connection between heme oxygenase-1 and the nuclear factor-kappaB pathway in vitro and in vivo. Inflamm Bowel Dis, 2006. **12**(7): p. 619-29.
148. Iskander, K., et al., NQO1 and NQO2 regulation of humoral immunity and autoimmunity. J Biol Chem, 2006. **281**(41): p. 30917-24.
149. Seldon, M.P., et al., Heme oxygenase-1 inhibits the expression of adhesion molecules associated with endothelial cell activation via inhibition of NF-kappaB RelA phosphorylation at serine 276. Journal of immunology, 2007. **179**(11): p. 7840-51.
150. Ayrton, A. and P. Morgan, Role of transport proteins in drug absorption, distribution and excretion. Xenobiotica, 2001. **31**(8-9): p. 469-97.
151. Gottesman, M.M., T. Fojo, and S.E. Bates, Multidrug resistance in cancer: role of ATP-dependent transporters. Nat Rev Cancer, 2002. **2**(1): p. 48-58.
152. Higgins, C.F., Multiple molecular mechanisms for multidrug resistance transporters. Nature, 2007. **446**(7137): p. 749-57.
153. Borst, P., et al., A family of drug transporters: the multidrug resistance-associated proteins. J Natl Cancer Inst, 2000. **92**(16): p. 1295-302.
154. Vollrath, V., et al., Role of Nrf2 in the regulation of the Mrp2 (ABCC2) gene. Biochem J, 2006. **395**(3): p. 599-609.
155. Ji, L., et al., Nrf2 pathway regulates multidrug-resistance-associated protein 1 in small cell lung cancer. PLoS One, 2013. **8**(5): p. e63404.
156. Singh, A., et al., Expression of ABCG2 (BCRP) is regulated by Nrf2 in cancer cells that confers side population and chemoresistance phenotype. Mol Cancer Ther, 2010. **9**(8): p. 2365-76.
157. Maher, J.M., et al., Oxidative and electrophilic stress induces multidrug resistance-associated protein transporters via the nuclear factor-E2-related factor-2 transcriptional pathway. Hepatology, 2007. **46**(5): p. 1597-610.
158. Hirotsu, Y., et al., Nrf2-MafG heterodimers contribute globally to antioxidant and metabolic networks. Nucleic Acids Res, 2012. **40**(20): p. 10228-39.

159. Maher, J.M., et al., Induction of the multidrug resistance-associated protein family of transporters by chemical activators of receptor-mediated pathways in mouse liver. Drug Metab Dispos, 2005. **33**(7): p. 956-62.
160. Adachi, T., et al., Nrf2-dependent and -independent induction of ABC transporters ABCC1, ABCC2, and ABCG2 in HepG2 cells under oxidative stress. J Exp Ther Oncol, 2007. **6**(4): p. 335-48.
161. Yeh, C.T. and G.C. Yen, Induction of hepatic antioxidant enzymes by phenolic acids in rats is accompanied by increased levels of multidrug resistance-associated protein 3 mRNA expression. J Nutr, 2006. **136**(1): p. 11-5.
162. Anwar-Mohamed, A., et al., The effect of Nrf2 knockout on the constitutive expression of drug metabolizing enzymes and transporters in C57Bl/6 mice livers. Toxicol In Vitro, 2011. **25**(4): p. 785-95.
163. Kweon, M.H., et al., Constitutive overexpression of Nrf2-dependent heme oxygenase-1 in A549 cells contributes to resistance to apoptosis induced by epigallocatechin 3-gallate. J Biol Chem, 2006. **281**(44): p. 33761-72.
164. Wang, X.J., et al., Nrf2 enhances resistance of cancer cells to chemotherapeutic drugs, the dark side of Nrf2. Carcinogenesis, 2008. **29**(6): p. 1235-43.
165. Homma, S., et al., Nrf2 enhances cell proliferation and resistance to anticancer drugs in human lung cancer. Clin Cancer Res, 2009. **15**(10): p. 3423-32.
166. Shibata, T., et al., Cancer related mutations in NRF2 impair its recognition by Keap1-Cul3 E3 ligase and promote malignancy. Proc Natl Acad Sci U S A, 2008. **105**(36): p. 13568-73.
167. Primiano, T., et al., Intermittent dosing with oltipraz: relationship between chemoprevention of aflatoxin-induced tumorigenesis and induction of glutathione S-transferases. Cancer Res, 1995. **55**(19): p. 4319-24.
168. Fahey, J.W., Y. Zhang, and P. Talalay, Broccoli sprouts: an exceptionally rich source of inducers of enzymes that protect against chemical carcinogens. Proc Natl Acad Sci U S A, 1997. **94**(19): p. 10367-72.
169. Fahey, J.W., et al., Sulforaphane inhibits extracellular, intracellular, and antibiotic-resistant strains of Helicobacter pylori and prevents benzo[a]pyrene-induced stomach tumors. Proc Natl Acad Sci U S A, 2002. **99**(11): p. 7610-5.
170. Osburn, W.O., et al., Increased colonic inflammatory injury and formation of aberrant crypt foci in Nrf2-deficient mice upon dextran sulfate treatment. Int J Cancer, 2007. **121**(9): p. 1883-91.
171. Rangasamy, T., et al., Disruption of Nrf2 enhances susceptibility to severe airway inflammation and asthma in mice. J Exp Med, 2005. **202**(1): p. 47-59.
172. Padmanabhan, B., et al., Structural basis for defects of Keap1 activity provoked by its point mutations in lung cancer. Mol Cell, 2006. **21**(5): p. 689-700.
173. Ohta, T., et al., Loss of Keap1 function activates Nrf2 and provides advantages for lung cancer cell growth. Cancer Res, 2008. **68**(5): p. 1303-9.
174. Kim, Y.R., et al., Oncogenic NRF2 mutations in squamous cell carcinomas of oesophagus and skin. J Pathol, 2010. **220**(4): p. 446-51.
175. Zhang, P., et al., Loss of Kelch-like ECH-associated protein 1 function in prostate cancer cells causes chemoresistance and radioresistance and promotes tumor growth. Mol Cancer Ther, 2010. **9**(2): p. 336-46.
176. Jiang, T., et al., High levels of Nrf2 determine chemoresistance in type II endometrial cancer. Cancer Res, 2010. **70**(13): p. 5486-96.

177. Rushworth, S.A., et al., The high Nrf2 expression in human acute myeloid leukemia is driven by NF-kappaB and underlies its chemo-resistance. Blood, 2012. **120**(26): p. 5188-98.
178. Lister, A., et al., Nrf2 is overexpressed in pancreatic cancer: implications for cell proliferation and therapy. Mol Cancer, 2011. **10**: p. 37.
179. Sasaki, H., et al., Genotype analysis of the NRF2 gene mutation in lung cancer. Int J Mol Med, 2013. **31**(5): p. 1135-8.
180. Hu, X.F., et al., Nrf2 overexpression predicts prognosis and 5-fu resistance in gastric cancer. Asian Pac J Cancer Prev, 2013. **14**(9): p. 5231-5.
181. Solis, L.M., et al., Nrf2 and Keap1 abnormalities in non-small cell lung carcinoma and association with clinicopathologic features. Clin Cancer Res, 2010. **16**(14): p. 3743-53.
182. Satoh, H., et al., Nrf2 prevents initiation but accelerates progression through the Kras signaling pathway during lung carcinogenesis. Cancer Res, 2013. **73**(13): p. 4158-68.
183. Mitsuishi, Y., et al., Nrf2 redirects glucose and glutamine into anabolic pathways in metabolic reprogramming. Cancer Cell, 2012. **22**(1): p. 66-79.
184. Hanahan, D. and R.A. Weinberg, Hallmarks of cancer: the next generation. Cell, 2011. **144**(5): p. 646-74.
185. Kensler, T.W. and N. Wakabayashi, Nrf2: friend or foe for chemoprevention? Carcinogenesis, 2010. **31**(1): p. 90-9.
186. Jaramillo, M.C. and D.D. Zhang, The emerging role of the Nrf2-Keap1 signaling pathway in cancer. Genes Dev, 2013. **27**(20): p. 2179-91.
187. Xu, C., et al., Suppression of NF-kappaB and NF-kappaB-regulated gene expression by sulforaphane and PEITC through IkappaBalpha, IKK pathway in human prostate cancer PC-3 cells. Oncogene, 2005. **24**(28): p. 4486-95.
188. Ahmad, R., et al., Triterpenoid CDDO-Me blocks the NF-kappaB pathway by direct inhibition of IKKbeta on Cys-179. J Biol Chem, 2006. **281**(47): p. 35764-9.
189. Karuri, A.R., et al., 3H-1,2-dithiole-3-thione targets nuclear factor kappaB to block expression of inducible nitric-oxide synthase, prevents hypotension, and improves survival in endotoxemic rats. J Pharmacol Exp Ther, 2006. **317**(1): p. 61-7.
190. Marks, P.A. and W.S. Xu, Histone deacetylase inhibitors: Potential in cancer therapy. J Cell Biochem, 2009. **107**(4): p. 600-8.
191. Seidel, C., et al., Histone deacetylase modulators provided by Mother Nature. Genes Nutr, 2012. **7**(3): p. 357-67.
192. Fang, M., D. Chen, and C.S. Yang, Dietary polyphenols may affect DNA methylation. J Nutr, 2007. **137**(1 Suppl): p. 223S-228S.
193. Khor, T.O., et al., Pharmacodynamics of curcumin as DNA hypomethylation agent in restoring the expression of Nrf2 via promoter CpGs demethylation. Biochem Pharmacol, 2011. **82**(9): p. 1073-8.
194. Catala, A., Lipid peroxidation of membrane phospholipids generates hydroxy-alkenals and oxidized phospholipids active in physiological and/or pathological conditions. Chem Phys Lipids, 2009. **157**(1): p. 1-11.
195. Esterbauer, H., R.J. Schaur, and H. Zollner, Chemistry and biochemistry of 4-hydroxynonenal, malonaldehyde and related aldehydes. Free Radic Biol Med, 1991. **11**(1): p. 81-128.
196. Siems, W. and T. Grune, Intracellular metabolism of 4-hydroxynonenal. Mol Aspects Med, 2003. **24**(4-5): p. 167-75.

197. Awasthi, Y.C., G.A. Ansari, and S. Awasthi, Regulation of 4-hydroxynonenal mediated signaling by glutathione S-transferases. Methods Enzymol, 2005. **401**: p. 379-407.
198. Petersen, D.R. and J.A. Doorn, Reactions of 4-hydroxynonenal with proteins and cellular targets. Free Radic Biol Med, 2004. **37**(7): p. 937-45.
199. Smathers, R.L., et al., Overview of lipid peroxidation products and hepatic protein modification in alcoholic liver disease. Chem Biol Interact, 2011. **192**(1-2): p. 107-12.
200. Jaiswal, A.K., Nrf2 signaling in coordinated activation of antioxidant gene expression. Free Radic Biol Med, 2004. **36**(10): p. 1199-207.
201. Xie, T., et al., ARE- and TRE-mediated regulation of gene expression. Response to xenobiotics and antioxidants. J Biol Chem, 1995. **270**(12): p. 6894-900.
202. Shen, G. and A.N. Kong, Nrf2 plays an important role in coordinated regulation of Phase II drug metabolism enzymes and Phase III drug transporters. Biopharm Drug Dispos, 2009. **30**(7): p. 345-55.
203. Motohashi, H. and M. Yamamoto, Nrf2-Keap1 defines a physiologically important stress response mechanism. Trends Mol Med, 2004. **10**(11): p. 549-57.
204. Li, W. and A.N. Kong, Molecular mechanisms of Nrf2-mediated antioxidant response. Mol Carcinog, 2009. **48**(2): p. 91-104.
205. Yu, R., et al., p38 mitogen-activated protein kinase negatively regulates the induction of phase II drug-metabolizing enzymes that detoxify carcinogens. J Biol Chem, 2000. **275**(4): p. 2322-7.
206. Kim, J.H., et al., The nuclear cofactor RAC3/AIB1/SRC-3 enhances Nrf2 signaling by interacting with transactivation domains. Oncogene, 2012.
207. Chen, Z.H., et al., 4-Hydroxynonenal induces adaptive response and enhances PC12 cell tolerance primarily through induction of thioredoxin reductase 1 via activation of Nrf2. J Biol Chem, 2005. **280**(51): p. 41921-7.
208. Ishikado, A., et al., Low concentration of 4-hydroxy hexenal increases heme oxygenase-1 expression through activation of Nrf2 and antioxidative activity in vascular endothelial cells. Biochem Biophys Res Commun, 2010. **402**(1): p. 99-104.
209. Katoh, Y., et al., Evolutionary conserved N-terminal domain of Nrf2 is essential for the Keap1-mediated degradation of the protein by proteasome. Arch Biochem Biophys, 2005. **433**(2): p. 342-50.
210. Raza, H. and A. John, 4-hydroxynonenal induces mitochondrial oxidative stress, apoptosis and expression of glutathione S-transferase A4-4 and cytochrome P450 2E1 in PC12 cells. Toxicol Appl Pharmacol, 2006. **216**(2): p. 309-18.
211. Burczynski, M.E., et al., The reactive oxygen species--and Michael acceptor-inducible human aldo-keto reductase AKR1C1 reduces the alpha,beta-unsaturated aldehyde 4-hydroxy-2-nonenal to 1,4-dihydroxy-2-nonene. J Biol Chem, 2001. **276**(4): p. 2890-7.
212. Hayes, J.D., J.U. Flanagan, and I.R. Jowsey, Glutathione transferases. Annu Rev Pharmacol Toxicol, 2005. **45**: p. 51-88.
213. Burczynski, M.E., H.K. Lin, and T.M. Penning, Isoform-specific induction of a human aldo-keto reductase by polycyclic aromatic hydrocarbons (PAHs), electrophiles, and oxidative stress: implications for the alternative pathway of

PAH activation catalyzed by human dihydrodiol dehydrogenase. Cancer Res, 1999. **59**(3): p. 607-14.
214. Levonen, A.L., et al., Cellular mechanisms of redox cell signalling: role of cysteine modification in controlling antioxidant defences in response to electrophilic lipid oxidation products. Biochem J, 2004. **378**(Pt 2): p. 373-82.
215. Chen, J., et al., Phosphatidylinositol 3 kinase pathway and 4-hydroxy-2-nonenal-induced oxidative injury in the RPE. Invest Ophthalmol Vis Sci, 2009. **50**(2): p. 936-42.
216. Long, E.K., et al., Trans-4-hydroxy-2-hexenal is a neurotoxic product of docosahexaenoic (22:6; n-3) acid oxidation. J Neurochem, 2008. **105**(3): p. 714-24.
217. Vladykovskaya, E., et al., Lipid peroxidation product 4-hydroxy-trans-2-nonenal causes endothelial activation by inducing endoplasmic reticulum stress. J Biol Chem, 2012. **287**(14): p. 11398-409.
218. Copple, I.M., et al., The hepatotoxic metabolite of acetaminophen directly activates the Keap1-Nrf2 cell defense system. Hepatology, 2008. **48**(4): p. 1292-301.
219. Pettazzoni, P., et al., Nuclear factor erythroid 2-related factor-2 activity controls 4-hydroxynonenal metabolism and activity in prostate cancer cells. Free Radic Biol Med, 2011. **51**(8): p. 1610-8.
220. Gallagher, E.P., C.M. Huisden, and J.L. Gardner, Transfection of HepG2 cells with hGSTA4 provides protection against 4-hydroxynonenal-mediated oxidative injury. Toxicol In Vitro, 2007. **21**(8): p. 1365-72.
221. Lopez, J., et al., The context and potential of epigenetics in oncology. Br J Cancer, 2009. **100**(4): p. 571-7.
222. Nelson, W.G., A.M. De Marzo, and S. Yegnasubramanian, Epigenetic alterations in human prostate cancers. Endocrinology, 2009. **150**(9): p. 3991-4002.
223. Sigalotti, L., et al., Epigenetic drugs as pleiotropic agents in cancer treatment: biomolecular aspects and clinical applications. J Cell Physiol, 2007. **212**(2): p. 330-44.
224. Mai, A. and L. Altucci, Epi-drugs to fight cancer: from chemistry to cancer treatment, the road ahead. Int J Biochem Cell Biol, 2009. **41**(1): p. 199-213.
225. Goel, A. and B.B. Aggarwal, Curcumin, the golden spice from Indian saffron, is a chemosensitizer and radiosensitizer for tumors and chemoprotector and radioprotector for normal organs. Nutr Cancer, 2010. **62**(7): p. 919-30.
226. Barve, A., et al., Murine prostate cancer inhibition by dietary phytochemicals--curcumin and phenyethylisothiocyanate. Pharm Res, 2008. **25**(9): p. 2181-9.
227. Dhillon, N., et al., Phase II trial of curcumin in patients with advanced pancreatic cancer. Clin Cancer Res, 2008. **14**(14): p. 4491-9.
228. Aggarwal, B.B. and B. Sung, Pharmacological basis for the role of curcumin in chronic diseases: an age-old spice with modern targets. Trends Pharmacol Sci, 2009. **30**(2): p. 85-94.
229. Bora-Tatar, G., et al., Molecular modifications on carboxylic acid derivatives as potent histone deacetylase inhibitors: Activity and docking studies. Bioorg Med Chem, 2009. **17**(14): p. 5219-28.
230. Chen, Y., et al., Curcumin, both histone deacetylase and p300/CBP-specific inhibitor, represses the activity of nuclear factor kappa B and Notch 1 in Raji cells. Basic Clin Pharmacol Toxicol, 2007. **101**(6): p. 427-33.

231. Liu, H.L., et al., Curcumin, a potent anti-tumor reagent, is a novel histone deacetylase inhibitor regulating B-NHL cell line Raji proliferation. Acta Pharmacol Sin, 2005. **26**(5): p. 603-9.
232. Meja, K.K., et al., Curcumin restores corticosteroid function in monocytes exposed to oxidants by maintaining HDAC2. Am J Respir Cell Mol Biol, 2008. **39**(3): p. 312-23.
233. Balasubramanyam, K., et al., Curcumin, a novel p300/CREB-binding protein-specific inhibitor of acetyltransferase, represses the acetylation of histone/nonhistone proteins and histone acetyltransferase-dependent chromatin transcription. J Biol Chem, 2004. **279**(49): p. 51163-71.
234. Medina-Franco, J.L., et al., Natural products as DNA methyltransferase inhibitors: a computer-aided discovery approach. Mol Divers, 2011. **15**(2): p. 293-304.
235. Ullman, T.A. and S.H. Itzkowitz, Intestinal inflammation and cancer. Gastroenterology, 2011. **140**(6): p. 1807-1816 e1.
236. Balkwill, F. and A. Mantovani, Inflammation and cancer: back to Virchow? Lancet, 2001. **357**(9255): p. 539-45.
237. De Marzo, A.M., et al., Inflammation in prostate carcinogenesis. Nat Rev Cancer, 2007. **7**(4): p. 256-69.
238. Nguyen, T., P.J. Sherratt, and C.B. Pickett, Regulatory mechanisms controlling gene expression mediated by the antioxidant response element. Annu Rev Pharmacol Toxicol, 2003. **43**: p. 233-60.
239. Chen, C. and A.N. Kong, Dietary chemopreventive compounds and ARE/EpRE signaling. Free Radic Biol Med, 2004. **36**(12): p. 1505-16.
240. Keum, Y.S., W.S. Jeong, and A.N. Kong, Chemoprevention by isothiocyanates and their underlying molecular signaling mechanisms. Mutat Res, 2004. **555**(1-2): p. 191-202.
241. Kobayashi, A., T. Ohta, and M. Yamamoto, Unique function of the Nrf2-Keap1 pathway in the inducible expression of antioxidant and detoxifying enzymes. Methods Enzymol, 2004. **378**: p. 273-86.
242. Kwak, M.K., N. Wakabayashi, and T.W. Kensler, Chemoprevention through the Keap1-Nrf2 signaling pathway by phase 2 enzyme inducers. Mutat Res, 2004. **555**(1-2): p. 133-48.
243. Kang, K.W., S.J. Lee, and S.G. Kim, Molecular mechanism of nrf2 activation by oxidative stress. Antioxid Redox Signal, 2005. **7**(11-12): p. 1664-73.
244. Jeong, W.S., M. Jun, and A.N. Kong, Nrf2: a potential molecular target for cancer chemoprevention by natural compounds. Antioxid Redox Signal, 2006. **8**(1-2): p. 99-106.
245. Rigas, B., The use of nitric oxide-donating nonsteroidal anti-inflammatory drugs in the chemoprevention of colorectal neoplasia. Curr Opin Gastroenterol, 2007. **23**(1): p. 55-9.
246. Rushmore, T.H. and C.B. Pickett, Transcriptional regulation of the rat glutathione S-transferase Ya subunit gene. Characterization of a xenobiotic-responsive element controlling inducible expression by phenolic antioxidants. J Biol Chem, 1990. **265**(24): p. 14648-53.
247. Friling, R.S., S. Bergelson, and V. Daniel, Two adjacent AP-1-like binding sites form the electrophile-responsive element of the murine glutathione S-transferase Ya subunit gene. Proc Natl Acad Sci U S A, 1992. **89**(2): p. 668-72.

248. Li, Y. and A.K. Jaiswal, Regulation of human NAD(P)H:quinone oxidoreductase gene. Role of AP1 binding site contained within human antioxidant response element. J Biol Chem, 1992. **267**(21): p. 15097-104.
249. Khor, T.O., et al., Increased susceptibility of Nrf2 knockout mice to colitis-associated colorectal cancer. Cancer Prev Res (Phila), 2008. **1**(3): p. 187-91.
250. Kitamura, Y., et al., Increased susceptibility to hepatocarcinogenicity of Nrf2-deficient mice exposed to 2-amino-3-methylimidazo[4,5-f]quinoline. Cancer Sci, 2007. **98**(1): p. 19-24.
251. Frohlich, D.A., et al., The role of Nrf2 in increased reactive oxygen species and DNA damage in prostate tumorigenesis. Oncogene, 2008. **27**(31): p. 4353-62.
252. Weber, M., et al., Chromosome-wide and promoter-specific analyses identify sites of differential DNA methylation in normal and transformed human cells. Nat Genet, 2005. **37**(8): p. 853-62.
253. Cheung, H.H., et al., Genome-wide DNA methylation profiling reveals novel epigenetically regulated genes and non-coding RNAs in human testicular cancer. Br J Cancer, 2010. **102**(2): p. 419-27.
254. Brueckner, B., et al., Epigenetic reactivation of tumor suppressor genes by a novel small-molecule inhibitor of human DNA methyltransferases. Cancer Res, 2005. **65**(14): p. 6305-11.
255. Bestor, T.H., The DNA methyltransferases of mammals. Hum Mol Genet, 2000. **9**(16): p. 2395-402.
256. Davis, C.D. and E.O. Uthus, DNA methylation, cancer susceptibility, and nutrient interactions. Exp Biol Med (Maywood), 2004. **229**(10): p. 988-95.
257. Yang, C.S., et al., Reversal of hypermethylation and reactivation of genes by dietary polyphenolic compounds. Nutr Rev, 2008. **66 Suppl 1**: p. S18-20.
258. Xiang, N., et al., Selenite reactivates silenced genes by modifying DNA methylation and histones in prostate cancer cells. Carcinogenesis, 2008. **29**(11): p. 2175-81.
259. Nian, H., et al., Modulation of histone deacetylase activity by dietary isothiocyanates and allyl sulfides: studies with sulforaphane and garlic organosulfur compounds. Environ Mol Mutagen, 2009. **50**(3): p. 213-21.
260. Wang, L.G., et al., Dual action on promoter demethylation and chromatin by an isothiocyanate restored GSTP1 silenced in prostate cancer. Mol Carcinog, 2007. **46**(1): p. 24-31.
261. Wang, L.G., et al., De-repression of the p21 promoter in prostate cancer cells by an isothiocyanate via inhibition of HDACs and c-Myc. Int J Oncol, 2008. **33**(2): p. 375-80.
262. Fu, S. and R. Kurzrock, Development of curcumin as an epigenetic agent. Cancer, 2010. **116**(20): p. 4670-6.
263. Liu, H. and R.M. Pope, Apoptosis in rheumatoid arthritis: friend or foe. Rheum Dis Clin North Am, 2004. **30**(3): p. 603-25, x.
264. Morimoto, T., et al., The dietary compound curcumin inhibits p300 histone acetyltransferase activity and prevents heart failure in rats. J Clin Invest, 2008. **118**(3): p. 868-78.
265. Marcu, M.G., et al., Curcumin is an inhibitor of p300 histone acetylatransferase. Med Chem, 2006. **2**(2): p. 169-74.
266. Liu, Z., et al., Curcumin is a potent DNA hypomethylation agent. Bioorg Med Chem Lett, 2009. **19**(3): p. 706-9.

267. Jha, A.K., et al., Reversal of hypermethylation and reactivation of the RARbeta2 gene by natural compounds in cervical cancer cell lines. Folia Biol (Praha), 2010. **56**(5): p. 195-200.
268. Liu, Y.L., et al., Hypomethylation effects of curcumin, demethoxycurcumin and bisdemethoxycurcumin on WIF-1 promoter in non-small cell lung cancer cell lines. Mol Med Report, 2011.
269. Anand, P., et al., Biological activities of curcumin and its analogues (Congeners) made by man and Mother Nature. Biochem Pharmacol, 2008. **76**(11): p. 1590-611.
270. Ravindran, J., S. Prasad, and B.B. Aggarwal, Curcumin and cancer cells: how many ways can curry kill tumor cells selectively? AAPS J, 2009. **11**(3): p. 495-510.
271. Zhang, D.D., Mechanistic studies of the Nrf2-Keap1 signaling pathway. Drug Metab Rev, 2006. **38**(4): p. 769-89.
272. Khor, T.O., S. Yu, and A.N. Kong, Dietary cancer chemopreventive agents - targeting inflammation and Nrf2 signaling pathway. Planta Med, 2008. **74**(13): p. 1540-7.
273. Tam, N.N., et al., Differential attenuation of oxidative/nitrosative injuries in early prostatic neoplastic lesions in TRAMP mice by dietary antioxidants. Prostate, 2006. **66**(1): p. 57-69.
274. Foster, B.A., et al., Characterization of prostatic epithelial cell lines derived from transgenic adenocarcinoma of the mouse prostate (TRAMP) model. Cancer Res, 1997. **57**(16): p. 3325-30.
275. Meeran, S.M., A. Ahmed, and T.O. Tollefsbol, Epigenetic targets of bioactive dietary components for cancer prevention and therapy. Clin Epigenetics, 2010. **1**(3-4): p. 101-116.
276. Brigelius-Flohe, R. and M.G. Traber, Vitamin E: function and metabolism. FASEB J, 1999. **13**(10): p. 1145-55.
277. Helzlsouer, K.J., et al., Association between alpha-tocopherol, gamma-tocopherol, selenium, and subsequent prostate cancer. J Natl Cancer Inst, 2000. **92**(24): p. 2018-23.
278. Virtamo, J., et al., Incidence of cancer and mortality following alpha-tocopherol and beta-carotene supplementation: a postintervention follow-up. JAMA, 2003. **290**(4): p. 476-85.
279. Lippman, S.M., et al., Effect of selenium and vitamin E on risk of prostate cancer and other cancers: the Selenium and Vitamin E Cancer Prevention Trial (SELECT). JAMA, 2009. **301**(1): p. 39-51.
280. Ju, J., et al., A gamma-tocopherol-rich mixture of tocopherols inhibits colon inflammation and carcinogenesis in azoxymethane and dextran sulfate sodium-treated mice. Cancer Prev Res (Phila), 2009. **2**(2): p. 143-52.
281. Lambert, J.D., et al., Inhibition of lung cancer growth in mice by dietary mixed tocopherols. Mol Nutr Food Res, 2009. **53**(8): p. 1030-5.
282. Lee, H.J., et al., Mixed tocopherols prevent mammary tumorigenesis by inhibiting estrogen action and activating PPAR-gamma. Clin Cancer Res, 2009. **15**(12): p. 4242-9.
283. Barve, A., et al., Gamma-tocopherol-enriched mixed tocopherol diet inhibits prostate carcinogenesis in TRAMP mice. Int J Cancer, 2009. **124**(7): p. 1693-9.
284. Wu, T.Y., et al., In vivo pharmacodynamics of indole-3-carbinol in the inhibition of prostate cancer in transgenic adenocarcinoma of mouse prostate

(TRAMP) mice: Involvement of Nrf2 and cell cycle/apoptosis signaling pathways. Mol Carcinog, 2011.
285. Reeves, P.G., F.H. Nielsen, and G.C. Fahey, Jr., AIN-93 purified diets for laboratory rodents: final report of the American Institute of Nutrition ad hoc writing committee on the reformulation of the AIN-76A rodent diet. J Nutr, 1993. **123**(11): p. 1939-51.
286. Bird, A., DNA methylation patterns and epigenetic memory. Genes Dev, 2002. **16**(1): p. 6-21.
287. Ju, J., et al., Cancer-preventive activities of tocopherols and tocotrienols. Carcinogenesis, 2010. **31**(4): p. 533-42.
288. Morey Kinney, S.R., et al., Stage-specific alterations of DNA methyltransferase expression, DNA hypermethylation, and DNA hypomethylation during prostate cancer progression in the transgenic adenocarcinoma of mouse prostate model. Mol Cancer Res, 2008. **6**(8): p. 1365-74.
289. Mavis, C.K., et al., Expression level and DNA methylation status of glutathione-S-transferase genes in normal murine prostate and TRAMP tumors. Prostate, 2009. **69**(12): p. 1312-24.
290. Dashwood, R.H. and E. Ho, Dietary histone deacetylase inhibitors: from cells to mice to man. Semin Cancer Biol, 2007. **17**(5): p. 363-9.
291. Pandey, M., S. Shukla, and S. Gupta, Promoter demethylation and chromatin remodeling by green tea polyphenols leads to re-expression of GSTP1 in human prostate cancer cells. Int J Cancer, 2010. **126**(11): p. 2520-33.
292. Traber, M.G., Regulation of xenobiotic metabolism, the only signaling function of alpha-tocopherol? Mol Nutr Food Res, 2010. **54**(5): p. 661-8.
293. Xi Zheng, X.-X.C., Tin Oo Khor, Ying Huang, Robert S DiPaola, Susan Goodin, Mao-Jung Lee, Chung S Yang, Ah-Ng Kong, Allan H. Conney, Inhibitory Effect of a γ-Tocopherol-Rich Mixture of Tocopherols on the Formation and Growth of LNCaP Prostate Tumors in Immunodeficient Mice. Cancers, 2011. **3**: p. 3762-3772.
294. Li, G.X., et al., delta-tocopherol is more active than alpha - or gamma - tocopherol in inhibiting lung tumorigenesis in vivo. Cancer Prev Res (Phila), 2011. **4**(3): p. 404-13.
295. Conte, C., et al., Gamma-tocotrienol metabolism and antiproliferative effect in prostate cancer cells. Ann N Y Acad Sci, 2004. **1031**: p. 391-4.
296. Jiang, Q., et al., gamma-tocopherol and its major metabolite, in contrast to alpha-tocopherol, inhibit cyclooxygenase activity in macrophages and epithelial cells. Proc Natl Acad Sci U S A, 2000. **97**(21): p. 11494-9.
297. Jiang, Q. and B.N. Ames, Gamma-tocopherol, but not alpha-tocopherol, decreases proinflammatory eicosanoids and inflammation damage in rats. FASEB J, 2003. **17**(8): p. 816-22.
298. Hensley, K., et al., New perspectives on vitamin E: gamma-tocopherol and carboxyelthylhydroxychroman metabolites in biology and medicine. Free Radic Biol Med, 2004. **36**(1): p. 1-15.
299. Frei, B., Efficacy of dietary antioxidants to prevent oxidative damage and inhibit chronic disease. J Nutr, 2004. **134**(11): p. 3196S-3198S.
300. Jiang, Q., J. Wong, and B.N. Ames, Gamma-tocopherol induces apoptosis in androgen-responsive LNCaP prostate cancer cells via caspase-dependent and independent mechanisms. Ann N Y Acad Sci, 2004. **1031**: p. 399-400.

301. Yu, W., et al., Induction of apoptosis in human breast cancer cells by tocopherols and tocotrienols. Nutr Cancer, 1999. **33**(1): p. 26-32.
302. Zheng, X., et al., Inhibitory Effect of a gamma-Tocopherol-Rich Mixture of Tocopherols on the Formation and Growth of LNCaP Prostate Tumors in Immunodeficient Mice. Cancers (Basel), 2011. **3**(4): p. 3762-72.
303. Guan, F., et al., delta- and gamma-tocopherols, but not alpha-tocopherol, inhibit colon carcinogenesis in azoxymethane-treated F344 rats. Cancer Prev Res (Phila), 2012. **5**(4): p. 644-54.
304. Jiang, Q., et al., Gamma-tocopherol attenuates moderate but not severe colitis and suppresses moderate colitis-promoted colon tumorigenesis in mice. Free Radic Biol Med, 2013. **65**: p. 1069-77.
305. Takahashi, S., et al., Suppression of prostate cancer in a transgenic rat model via gamma-tocopherol activation of caspase signaling. Prostate, 2009. **69**(6): p. 644-51.
306. Smolarek, A.K., et al., Dietary administration of delta- and gamma-tocopherol inhibits tumorigenesis in the animal model of estrogen receptor-positive, but not HER-2 breast cancer. Cancer Prev Res (Phila), 2012. **5**(11): p. 1310-20.
307. Siegel, R., D. Naishadham, and A. Jemal, Cancer statistics, 2013. CA Cancer J Clin, 2013. **63**(1): p. 11-30.
308. Heinonen, O.P., et al., Prostate cancer and supplementation with alpha-tocopherol and beta-carotene: incidence and mortality in a controlled trial. J Natl Cancer Inst, 1998. **90**(6): p. 440-6.
309. Jiang, Q., et al., gamma-tocopherol, the major form of vitamin E in the US diet, deserves more attention. Am J Clin Nutr, 2001. **74**(6): p. 714-22.
310. Opoku-Acheampong, A.B., et al., Preventive and Therapeutic Efficacy of Finasteride and Dutasteride in TRAMP Mice. PLoS One, 2013. **8**(10): p. e77738.
311. Shukla, S., et al., Apigenin inhibits prostate cancer progression in TRAMP mice via targeting PI3K/Akt/FoxO pathway. Carcinogenesis, 2013.
312. Hahm, E.R., et al., Honokiol inhibits androgen receptor activity in prostate cancer cells. Prostate, 2013.
313. Ru, P., et al., Bitter melon extract impairs prostate cancer cell-cycle progression and delays prostatic intraepithelial neoplasia in TRAMP model. Cancer Prev Res (Phila), 2011. **4**(12): p. 2122-30.
314. Wu, T.Y., et al., In vivo pharmacodynamics of indole-3-carbinol in the inhibition of prostate cancer in transgenic adenocarcinoma of mouse prostate (TRAMP) mice: involvement of Nrf2 and cell cycle/apoptosis signaling pathways. Mol Carcinog, 2012. **51**(10): p. 761-70.
315. Greenberg, N.M., et al., Prostate cancer in a transgenic mouse. Proc Natl Acad Sci U S A, 1995. **92**(8): p. 3439-43.
316. Barve, A., et al., Pharmacogenomic profile of soy isoflavone concentrate in the prostate of Nrf2 deficient and wild-type mice. J Pharm Sci, 2008. **97**(10): p. 4528-45.
317. Nair, S., et al., Toxicogenomics of endoplasmic reticulum stress inducer tunicamycin in the small intestine and liver of Nrf2 knockout and C57BL/6J mice. Toxicol Lett, 2007. **168**(1): p. 21-39.
318. Bolstad, B.M., et al., A comparison of normalization methods for high density oligonucleotide array data based on variance and bias. Bioinformatics, 2003. **19**(2): p. 185-93.

319. Bolstad, B.M., preprocessCore: A collection of pre-processing functions. R package version 1.20.0.
320. Su, Z.Y., et al., A perspective on dietary phytochemicals and cancer chemoprevention: oxidative stress, nrf2, and epigenomics. Top Curr Chem, 2013. **329**: p. 133-62.
321. Slocum, S.L. and T.W. Kensler, Nrf2: control of sensitivity to carcinogens. Arch Toxicol, 2011. **85**(4): p. 273-84.
322. Nilsson, U., et al., Examination of substrate binding in thiamin diphosphate-dependent transketolase by protein crystallography and site-directed mutagenesis. J Biol Chem, 1997. **272**(3): p. 1864-9.
323. Kahn, A., et al., Phosphofructokinase (PFK) isozymes in man. I. Studies of adult human tissues. Hum Genet, 1979. **48**(1): p. 93-108.
324. Elshourbagy, N.A., et al., Cloning and expression of a human ATP-citrate lyase cDNA. Eur J Biochem, 1992. **204**(2): p. 491-9.
325. Tatibana, M., et al., Mammalian phosphoribosyl-pyrophosphate synthetase. Adv Enzyme Regul, 1995. **35**: p. 229-49.
326. Kim, Y.O., et al., Characterization of a cDNA clone for human NAD(+)-specific isocitrate dehydrogenase alpha-subunit and structural comparison with its isoenzymes from different species. Biochem J, 1995. **308 (Pt 1)**: p. 63-8.
327. Eng, C., et al., A role for mitochondrial enzymes in inherited neoplasia and beyond. Nat Rev Cancer, 2003. **3**(3): p. 193-202.
328. Torricelli, P., et al., gamma-Tocopherol inhibits human prostate cancer cell proliferation by up-regulation of transglutaminase 2 and down-regulation of cyclins. Amino Acids, 2013. **44**(1): p. 45-51.
329. Ni, J., et al., Vitamin E succinate inhibits human prostate cancer cell growth via modulating cell cycle regulatory machinery. Biochem Biophys Res Commun, 2003. **300**(2): p. 357-63.
330. Gysin, R., A. Azzi, and T. Visarius, Gamma-tocopherol inhibits human cancer cell cycle progression and cell proliferation by down-regulation of cyclins. FASEB J, 2002. **16**(14): p. 1952-4.
331. Sigounas, G., A. Anagnostou, and M. Steiner, dl-alpha-tocopherol induces apoptosis in erythroleukemia, prostate, and breast cancer cells. Nutr Cancer, 1997. **28**(1): p. 30-5.
332. Xi Zheng, X.-X.C., Tin Oo Khor, Ying Huang, Robert S DiPaola, Susan Goodin, Mao-Jung Lee, Chung S yang, Ah-Ng Kong, and Allan H. Conney, Inhibitory Effect of a γ-Tocopherol-Rich Mixture of Tocopherols on the Formation and Growth of LNCaP Prostate Tumors in Immunodeficient Mice. Cancer, 2011. **3**(4): p. 3762-3772.
333. Finkel, T., Signal transduction by reactive oxygen species. J Cell Biol, 2011. **194**(1): p. 7-15.
334. Fryer, A.A., et al., Polymorphisms in glutathione S-transferases and non-melanoma skin cancer risk in Australian renal transplant recipients. Carcinogenesis, 2005. **26**(1): p. 185-91.
335. Carlsten, C., et al., Glutathione S-transferase M1 (GSTM1) polymorphisms and lung cancer: a literature-based systematic HuGE review and meta-analysis. Am J Epidemiol, 2008. **167**(7): p. 759-74.
336. Ward, P.S. and C.B. Thompson, Metabolic reprogramming: a cancer hallmark even warburg did not anticipate. Cancer Cell, 2012. **21**(3): p. 297-308.

337. Warburg, O., On the origin of cancer cells. Science, 1956. **123**(3191): p. 309-14.
338. Reiter, E., Q. Jiang, and S. Christen, Anti-inflammatory properties of alpha- and gamma-tocopherol. Mol Aspects Med, 2007. **28**(5-6): p. 668-91.
339. ASH, O., *Natural sources of tocotrienols in vitamin E in health and disease*, ed. F.J. Packer L. 1993, New York: Marcel Dekker. 3-8.
340. Kunnumakkara, A.B., et al., {Gamma}-tocotrienol inhibits pancreatic tumors and sensitizes them to gemcitabine treatment by modulating the inflammatory microenvironment. Cancer Res, 2010. **70**(21): p. 8695-705.
341. Hodul, P.J., et al., Vitamin E delta-tocotrienol induces p27(Kip1)-dependent cell-cycle arrest in pancreatic cancer cells via an E2F-1-dependent mechanism. PLoS One, 2013. **8**(2): p. e52526.
342. Manu, K.A., et al., First evidence that gamma-tocotrienol inhibits the growth of human gastric cancer and chemosensitizes it to capecitabine in a xenograft mouse model through the modulation of NF-kappaB pathway. Clin Cancer Res, 2012. **18**(8): p. 2220-9.
343. Pierpaoli, E., et al., Effect of annatto-tocotrienols supplementation on the development of mammary tumors in HER-2/neu transgenic mice. Carcinogenesis, 2013. **34**(6): p. 1352-60.
344. Jiang, Q., et al., Gamma-tocotrienol induces apoptosis and autophagy in prostate cancer cells by increasing intracellular dihydrosphingosine and dihydroceramide. Int J Cancer, 2012. **130**(3): p. 685-93.
345. Yap, W.N., et al., In vivo evidence of gamma-tocotrienol as a chemosensitizer in the treatment of hormone-refractory prostate cancer. Pharmacology, 2010. **85**(4): p. 248-58.
346. Barve, A., et al., Mixed tocotrienols inhibit prostate carcinogenesis in TRAMP mice. Nutr Cancer, 2010. **62**(6): p. 789-94.
347. Bachawal, S.V., V.B. Wali, and P.W. Sylvester, Combined gamma-tocotrienol and erlotinib/gefitinib treatment suppresses Stat and Akt signaling in murine mammary tumor cells. Anticancer Res, 2010. **30**(2): p. 429-37.
348. Krycer, J.R., L. Phan, and A.J. Brown, A key regulator of cholesterol homoeostasis, SREBP-2, can be targeted in prostate cancer cells with natural products. Biochem J, 2012. **446**(2): p. 191-201.
349. Constantinou, C., et al., Induction of caspase-independent programmed cell death by vitamin E natural homologs and synthetic derivatives. Nutr Cancer, 2009. **61**(6): p. 864-74.
350. Korenchuk, S., et al., VCaP, a cell-based model system of human prostate cancer. In Vivo, 2001. **15**(2): p. 163-8.
351. FDA, Guidance for Industry: Estimating the Maximum Safe Starting Dose in Initial Clinical Trials for Therapeutics in Adults Healthy Volunteers. 2005.
352. Husain, K., et al., Vitamin E delta-tocotrienol levels in tumor and pancreatic tissue of mice after oral administration. Pharmacology, 2009. **83**(3): p. 157-63.
353. Fernandes, N.V., P.K. Guntipalli, and H. Mo, d-delta-Tocotrienol-mediated cell cycle arrest and apoptosis in human melanoma cells. Anticancer Res, 2010. **30**(12): p. 4937-44.
354. Makpol, S., et al., Tocotrienol-rich fraction prevents cell cycle arrest and elongates telomere length in senescent human diploid fibroblasts. J Biomed Biotechnol, 2011. **2011**: p. 506171.
355. Wu, S.J., G.Y. Huang, and L.T. Ng, gamma-Tocotrienol induced cell cycle arrest and apoptosis via activating the Bax-mediated mitochondrial and

AMPK signaling pathways in 3T3-L1 adipocytes. Food Chem Toxicol, 2013. **59**: p. 501-13.
356. Gaziano, J.M., et al., Multivitamins in the prevention of cancer in men: the Physicians' Health Study II randomized controlled trial. JAMA, 2012. **308**(18): p. 1871-80.
357. Yossepowitch, O., et al., Advanced but not localized prostate cancer is associated with increased oxidative stress. J Urol, 2007. **178**(4 Pt 1): p. 1238-43; discussion 1243-4.
358. Kumar, B., et al., Oxidative stress is inherent in prostate cancer cells and is required for aggressive phenotype. Cancer Res, 2008. **68**(6): p. 1777-85.
359. Barocas, D.A., et al., Oxidative stress measured by urine F2-isoprostane level is associated with prostate cancer. J Urol, 2011. **185**(6): p. 2102-7.
360. Gupta-Elera, G., et al., The role of oxidative stress in prostate cancer. Eur J Cancer Prev, 2012. **21**(2): p. 155-62.
361. Khandrika, L., et al., Oxidative stress in prostate cancer. Cancer Lett, 2009. **282**(2): p. 125-36.
362. Nakayama, M., et al., GSTP1 CpG island hypermethylation as a molecular biomarker for prostate cancer. J Cell Biochem, 2004. **91**(3): p. 540-52.
363. Khor, T.O., et al., Epigenetic DNA Methylation of Antioxidative Stress Regulator NRF2 in Human Prostate Cancer. Cancer Prev Res (Phila), 2014. **7**(12): p. 1186-97.